TÉCNICO LISBOA

Inverse Dynamics of Change of Direction Manoeuvres in Elite Athletes

Adriana Guedes Cameirão Jorge

Thesis to obtain the Master of Science Degree in

Biomedical Engineering

Supervisor: Prof. Dr. Carlos Miguel Fernandes Quental

Examination Committee

Chairperson: Prof. Dr. João Orlando Marques Gameiro Folgado
Supervisor: Prof. Dr. Carlos Miguel Fernandes Quental
Members of the Committee: Profª. Dra. Silvia Arsénio Rodrigues Cabral
Prof. Dr. Pedro Filipe Lima Marques

October 2022

The work presented in this thesis was performed at the Biomechanics Group of Instituto Superior Técnico (Lisbon, Portugal), during the period February 2020-October 2022, under the supervision of Prof. Dr. Carlos Miguel Fernandes Quental.

I declare that this document is an original work of my own authorship and that it fulfills all the requirements of the Code of Conduct and Good Practices of the Universidade de Lisboa.

Acknowledgments

Firstly, I would like to thank my supervisor Professor Carlos Quental for accepting my proposition and embarking on this project with me. An important acknowledgement to Ivo Fialho Roupa whose guidance and contributions were invaluable to this work. A great thank you to both for being so patient with me throughout this process. To Sérgio Gonçalves, a big thank you for all the help in the lab.

Thank you to my fellow handball players from Núcleo de Antigos Alunos do Liceu Passos Manuel, without whom this work would not have been possible.

A special thank you to João, the best coach I ever had, who was the perfect guinea pig to try out all my ideas.

To Pimentel, Bruno, Joana and Dalila, thank you for always being available to help, discuss and reassess every time I had a set-back. Above all, thank you for the support, compassion and motivational speeches.

Thank you to my parents, who have always allowed me to pursue my passions and continuously push me to be a better student, better colleague, better player, better engineer, better person.

Finally, a very special thank you to Miguel, for always believing in me. Never too busy to help, never to tired to listen and never out of words of encouragement.

Abstract

Performance enhancement and injury prevention are key to the success of elite athletes. Biomechanics is a valuable tool to provide insight into the behaviour of the musculoskeletal system during the execution of sport specific tasks. The aim of this work is to assess muscle force of the human lower limbs during the execution of handball specific changes of direction (CODs) (45°, 90° and 135°). Eleven elite female handball players performed 6 COD tasks (3 with each limb). Musculoskeletal models were scaled and used to execute inverse kinematic and inverse dynamic analyses in OpenSim. Static optimization was utilised to estimate muscles' activity and force. Statistical parametric mapping was employed to compare average joint angles, joint moments, and muscle forces between the different COD angles. Sharper CODs were found to be associated with steeper deceleration and smaller hip flexion moments. The 90° CODs were found to have the smallest knee flexion and largest knee extension joint moments, together with the smallest ankle plantarflexion and largest dorsiflexion joint moments. The *rectus femoris*, the *adductors*, the *psoas* and the *tibialis anterior* muscles showed largest peak forces for the 90° CODs, while the *soleus*, the *gastrocnemius* and the *tibialis posterior* muscles showed the smallest peak forces for those CODs. All the remaining muscles showed decreasing peak force with the increase in COD angle. Statistical comparisons between dominant and non-dominant limbs showed no significant difference between them, regardless of the evaluated variables.

Keywords

Change of direction, Musculoskeletal modeling, Inverse kinematics, Inverse dynamics, Static optimisation

Resumo

A melhoria do desempenho e a prevenção de lesões são fundamentais para o sucesso dos atletas de elite. A biomecânica é uma ferramenta valiosa para fornecer informações sobre o comportamento do sistema musculoesquelético durante a execução de tarefas específicas do desporto. O objetivo deste trabalho é avaliar os momentos articulares e as forças musculares nas articulações e nos músculos dos membros inferiores durante exercícios de mudanças de direção específicas do andebol (CODs) (45°, 90° e 135°). Onze jogadoras de andebol de elite realizaram 6 tarefas de COD (3 com cada perna). Modelos musculoesqueléticos foram dimensionados e usados para executar análises cinemática e dinâmica inversas no OpenSim. Foi utilizada otimização estática para estimar atividades e forças musculares. O mapeamento paramétrico estatístico (SPM) foi empregue para comparar as médias dos ângulos articulares, momentos articulares e forças musculares entre os diferentes ângulos de COD. CODs mais acentuadas foram associadas a desacelerações mais acentuadas e menores momentos de flexão da anca. Nas CODs de 90° foram encontrados os menores momentos articulares de flexão e os maiores momentos articulares de extensão do joelho, juntamente com os menores momentos articulares de flexão plantar e os maiores momentos articulares de dorsiflexão do tornozelo. O *Rectus femoris*, os *Adductors*, o *Psoas* e o *Tibialis anterior* apresentaram os maiores picos de força para as CODs de 90°, enquanto o *Soleus*, o *Gastrocnemius* e o *Tibialis posterior* apresentaram os picos de força mais pequenos para essas mesmas CODs. Todos os restantes músculos mostraram diminuição do pico de força com o aumento do ângulo de COD. Foi também realizada uma comparação estatística entre a execução das CODs com o membro dominante e não dominante, não tendo sido encontradas diferenças significativas entre eles em nenhuma das variáveis avaliadas.

Palavras Chave

Mudança de direção, Modelação musculoesquelética, Cinemática inversa, Dinâmica inversa, Otimização estática

Contents

List of Figures

List of Tables

Acronyms

ACL	Anterior Cruciate Ligament
CM	Centre of Mass
COD	Change of Direction
DOF	Degrees of Freedom
ES	Effect Size
EoM	Equations of Motion
GRF	Ground Reaction Forces
IC	Initial Contact
ID	Inverse Dynamics
IK	Inverse Kinematics
MOCAP	Motion Capture
MTU	Muscle Tendon Unit
RFT	Random Field Theory
SO	Static Optimization
SPM	Statistical Parametric Mapping
WA	Weight Acceptance

1

Introduction

Contents

1.1 Motivation

From individual sports, like tennis or athletics, to team sports, like football or basketball, whether they are practiced recreationally or professionally, two words are always present in an athlete's mind: performance and injury. In the case of competitive sports, there is a desire to continuously become faster, stronger, better in every way, in order to achieve the ultimate goal, winning. That objective drives the athletes to constantly push their limits, both mentally and physically. The extremely high intensity of their training, combining fitness and sport specific skills, potentiated by the athlete's inherent capabilities, together with mental coaching and tactical training are what allows athletes to reach those goals. However, it can also be their undoing, since the higher the intensity, the higher the risk of injury for an athlete.[1]

Specificity in training is crucial. A marathon runner has very different physical requirements to a volleyball player. Therefore, training programs are designed to develop specific sets of characteristics in athletes, which differ greatly across sports.[9] These differences also mean that athletes of one particular sport are more prone to certain types of injuries than others. For instance, tennis players are known to struggle with tendon inflammation in the elbow region, whereas the most prevalent injury in handball players is damage to the anterior cruciate ligament of the knee.[1]

Taking the example of handball players, injuries are strongly associated with very fast Change of Direction (COD) manoeuvres, which are an integral part of the sport. Rapid CODs are whole-body movements composed of an acceleration phase and a deceleration phase in a certain direction followed by acceleration in a different direction.[9] CODs are present in several aspects of the game, from trying to pass an opponent to rapidly going from an attacking position to a defensive position. The athlete's ability to perform these CODs is greatly tied to their success as a player.[9]

COD performance ability depends of three major characteristics: technique (foot placement, posture and stride adjustment), straight sprinting speed and leg muscle quality (strength, power and reactive strength).[9] A deep understanding of the mechanisms that are involved in producing the rapid COD can lead to better, more specific, training of these manoeuvres, improving performance and minimizing injury risks. Hence the necessity to study these movements and how athletes perform them.

Biomechanics is *"the study of the mechanical laws relating to the movement or structure of living organisms"* as per the Oxford Languages definition. It is the area of science that explains structure and motion of biological systems in response to forces or displacements, by applying mechanical methods. It is imperative for biomechanical studies in the context of sports' analysis to take into account the internal forces acting within the body. Direct methods to obtain this kind of information are invasive and therefore not a viable option. Musculoskeletal modelling provides a solution to that problem, by allowing the computation of mechanical variables such as joint angles, velocities and accelerations as well as the estimation of the internal joint moments, reaction forces and muscle forces that are present during the

body's movement. This strategy relies on the development of multi-body systems articulated by joints and actuated by muscles that replicate human motion.

Consequently, the biomechanical study of sport specific tasks utilizing musculoskeletal modelling can be used as a tool to deepen the knowledge regarding athletes' bodies and their physical capabilities, which can contribute significantly to performance analysis and even the development of injury prevention programs in elite level sports.

1.2 Scopes and Objectives

Several studies have focused on the kinematics, kinetics or muscle behaviour of COD motions in either generally active subjects or athletes. However, COD technique is not only specific to each sport, but its biomechanics also greatly depend on biological sex and age.[10,11] Few studies have focused on muscles' role in handball specific CODs. Although knee injury risk and performance are not directly evaluated in this work, they serve as the basis to define the variables of interest to be studied.

The main goal of this work is therefore to assess the joint moments and muscle activity of the lower limb joints and muscles during the execution of handball specific CODs in elite female athletes and evaluate their dependency on COD angle and limb preference. For this purpose, several tasks are envisaged:

- To acquire of kinematic data from a population of elite female handball players executing different COD manoeuvres.
- To calculate lower limbs' joint angles and moments during the execution of the collected COD tasks.
- To estimate muscles' activation and force for the lower limbs during the execution of the COD tasks.
- To evaluate kinematic and dynamic differences during CODs with different angles.
- To compare kinematic and dynamic results from COD execution between subjects' dominant and non-dominant limbs.

1.3 Literature Review

Many studies have exploited the advantages brought on by musculoskeletal modelling and analysis to provide insight on the performance of sports' related tasks, subsequent injuries and even rehabilitation.[9,12–31]

Developing injury prevention programs requires the definition of injury patterns, from the tasks that entail the most injury risk to the intrinsic risk factors of athletes, and injury mechanisms. The relationship between internal and external factors and the event of an injury can be represented by the diagram in Figure 1.1.[1]

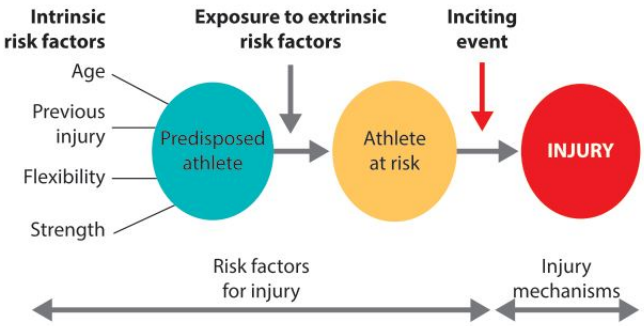

Figure 1.1: Multi-factorial model explaining injury risk in an athlete.[1]

Fully understanding a sports injury, how to prevent it and how to rehabilitate athletes to the performance level they had before the injury requires extensive knowledge of not only the risk factors and injury mechanisms, but also the athletes' execution of specific tasks as well. The description of the biomechanics by which the injury occurs is critical to identify which intrinsic factors and which specific tasks put the athletes more at risk.[1]

Knee injuries are the most prevalent in sports.[1] The most debilitating of the knee injuries is the rupture of the Anterior Cruciate Ligament (ACL), which still poses one of the greatest challenges in sports medicine.[1] Non-contact ACL injuries have clearly been associated with twisting impacts, where the joint's internal or external rotation and hyperextension play a definitive role. Motions like landing from jumps and suddenly changing direction while running carry the most risk for this type of injury.[1] Therefore, athletes that practice sports like football, rugby or handball are particularly susceptible. Furthermore, the ratio between female and male athletes that sustain ACL injuries is about 2.6, which implies women as the most vulnerable population.[1]

Several papers have focused on the relationship between ACL injury and the biological sex of the athletes. According to Hahn et al.(2021), regardless of the type and amount of sports practiced by athletes, knee instability is very common, especially among women.[32] A review of scientific papers regarding handball injuries, by Raya-González et al. (2020), reported that male athletes most commonly injured the knees and ankles, whereas female athletes primarily injured the knees.[11] This means that not only is it more common for female athletes to sustain knee injuries than male athletes, but also that it is the most prevalent handball related injury in women. Impairments of the motion of the hip have been reported by Powers (2010) to strongly affect the kinematics and dynamics of the knee joint.

He also suggested females may be more susceptible to this influence than males, potentiating ACL injury risk.[14] A review paper by Bencke et al. (2018) on gender disparities of muscle activation during the performance of sports' tasks greatly associated with ACL injury found that young female athletes present reduced activity of hamstring muscles and elevated activity of the quadriceps when compared to men.[10]

Pappas et al. (2013) reported several risk factors for ACL rupture, such as limb asymmetry, excessive quadriceps forces, excessive knee valgus and poor trunk control. This information indicates that motions that potentiate these characteristics, such as CODs, carry higher risk for ACL tear.[33] The risk factors associated with sports injuries were also investigated by Van Der Does et al. (2016) in a kinematic and dynamic study of counter-movement jump landings across female and male korfball, volleyball and basketball players. They reported that landing with smaller knee flexion moments, combined with greater ground reaction forces, carries higher risk for knee injury through overuse, and that greater ankle dorsiflexion moments increases risk of acute injury of the ankle.[21] Therefore, studying how athletes perform these manoeuvres can provide key information for injury prevention and rehabilitation. The need for skill-specific training of high risk maneuvers like CODs, with the purpose of correcting mechanical behaviours of the lower limbs joints, was highlighted by Weiss and Whatman (2015) as an effective way to reduce ACL injury risk.[19] This claim is supported by Dos'Santos et al. (2019) in a review paper that states that the most effective training programs to reduce knee injury risk consisted of balance training and changing of the COD technique.[34]

The question then arises as to whether the best for injury management is also the best for performance. Dos'Santos et. al (2018) explored the influence of angle and velocity in COD manoeuvres in sports and the relation of these parameters to a performance-injury conflict. They reported that the most desirable angles and speeds for athletic success also carry the most risk for injury. Identifying the existence of a necessary trade-off between approach velocity and the ability to execute the COD manoeuvre is one of the highlights of this analysis. Furthermore, it reinforced the need for further biomechanical studies considering the impact of these two parameters in the performance of COD motions.[25] This theme was further investigated by Fox (2018). The main conclusions drawn from this analysis were that executing the manoeuvre with toe landing and trunk rotation and lateral flexion in the direction of the cutting may reduce ACL injury risk as well as improve performance. A narrow foot placement combined with greater knee flexion were also found to reduce injury risk, but at the expense of performance quality. The key takeaway from this study is that prevention programs must take into account the performance of the COD task, to make sure they can be used without compromising athletic success.[26] Different types of training and their effects on COD execution were analysed by Nygaard et al. (2019), reporting that their effectiveness is strongly dependent on the type of the COD task.[9] This study reports the need to adapt training to the specific requirements of the manoeuvres, highlighting the importance of knowing

the biomechanical specificities of each sports' CODs, in order to develop optimal training procedures.

Angle dependence of the biomechanical behaviour of lower limb joints during COD motions was the focus of another work developed by Dos'Santos et al. (2021). Kinematic and dynamic data obtained for healthy males changing direction to three different angles (45°, 90° and 180°) revealed that higher cutting angles are associated with greater knee internal rotation and abduction moments, supporting the previously mentioned notion that sharper changes of direction are riskier for the knee. This work also states that the use of biomechanical analysis of these motions, to assess injury risk or to help in training, must consider the COD angle, since it affects joint movement patterns.[30] João et al. (2014) analysed a population of 5 physically active subjects (3 female, 2 male) performing single leg hopping motions and found that the vertical acceleration of the centre of mass of the subjects was mostly due to knee extensor muscles whereas stability of the foot was mostly influenced by the ankle plantar-flexor muscles.[35] These findings support the notion of synergies between joints (the knee and ankle in this case) in the control of complex motions, such as hopping or changing direction. Therefore, to better understand the biomechanical behaviour of the lower limbs during sports related tasks, the various joints acting together must be considered.

Raya-González et al. (2020) proposed another factor that influences COD performance, reporting a higher number of injury occurrences in both male and female players when comparing matches to training, and when comparing international to national league games, implying that movement intensity is a key factor in injury risk.[11] The lack of capability to assess the biomechanics of movements performed in-game was also reported by Weiss and Whatman (2015) as an important improvement to make in research in this field.[19]

Considering the sport specificity and the other aforementioned factors that influence COD performance, the biomechanical analysis of this manoeuvre requires the usage of reproducible tasks. By describing the differences in kinematic and dynamic behaviour of the knee between drop-jump and COD tasks in elite female handball athletes, Kristianslund and Krosshaug (2013) concluded that drop-jump motions cannot be used to infer about knee torques in CODs.[16] Later, Nedergaard et al. (2020) also evaluated the validity of using jump landings as replacement tasks to test for the risk of injuring the ACL in COD manoeuvres. They found that single-planar jump landings and multi-planar jumps do not replicate the biomechanical behaviour of young female football and handball players changing direction abruptly and therefore advised for extra caution when using these tasks to investigate ACL injury risk factors in these populations.[28] These finds support the need for specific tasks to be designed to emulate the in-game situations of interest.

A research study conducted on collegiate level football players by Sasaki et al. (2011) aimed at relating trunk kinematics to performance of COD tasks. The evaluated task was designed based on the 5-0-5 agility test, which has been used as a reliable substitute task to evaluate a person's general ability

to change direction rapidly. During this test, the subject is instructed to sprint in a straight line during 15 meters, at which point they must turn 180 degrees and sprint back another 5 meters. Although this task is highly reproducible, adjustments must be made in order to better represent sport specific COD tasks.[15] Variations of the 5-0-5 agility test have been used across studies to represent CODs. For example, Schreurs et al. (2017) focused on the influence of angle on knee kinematic and dynamic behaviour during CODs in athletes. The COD tasks consisted of a 5 meter run towards a force plate, performing the cutting manoeuvre and then sprinting 5 meters in the desired direction (45°, 90°, 135° and 180°). The results reported in this work are consistent with previous studies, stating that considerable differences exist between males and females, and that regardless of gender, sharper cutting angles involve higher knee valgus moments, placing the subject at higher risk of injuring the ACL.[24]

This type of task has also successfully been employed in research aimed at understanding the specificity of COD manoeuvres performed by female handball athletes. A group of elite female handball players was analysed by Bencke et al. (2013) performing handball-specific COD tasks, which consisted of a 5 step run-up followed by their individual side-step cutting maneuver, without COD angle constraints and executed with similar intensity to a game situation. The purpose of this work was to obtain knee and hip kinematic and dynamic data for both dominant (preferred push-off leg) and non-dominant leg.[17] Similarly, using an adaptation of the 5-0-5 test, Thomas et al. (2018) verified significant asymmetries between dominant and non-dominant limbs and directional preference in the executions of the COD tasks. These findings pertain to male and female athletes of a variety of team sports, when changing direction to 180°.[36] Kristianslund et al. (2014) performed another study on elite female athletes, aimed at explaining how technique differences in COD influence knee abduction moments. A standardised COD task was defined in order to replicate an in-game situation, where each subject ran for about 6 meters, received a ball passed from a colleague, and then performed the side-step cutting maneuver to pass a static defender. They found that the COD parameters they analysed (width of cut, hip abduction, hip internal rotation, foot rotation, torso rotation, torso lateral flexion, knee valgus and knee flexion), measured at initial contact, were dependent on individual technique. Together with approach speed, cutting angle and type of landing, these parameters accounted for over half of the variability observed in knee abduction moments (calculated using the centre of pressure of the foot and the Ground Reaction Forces (GRF) vector) across subjects.[18] These results suggest that studying COD manoeuvres should consider the difference in side of the cutting and subjects' limb preference.

Other factors, such as fatigue level and chronic pains, have also been reported to influence the ability of athletes to perform COD manoeuvres and they may lead to different adaptation strategies for each subject, which impact the kinematics of the COD, as stated by Franklyn-Miller et al. (2017) and Hosseini et al. (2020). This underlies the need to try to minimise the influence of such factors when designing a biomechanical study with the objective of analysing CODs in a population of athletes.

Several studies have been performed with the intent of estimating muscle participation in motor tasks, with human gait being the one of the most studied.[37–41] Arnold et al. (2005) used a musculoskeletal model with 54 muscle-tendon actuators to compute muscle forces of the lower limb during gait, from data from 5 healthy male subjects.[38] The same type of model and strategy was adapted by Shelburne et al. (2005) to estimate muscle, ligament and joint forces at the knee during walking,[42] and by Sritharan et al. (2012) to compare the contribution of knee-spanning and non-knee-spanning muscles on knee loading during gait.[43] One critical factor to consider when analysing kinematic and dynamic results obtained from these analysis is their great dependency on subject specific anthropometric and geometric data, as reported by Dao et al. (2009), reinforcing the importance of scaling the model according to subject specific parameters.[44] The capability of this type of actuated musculoskeletal models to analyse human gait, calculate joint angle variations, joint moments and muscle forces becomes the starting point for studying more complex motions.

To facilitate musculoskeletal based analysis, several software have been developed for research and commercial purposes. Among the available software, OpenSim, a free, open source software that allows for the development of musculoskeletal models and dynamic simulations of a multitude of motions, is one of the most used.[45] It provides the tools to design a model of a desired structure, its actuators, and perform a series of analysis, such as inverse kinematics and inverse dynamics. Researchers can use this software and its models, customise them to meet their needs and perform their own analysis.[46,47] Hamner et al. (2011) successfully used it to develop a muscle-actuated musculoskeletal model to evaluate muscle contribution in propulsion and support of a male subject when running.[48] Maniar et al. (2017) utilised a freely available muscle-actuated musculoskeletal model[7] and the capabilities of OpenSim[46,47] (inverse kinematics, inverse dynamics and static optimisation) to estimate the participation of different lower limb muscles during side-step cutting manoeuvres (not sport related) in healthy subjects and assess their individual role in loading the ACL. This study reported that the hamstring and gluteal muscles contribute the most to protecting the ACL, by opposing the forces it sustains.[49,50]

Different approaches have been used to investigate muscle participation in sports related tasks and injury mechanisms. For example, Steffen et al. (2016) tried to associate muscle strength to ACL injury risk in elite female handball and football players. Peak muscle strength, measured with dynamometers and an altered leg press, was found not to be related to an increased risk of ACL injury.[51] The relationship between the directions of jump landing and knee injury risk in basketball and volleyball athletes was studied by Sinsurin et al. (2016) by analysing muscle participation in knee flexion while jump landing in different directions. The analysis of electromyography data led to the conclusion that landing laterally is riskier than landing forward or diagonally, highlighting the need for specific training of such landings for knee injury prevention.[52] A fully computational strategy to estimate muscle forces was employed by Schache et al. (2010) in order to understand the loads in the hamstring muscles during sprinting and

their relation to the risk of injuring said muscles. The study consisted of inverse dynamic analysis of one australian rules football player. It was performed utilizing an actuated musculoskeletal model[38] to report joint angles, moments and muscle forces of the lower limbs.[13]

The OpenSim[46,47] software and its biomechanical analysis tools were also used in a study by Mateus et al. (2020) aimed at describing lower limb muscles' role in joint behaviour during abrupt deceleration tasks. Abrupt deceleration can be viewed as a part of several manoeuvres elite level athletes perform, including CODs. This work analysed elite male indoor-sports players using a muscle driven analysis in OpenSim,[46,47] referred to as computed muscle control, which is a dynamic optimisation technique to estimate muscle forces.[29] The obtained results were also compared to those computed through static optimisation, showing no significant differences between the two strategies.[12] Another comparison between the computed muscle control and the static optimisation methods was done by Roelker et al. (2020). The reported results showed that both methods' accuracy to experimental data obtained for gait varied according to specific muscle and was dependent on the musculoskeletal model used. The main conclusion was that no method was objectively better than the other and therefore neither should be used in detriment of the other. It was also advised that validation of estimated muscle activations and forces should not be done utilizing results produced using different models or simulation strategies.[37]

Time continuous statistical analysis have been employed in biomechanical studies to assess differences between limbs, populations and interventions.[53] It has also proven useful in studying sports injury and performance. Huges-Oliver et al. (2019) used Statistical Parametric Mapping (SPM)[54] to assess inter-limb differences in lower-limb kinematics of healthy athletes and athletes with ACL reconstruction, during runing and landing tasks.[55] Whyte et al. (2018) utilised SPM to investigate the influence of a high-intensity intermittent exercise protocol on trunk and lower-limb kinematics and kinetics of male gaelic football players executing COD manoeuvres. Results from this study suggest hip and knee control plays an important role in the execution of COD manoeuvres.[56] Dos'Santos et al. (2021) also employed SPM to asses inter-limb differences in joint kinematics and kinetics in female football players changing direction to 180◦. They found no significant differences between COD execution with dominant and non-dominant limbs on their population of athletes.[57] These studies used kinematic and dynamic analysis of experimentally acquired motion data to perform the SPM.[55–57]

In order to summarise what has been done in the past 20 years in terms of research on COD manoeuvres in elite female handball players, it is possible to highlight some key points. Firstly, this population is very vulnerable to knee injury, in particular, ACL damage. Preventing this type of injury is critical to athletic success, and requires specific training to make sure the manoeuvre is performed safely and efficiently. Execution technique, limb dominance and cutting angle are the parameters that most affect kinematic behaviour of joints during COD manoeuvres. Variations of the 5-0-5 test have effectively been used to mimic handball specific COD. Not many studies have considered hip, knee

and ankle joint kinematics together and their interactions in producing COD. Although musculoskeletal modelling and muscle-driven analysis have been applied successfully to study side-step cutting and similar tasks in non-athlete healthy men, muscles' activation and force have never been analysed in female athletes. Almost every work done so far in this area identifies the need for further research considering muscle participation, since it can provide the basis for the development of prevention and performance enhancing training programs. The most reported limitation when applying biomechanical analysis to sport's tasks like COD is the difficulty in mimicking in-game situations and therefore obtaining reliable data regarding the conditions under which injury COD execution is more crucial.

1.4 Main Contributions

The kinematic data acquired in this work constitutes an important contribution to the scientific community, as they can be utilised in future research.

Muscle participation in COD motions is in need of further investigation. The results of this study provide a valuable insight into the participation of muscles of the lower limbs during COD tasks. Moreover, muscle-driven computed analysis have not been applied before in the study of lower limb function in female handball players. Hence, this study is expected to provide valuable insight on muscles' participation and force in these athletes.

The inclusion of statistical analysis constitutes an important step towards better understanding the importance of cutting angle and limb preference in execution of these tasks. Utilizing SPM provides the advantage of evaluating the entirety of the movements, instead of focusing on just a few discrete time points.

As a result of studying COD manoeuvres to this extent and with such a level of specificity, the findings of this work can contribute to the development of training strategies that will maximise a female handball player's ability to change direction abruptly, improving her performance and minimizing injury risks.

1.5 Thesis Outline

This document is organised into 6 chapters, in the following manner:

- **Chapter 1** explains the motivation behind this work, describes the context it is inserted in and states its objectives and major contributions.
- **Chapter 2** contains the theoretical knowledge and concepts which are necessary for fully understanding this work. It is divided into 3 subsections, where the first relates to the anatomy and functioning of the musculoskeletal system, the second focuses on musculoskeletal modelling and joint biomechanics and the third regards muscle-tendon dynamics and their modelling.

- **Chapter 3** provides a detailed description of the design of the study, the implemented methods and the tools used to produce the desired outcomes.
- **Chapter 4** presents the results obtained from the biomechanical and statistical analysis of the acquired data.
- **Chapter 5** contains the interpretation and discussion of the results.
- **Chapter 6** includes a summary of the findings of this work, addresses the study's limitations and suggests future complementary work.

2

Theoretical Background

Contents

Before delving into the computational modelling of a musculoskeletal system, it is necessary to understand how the human body is able to move. Therefore, this section will provide a brief explanation of the anatomy, physiology and function of the musculoskeletal system.

2.1 Musculoskeletal System

The musculoskeletal system is composed of bones, muscles, tendons, ligaments and joints. Its main function is to support the body, maintain posture and allow the human body to move.

In order to originate a motion, the central nervous system produces a stimulus that is transmitted down through a motor neuron. The axons of that motor neuron connect to motor endplates of skeletal muscle fibres, forming neuromuscular junctions. Since motor neuron axons have multiple branches, one motor neuron innervates several muscle fibres, forming a motor unit, as illustrated in Figure 2.1.

When a sufficiently strong stimulus reaches the endplate of a muscle fibre, it stimulates a muscle impulse that spreads across the fibre, causing the myosin and actin filaments of the sarcomeres (the functional unit of the skeletal muscle) to interact and change its length. The shortening of the sarcomeres inside a muscle fibre drives the skeletal muscle to contract. The summation of the contractile responses of a group of fibres generates muscle force. A representation of the tissue organisation of a skeletal muscle, including its functional unit (sarcomere) can be found in Figure 2.2.[2]

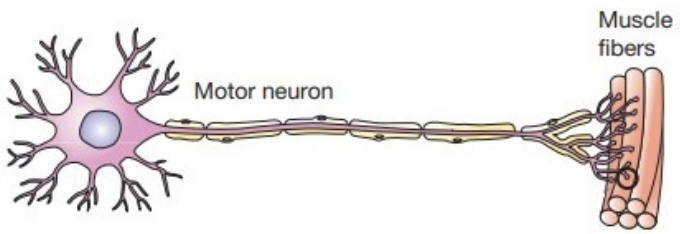

Figure 2.1: Representation of a motor unit.[2]

One muscle is composed of several fascicles, which are formed by hundreds of muscle fibres. Each muscle fibre is covered by connective tissue. Another layer of connective tissue bundles muscle fibres together, creating fascicles. A third sheath of connective tissue, encasing the fascicles together, surrounds the whole muscle. These layers of connective tissue gradually blend together, forming tendons and binding the muscle to its origin and insertion on the bone (Figure 2.2).[3,58]

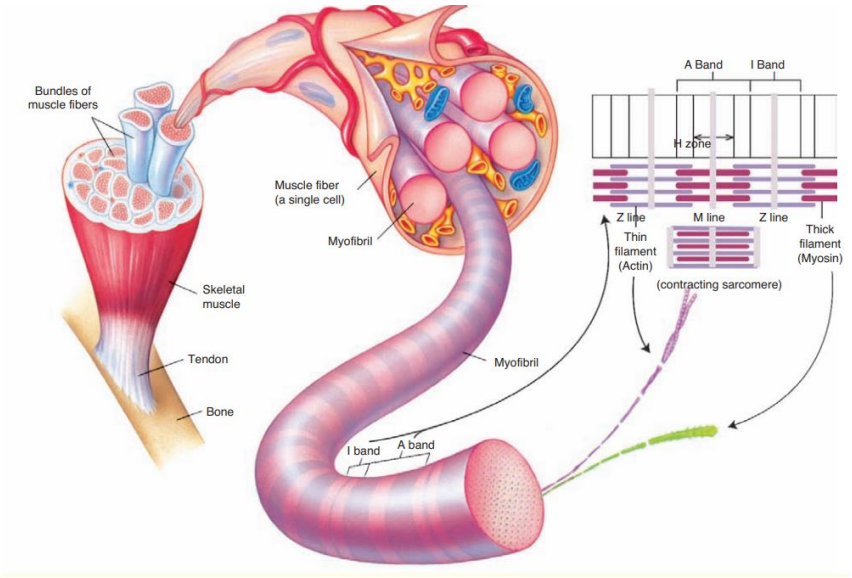

Figure 2.2: Structural organisation of skeletal muscle.[2]

Fascicle arrangement inside a muscle can be classified as parallel or pennate, whether the fibres are aligned with the long axis of the muscle or at a small angle to a tendon running along that axis. Figure 2.3 shows the distinction between the two. Pennation angle of a muscle is related to its capacity to generate force.[3,58]

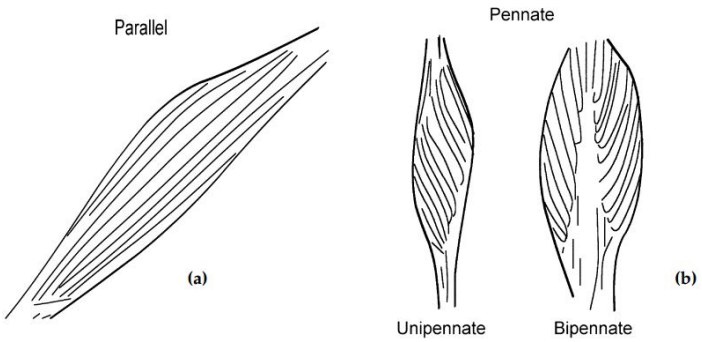

Figure 2.3: Parallel (a) and pennate (b) arrangement of skeletal muscle fascicles according to the muscle's long axis.[3]

The force produced by a muscle is the result of it pulling on its origin and insertion. The interfaces between two or more bones are composed of joints, which allow for movement of one or more bones in relation to an immovable bone. Most joints in the human body are synovial joints, which comprehend a joint capsule, a joint cavity filed with synovial fluid and articular cartilage covering the ends of the bones connected by that joint, as illustrated in Figure 2.4. The synovial fluid allows for lubrication, facilitating the movement of bones. The articular cartilage protects bones from rubbing against each other and helps to absorb impacts.[4,58]

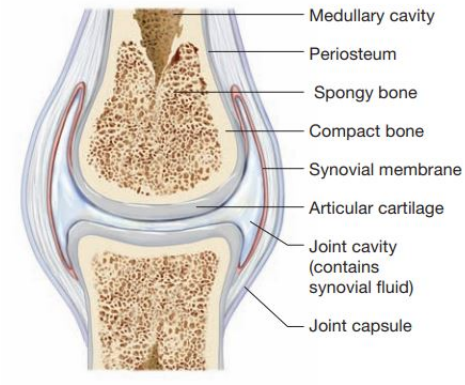

Figure 2.4: Structure of a generalised synovial joint.[4]

The origin of a muscle is located on the immovable bone, whereas its insertion is located on the movable bone, on the other side of the joint, as can be seen in Figure 2.5.[2] By creating tensile force on both its ends, a skeletal muscle pulls on the attached bones, creating movement at the joint.[58] Joint motions can be classified according to the direction of movement. Relative joints angles are measured between the longitudinal axis of the articulating body segments. A decrease in relative joint angle in the sagittal plane is called flexion, and an increase in relative joint angle in the same plane is called extension. Internal and external rotations consist of inward or outward rotations, respectively, of the moving segment in the transverse plane. In the frontal plane, if the moving segment moves towards the midline of the plane, it is called adduction, and the contrary motion, away from the midline of the plane, is called abduction.[2,3,58]

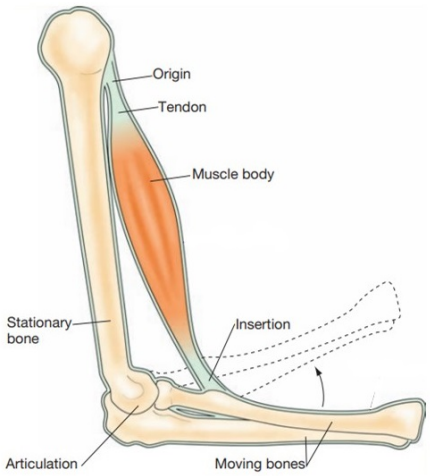

Figure 2.5: Representation of a skeletal muscle's origin and insertion in relation to a joint.[2]

In order to actually produce a controlled motion across a joint, the combined action of different muscles is necessary. Agonist and synergistic muscles are the ones responsible for generating the

desired movement, and do so through their contraction. Antagonist muscles are tasked with slowing down or stopping that movement. Each motion has several agonist and antagonist muscles. Muscle roles also change according to the action to be produced. For instance, agonist muscles in knee flexion behave as antagonists in knee extension. This activation of different muscles is called muscle synergy.[2]

A muscle can produce three types of actions, depending on the force created by the muscles and the forces they must overcome. If a muscle produces a force that is greater than the resistance, the muscle-tendon unit shortens, creating a concentric contraction. If the force generated by the muscle is equal to the resistance, the length of the muscle-tendon unit does not change, creating an isometric contraction. If the force applied to the muscle is greater than the force the muscle is producing, there is a lengthening of the muscle-tendon unit, creating an eccentric contraction.[3,58] Furthermore, the force the muscle-tendon unit exerts on the bones can be of two types, active or passive, depending on the structures it is produced by. The force generated by contraction of the muscle fibres is referred to as active force, which is the greatest contributor to the total muscle force during normal movement. The remaining of the total muscle force is due to the ability of tendons and connective tissues to deform, thus producing passive force.[3,58]

Tendon's main function is to connect and transfer loads between muscle and bone. Human tendons are filamentous structures mainly composed of collagen arranged in a well-defined hierarchical structure. Fibrils of Type-I collagen are bundled together to form fibres, which align together to create fascicles, as is illustrated in Figure 2.6.

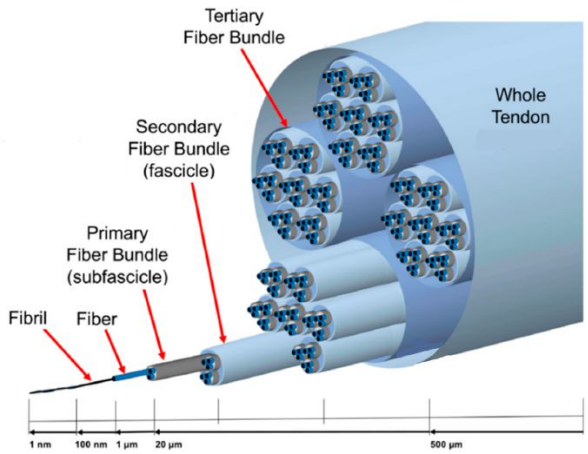

Figure 2.6: Tendon tissue hierarchical structure. Adapted from[5]

Muscle forces depend on several factors, such as number and synchronisation of activated fibres, pennation angle and passive elements.[3] For that reason, understanding and analysing human motion requires modelling of the musculoskeletal system in a way that considers these characteristics and their implications in the production of movement.

The lower limbs are divided into three segments, the thighs, between the hip and the knee joints, the legs, between the knee and the ankle joints, and finally, the feet. As can be seen in Figure 2.7 each limb is composed of thirty bones: femur, patella tibia, fibula, seven tarsal bones, five metatarsal bones and fourteen phalanges.[6]

Figure 2.7: Right lower limb bones and joints: anterior (a) and posterior (b) views.[6]

The hip joint is a spherical joint and therefore allows motion about the three principal axes, as illustrated in Figure 2.8. Flexion and extension happen about the transverse axis, abduction and adduction about the sagittal axis and internal and external rotation about the longitudinal axis.[6]

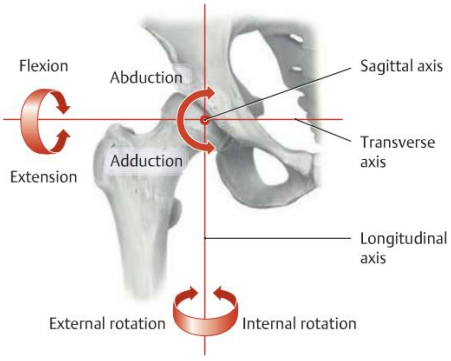

Figure 2.8: Motion of the hip joint.[6]

The knee joint, represented in Figure 2.9, is formed by two individual joints, the tibiofemoral joint

connecting the femur and the tibia and the patellofemoral joint articulating the femur and the patella, which are encapsulated together. The principal motions of the knee joint are flexion and extension and they occur about its transverse axis. Even so, the human knee joint still allows for small degrees of internal and external rotation of the tibia with respect to the femur.[6]

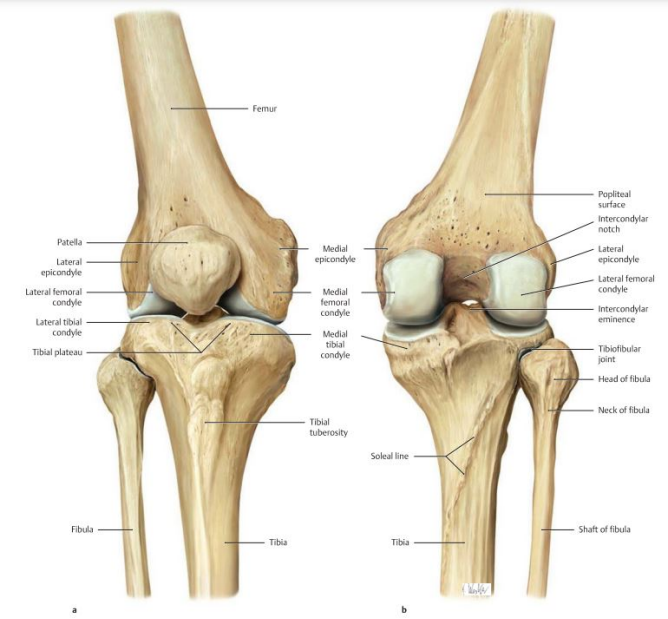

Figure 2.9: Anterior (a) and posterior (b) view of the right knee joint.[6]

The foot is composed of several joints, as illustrated in Figure 2.10, with the most significant for its range of motions being the talocrural joint (ankle joint), the subtalar joint (which articulates the talus with the calcaneus and the navicular bone), the transverse tarsal joint, the tarsometatarsal joints and the metatarsophalangeal joints.[6]

The foot possesses three principal motions, about three different axis, as can be seen in Figure 2.11. Plantar flexion and dorsiflexion occurs about an almost tranversal axis to the malleoli and is the primary motion produced by the ankle joint. The subtalar joint is responsible for the inversion and eversion of the foot, which happens about an oblique upward axis that runs from the lateral calcaneus to the centre of the navicular bone. The transverse tarsal joint, together with the tarsometatarsal joints are responsible for the motions of the foot on the sagittal plane, which are called pronation and supination.[6]

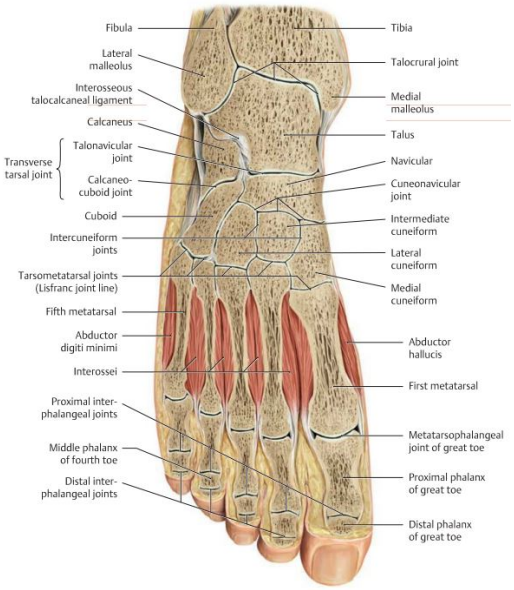

Figure 2.10: Bones and joints of the right foot (Oblique transverse section through the foot).[6]

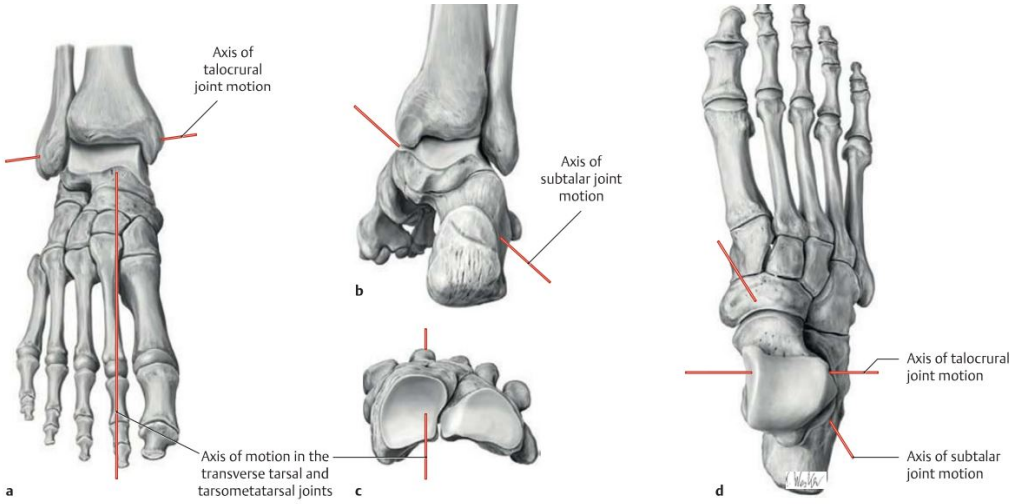

Figure 2.11: Primary axis of motion of the right foot: plantar flexion/dorsiflexion (a,d), pronation/supination (a,c) and inversion/eversion (b,d).[6]

Most muscles that generate the different motions of the hip joint originate in the pelvis and insert on the femur. Since many hip-spanning muscles produce motion across more than one of its movement axes, they cannot be correctly categorised according only to their function. On the other hand, muscles that act on the knee and foot joints are mostly topologically arranged according to their function.[2,6,8] Principal muscles of the lower limb and their respective functions are summarised in Table 2.1. A schematic representation of these muscles' location on the body is provided in Figures 2.12, 2.13 and 2.14.

Table 2.1: Hip, gluteal, thigh, leg and foot muscles and their functions.[6,8]

Hip and Gluteal Muscles	
Muscle	**Function**
Inner Hip	
Psoas	Flex thigh at hip joint
Iliacus	Flex thigh at hip joint
Outer Hip	
Gluteos maximus	Extends, laterally rotates and abducts thigh at hip joint; stabilises hip and knee joints
Gluteos medius	Abducts and medially rotates thight at hip joint; stabilises pelvis
Gluteos minimus	Abducts and medially rotates thigh at hip joint; stabilises pelvis
Tensor fasciae latae	Abducts and medially rotates thigh at hip joint; Stabilises extension of the knee joint
Piriformis	Abducts and laterally rotates thigh at hip joint
Adductor Group	
Adductor brevis	Adducts thigh at hip joint
Adductor longus	Adducts and medially rotates thigh at hip joint
Adductor magnus	Adducts and medially rotates thigh at hip joint
Gracilis	Adducts thigh at hip joint and flexes leg at knee joint
Thigh Muscles	
Muscle	**Function**
Anterior Thigh	
Sartorius	Flexes thigh at hip joint; Extends leg at knee joint
Rectus femoris	Flexes thigh at hip joint; Flexes leg at knee joint
Vastus medialis	Extends leg at knee joint
Vastus lateralis	Extends leg at knee joint
Vastus intermidius	Extends leg at knee joint
Posterior Thigh	
Biceps femoris	Extends and laterally rotates thigh at hip joint; Flexes and laterally rotates leg at knee joint
Semimembranosus	Extends and medially rotates thigh at hip joint; Flexes and medially rotates leg at knee joint
Semitendinosus	Extends and medially rotates thigh at hip joint; Flexes and medially rotates leg at knee joint
Leg Muscles	
Muscle	**Function**
Anterior Compartment	
Tiabilis anterior	Dorsiflexes foot at ankle joint; Inverts foot at subtalar joint
Extensor digitorum longus	Dorsiflexes foot at ankle joint; Extends lateral four toes
Extensor hallucis longus	Dorsiflexes foot at ankle joint; Extends great toe
Posterior Compartment	
Soleus	Plantarflexesd foot at ankle joint
Gatrocnemius	Flexes leg at knee joint; Plantarflexes foot at ankle joint
Tibialis posterior	Plantarflexes foot at ankle joint; Inverts foot at subtalar joint
Flexor digitorum longus	Flexes lateral four toes
Flexor hallucis longus	Flexes great toe
Foot Muscles	
Muscle	**Function**
Dorsal	
Extensor digitorum brevis	Extends lateral four toes at metatarsophalangeal joints
Extensor hallucis brevis	Extends great toe at metatarsophalangeal joint
Plantar	
Abductor hallucis	Abducts and flexes great toe at metatarsophalangeal joint
Abductor digiti minimi	Abducts little toe at metatarsophalangeal joint
Flexor hallucis brevis	Flexes great toe at metatarsophalangeal joint
Flexor digiti minimi	Flexes little toe at metatarsophalangeal joint
Flexor digitorum brevis	Flexes lateral four toes at metatarsophalangeal joints
Adductor hallucis	Adducts and flexes great toe at metatarsophalangeal joint

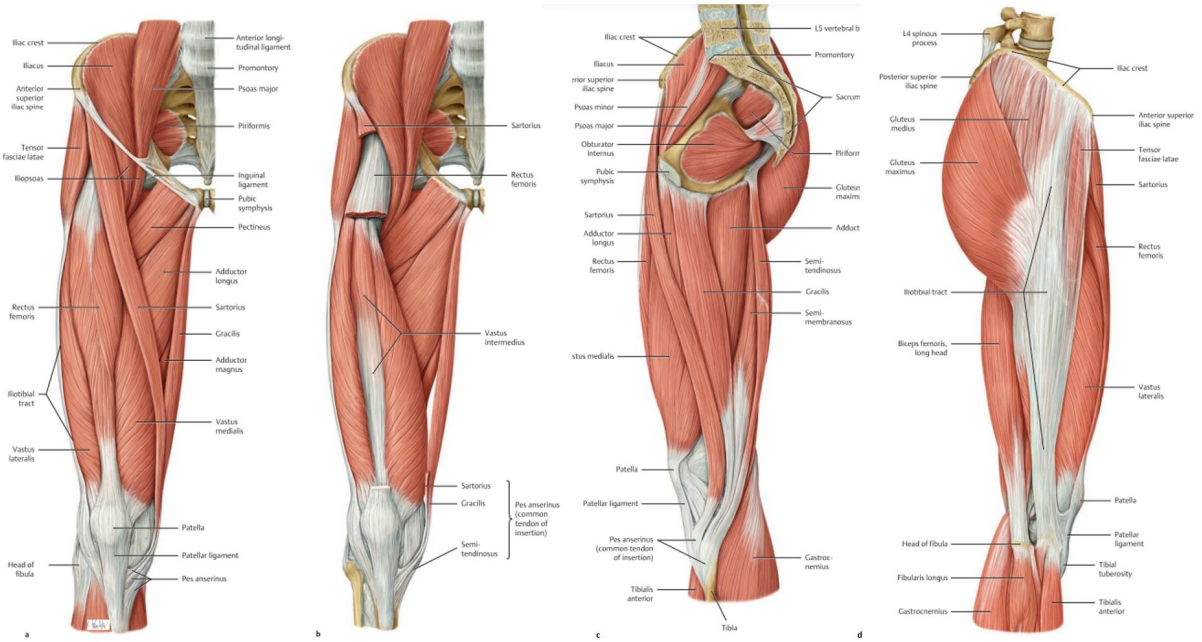

Figure 2.12: Right hip, thigh and gluteal muscles: anterior (a,b), midial (c) and lateral (b) views.

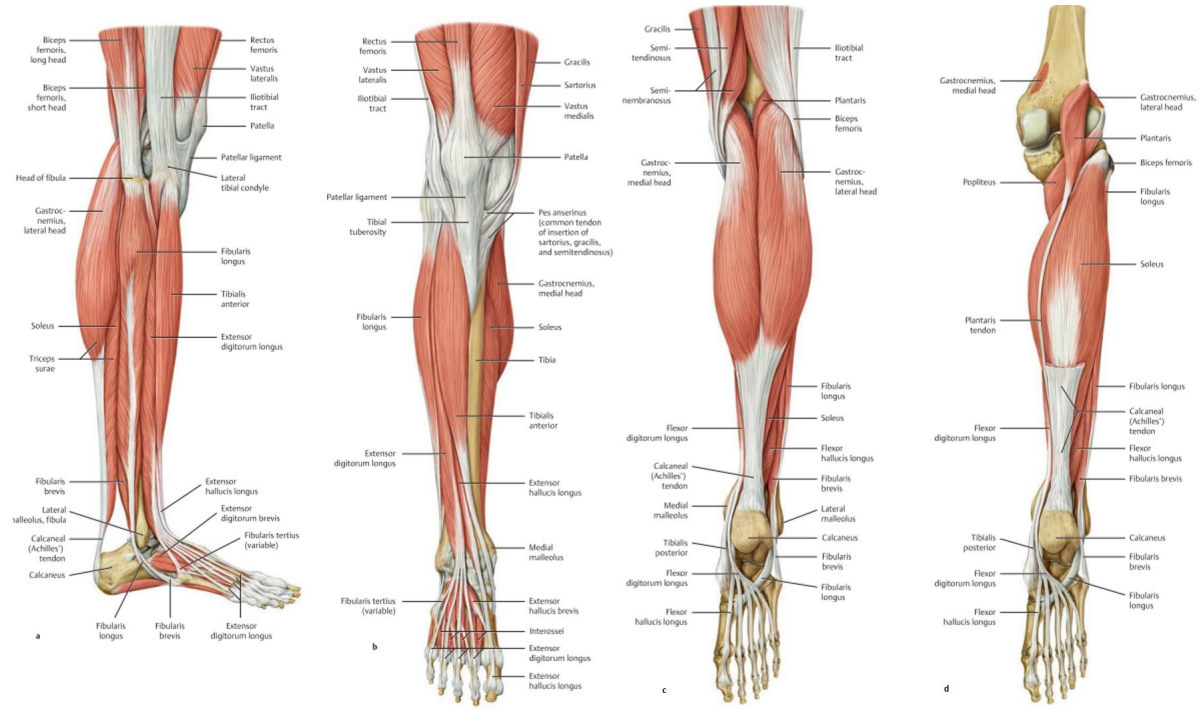

Figure 2.13: Right leg muscles: lateral (a), anterior (b) and posterior (c,d) views.

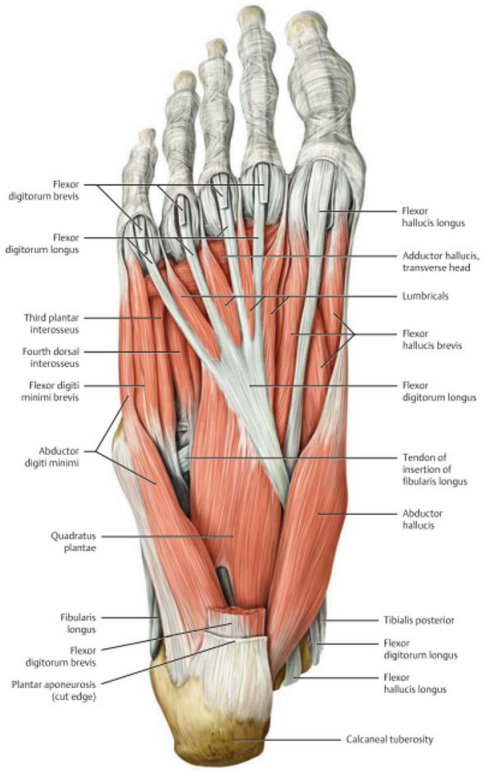

Figure 2.14: Right foot muscles: plantar view.

2.2 Musculoskeletal Modelling and Joint Biomechanics

The strategies used to model human bones and joints, as well as their mechanical behaviour are the focal point of this section. Moreover, it describes the mechanical properties of muscle-tendon units, the dynamics associated with force production and how they are modelled.

The use of a skeletal model makes it possible to render the human body and perform computational analysis in order to study a desired characteristic, in this case, related to how a certain motion is executed. Studies that focus on larger body segments and their movement opt to represent bones as rigid bodies, assuming the deformations resulting from the forces applied to them are negligible.[3] Joints, which connect the body segments in the multi-body system, must be modelled to represent the specificity of human joints, such as their range of motion and the correct definition of their axes of rotation.[47] Musculoskeletal models include actuators that represent the human muscles, allowing for more detailed studies of human motion, which include muscle's activation and force.

Describing a multi-body system requires utilising a set of coordinates that allow for its position, velocity, and acceleration to be defined unequivocally. The most common formulations use cartesian, natural or relative coordinates. This work utilises relative coordinates, which define the position and orientation

of a child body with respect to its parent body.[59]

Biological joints are usually modelled as ideal mechanical joints that represent the kinematic behaviour of the desired joint. For instance, a ball-and-socket joint allows for 3 rotations, but no translations between child and parent body segment, whereas a pin joint only allows for rotation around one of its axes.[59] This makes the ball-and-socket ideal to model the human hip joint and the pin joint to model the ankle joint, for example.[7]

This formulation of joint models allows for the kinematic and dynamic analysis of human movement, including estimation of muscle forces.[47]

The muscle-tendon unit participation on generating a motion, as explained in section 2, can be summarised by the scheme presented in Figure 2.15.

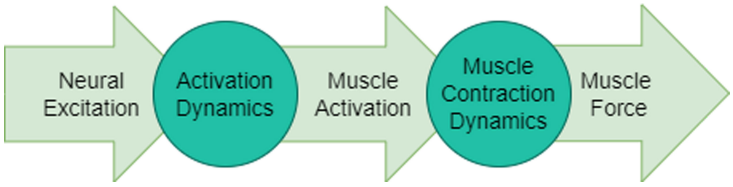

Figure 2.15: Muscle tissue dynamics

The most widely used model to represent muscle behaviour in biomechanical studies is the Hill-type model,[60,61] which is also the one used in this work.[3,47,62] The properties that define this model are activation dynamics, active and passive force-length relationship, force-velocity relationship and tendon's slack length .[7,47,62]

Activation dynamics is the process by which muscle tissue converts the nervous signal into muscle activation.

Following activation dynamics, the muscle needs to transform its activation into muscle force, a process referred to as contraction dynamics. This capability is greatly dependent on muscle length and velocity of contraction.[3,58]

The force-velocity relationship of a muscle describes how its ability to produce force varies according to the velocity of the motion that is being executed. This relationship states that as the shortening speed of muscle increases, its capacity to produce force decreases. In other words, during concentric muscle action, the muscle can produce the most tension when its shortening occurs at the lowest velocity. In the limit case, when the shortening velocity is 0, the contraction becomes isometric. Negative shortening velocities mean that the muscle is performing an eccentric action, elongating its fibres in order to resist force. In this situation, as the speed of lengthening increases (velocity becomes more negative), so does the amount of tension the muscle is able to sustain.[3,58] The force-length curve of a muscle was first described by A. V. Hill in 1949,[61] and takes the shape illustrated in Figure 2.16.

The most important implication of this relation for human movement is the inability to create high

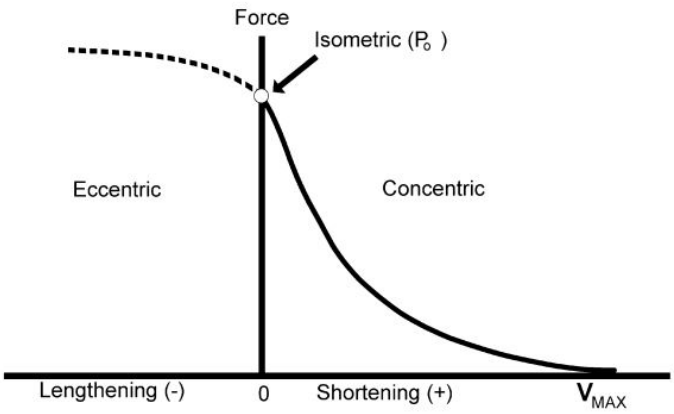

Figure 2.16: Muscle's force-velocity relationship observed *in vitro*.[3]

forces at high shortening speeds, which implies a trade-off between the force needed to execute a certain motion and the speed at which the motion can be performed. However, even though the shape of the curve is always maintained, it is possible to shift it with adequate training. This allows athletes to maximise their muscle capabilities to suit the needs of their sport. Weight training with lighter loads and more, faster, repetitions results in muscle being able to produce higher forces in the region close to their maximum concentric contraction speed, whereas training with higher loads and fewer repetitions increases the force muscles produce at slower contraction speeds.[3] Thus, athletes that undergo specific training will have slightly altered force-velocity curves, as is represented in Figure 2.17.

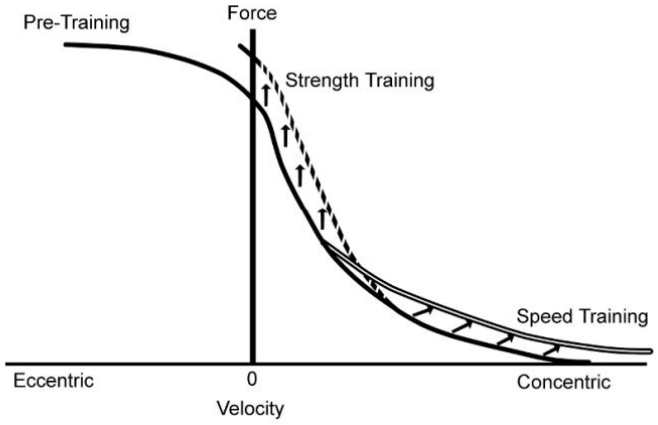

Figure 2.17: Effects of speed and weight training on the force-velocity relationship of muscles.[3]

The actual force a muscle is able to produce in relation to its contraction velocity strongly depends on the type of fibres that constitute it. Muscle fibres can be fast-twitching or slow-twitching, depending on their specific activation and relaxation delays. Human muscles are composed of both types of fibres, but their distribution varies across muscles.[3,58] This introduces differences among muscle's force-velocity

curves. Muscles with a predominance of slow-twitch fibres show greater curvature compared to muscles with a predominance of fast-twitch fibres.[62]

The force-length relationship of a muscle describes the capability of producing force depending on fibre length. As mentioned above, total muscle force is a sum of passive and active force. As such, the curve that describes this relationship is determined by both. The force-length curve for active contractile sources is characterised by reaching peak force near the midpoint of the range of motion, where the fibre length maximises linkage between actin and myosin filaments. This fibre length is referred to as optimal muscle fibre length (L_0). Active muscle has the ability to produce force for fibre lengths that range from 0.5 times to 1.5 times optimal fibre length.[3,62] As fibre length approaches these limits, active force decreases rapidly. Overly stretched or shortened sarcomeres have impaired ability to create links between actin and myosin filaments.[12] For shorter fibre lengths, up to optimal fibre length, passive elements of the muscle-tendon unit do not produce any force. If the fibre stretches over the optimal length, the passive elements start exerting tension. As fibres stretch past that point, the passive force increases exponentially.[3,62] The force-length relationship can be represented as seen in Figure 2.18.

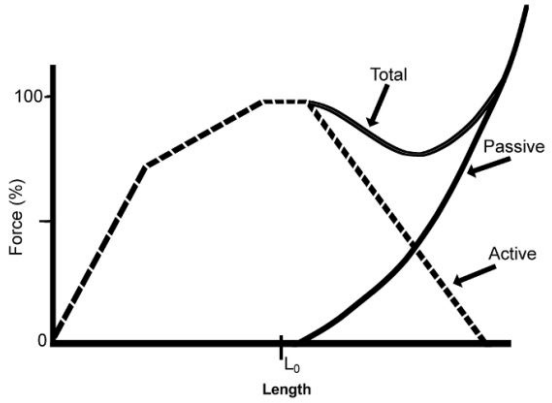

Figure 2.18: Force-length curve of a skeletal muscle.[3]

The Hill-type model is a musculoskeletal model used to represent muscle according to the characteristics explained in this section[60,61] This model is composed of a contractile component and an elastic component connected in parallel with each other, and another elastic component connected in series. The contractile component accounts for the active force produced by the muscle-tendon unit. More specifically, it is responsible for the contraction dynamics of the muscle. The elastic element in series represents the passive force production of tendons, and is rendered as a non-linear spring, in an effort to reproduce the stress-strain behaviour correctly. The elastic element in parallel represents the elasticity of connective tissue and intrinsic components of muscle, which present some resistance to stretching when the muscle is not activated. This model of the muscle-tendon unit is depicted in Figure 2.19.[3,63]

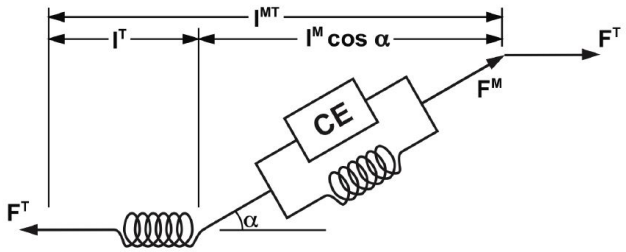

Figure 2.19: Hill-type computational model of muscle-tendon units in equilibrium, where l^{MT} is the length of the Muscle Tendon Unit (MTU), l^{M} is the muscle fibre length, l^{T} is the tendon length, α is the muscle pennation angle, F^{M} is muscle force, F^{T} is tendon force and CE represents the contractile element.[7]

As Figure 2.19 denotes, this musculotendon model relates the tension generated with the lengthening capacity of its elements, as well as the MTU unit as a whole, which in turn is dependent on pennation angle.[63] Muscles with a parallel arrangement of fibres, such as the sartorious, produce less force but allow for a greater range of motion when compared to muscles with a pennate arrangement of the fibres, such as the rectus femoris.[3]

In order to produce a biologically accurate model, the intrinsic characteristics of muscle-tendon units must be taken into account. Depending on the ultimate goal, the level of detail of the model must be adjusted in such a way that it balances computational cost and biological realism.[62] When it comes to modelling the MTU in these types of studies, they must accurately represent the mechanics of each muscle. The strategy for this revolves around utilising a musculotendon actuator model based on dimensionless muscle properties that can be scaled to represent a specific muscle-tendon unit.[7,47,62]

In order to properly model the mechanical properties of different muscles and estimate their active forces, the muscle's optimal fibre length ($l^{M}{}_{0}$), its peak isometric active force ($F^{M}{}_{0}$), maximum shortening velocity (v_{max}) and pennation angle for when the fibres are at optimal length (optimal pennation angle (α_0)) must be known, to enable scaling of the generic curves depicted in Figure 2.20.[7,62]

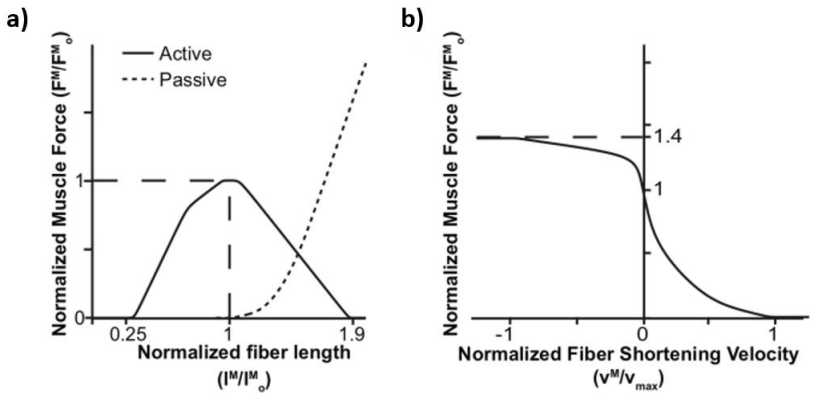

Figure 2.20: Generic force-length (a) and force-velocity (b) curves used to scale muscle actuators' properties in this work. F^{M} is the active muscle's force, l^{M} is the muscle's fiber length and v^{M} is the muscle fibres' shortening velocity.[7]

3

Methodology

Contents

The present chapter describes the framework of the experimental work developed in order to calculate joint angles and moments and estimate muscles' activation and force. It is divided into 3 main sections, Data Acquisition, Data Processing and Data Analysis, which in turn are composed of different subsections, as illustrated in Figure 3.1.

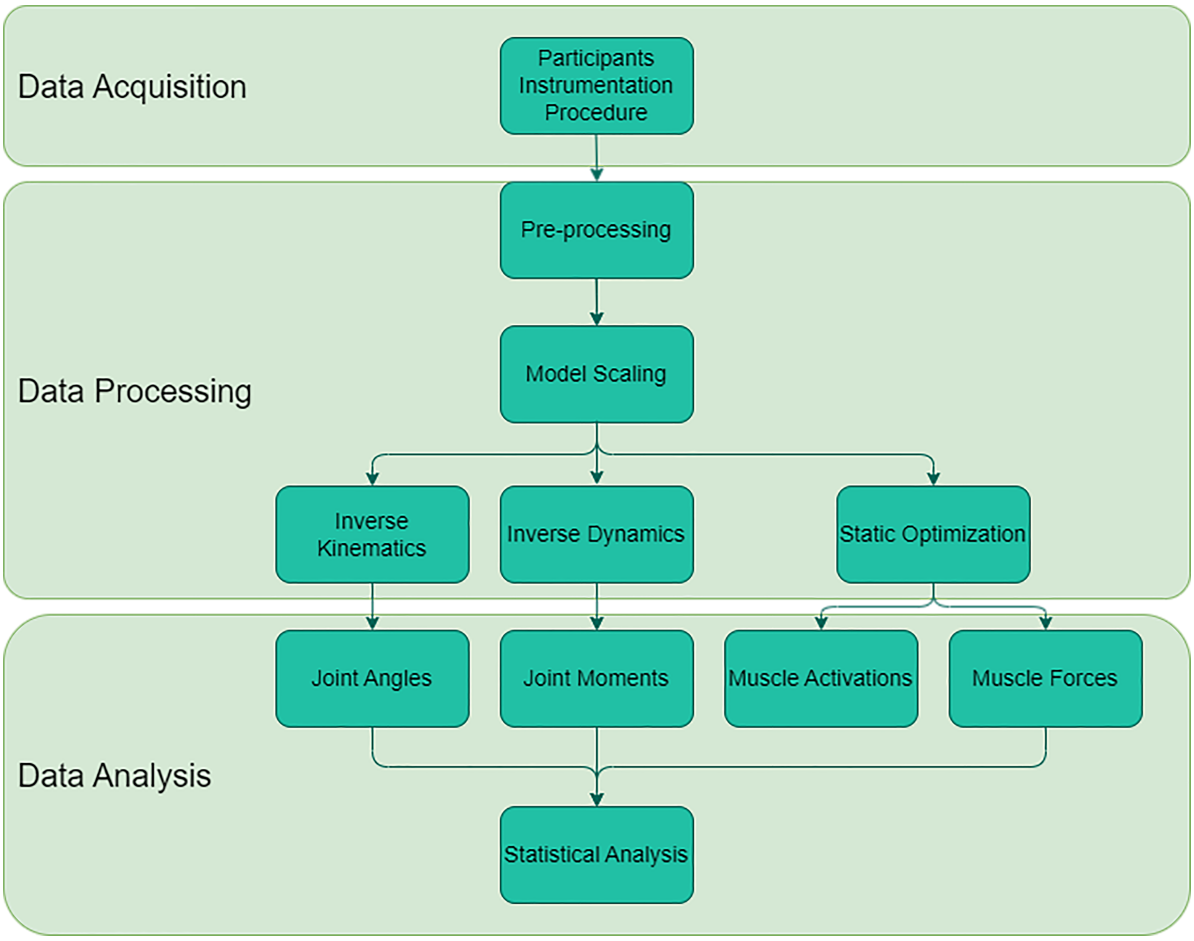

Figure 3.1: Diagram of the experimental work's architecture.

3.1 Data Acquisition

3.1.1 Participants

Eleven healthy female handball players (age: 22 $\pm$ 4 years, height: 1.69 $\pm$ 0.08 m, weight: 67 $\pm$ 12 kg) participated in this study. All subjects were part of the same team, participating in the Portuguese female handball second league. They were all subject to similar training, practicing 3-4 times per week. There were no cases of current or prior musculoskeletal injury that would affect their ability to perform the COD tasks. This work was approved by Instituto Superior Técnico Ethics Comitee (12/2021 CE/IST), and all

participants provided an informed written consent to be included in the work.

3.1.2 Instrumentation

The acquisition of three-dimensional marker data was carried out in the Laboratory of Biomechanics of Lisbon (Instituto Superior Técnico) using a motion capture system Motion Capture (MOCAP) composed of 14 infrared ProReflex 1000 cameras (Qualisys ©, Göteborg, Sweden). GRF were also acquired, by means of 3 force plates (AMTI, OR 6-7-1000 508x464mm, Watertown, MA). The acquisition frequency of the MOCAP system and of the force plates was set to 100 Hz for both.

All subjects wore a sports bra, shorts and their sports shoes. 71 reflective markers were placed on the subjects, as seen in Figure 3.2.[49] 47 markers were affixed to defined anatomical locations throughout the body: 5 on the head (left and right frontal and occipital bones and the top of the head); 6 on the torso (the spinous process of the 7^{th} cervical vertebra, the spinous process of the 8^{th} thoracic vertebra, the mid-point of the clavicles, the xiphoid process and the tip of each acromion); 4 on the pelvis (anterior and posterior superior iliac spines); 12 on the upper limbs (medial and lateral elbow, distal radius and ulna and second and fifth metacarpophalangeal joints of each arm); and 20 on the lower limbs (greater trochanter, medial and lateral femoral epicondyles, medial and lateral malleoli, first and fifth metatarsophalangeal joints, distal phalanx of the first toe, medial phalanx of the second toe and calcaneus of each leg and foot). 24 extra markers were added as clusters on the upper arms, thighs and shins.

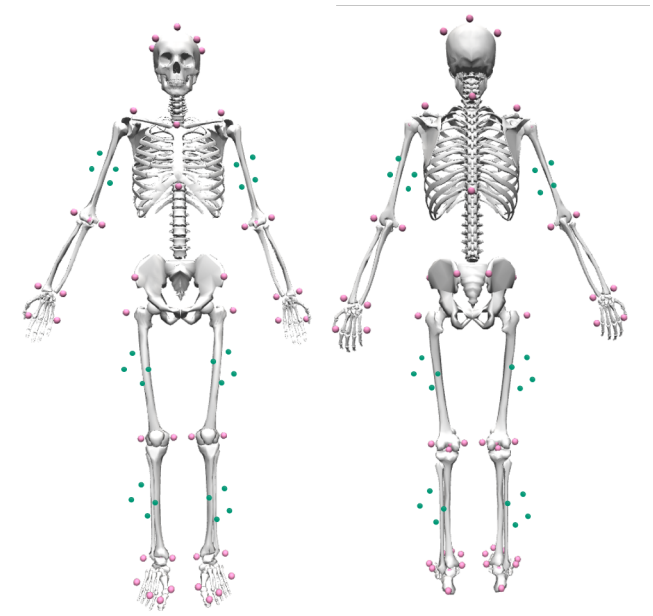

Figure 3.2: Schematic representation of the marker's placement on the body. Anatomical sites are identified with pink dots and clusters with green dots. Image obtained with OpenSim.

3.1.3 Experimental Procedure

Before the acquisition started, the participants were instructed to perform a 5-minute warm-up consisting of running and joint mobility exercises. After that, the subjects were allowed free time to get familiar with the tasks they had to perform, until they felt comfortable with them.

The task design consisted of three CODs, at 45°, 90° and 135° angles. Each COD was performed using both the left and right legs. Subjects were running in place at the start of a 1m line placed on the floor. Upon a signal, they took a small support step and then a second step along that line in order to place the stance foot on the centre of the force plate. Then they changed directions to sprint along another line marked on the floor, at the desired angle. Figure 3.3 illustrates the task design. The participants were asked to execute these manoeuvres with high intensity, since these would be emulating a variety of game-like situations.

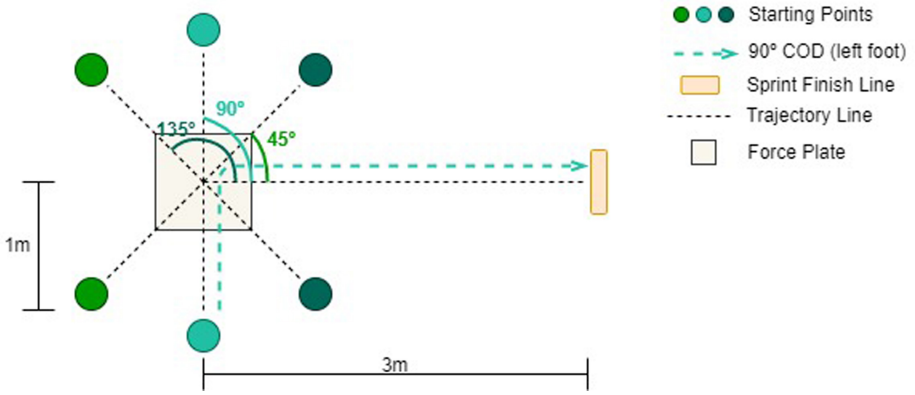

Figure 3.3: Schematic representation of the laboratory setup and the execution of the 90° COD with the left foot.

After calibration of the system and acquisition of a static trial, 5 successful trials were acquired for each COD, making a total of 30 dynamic trials per subject. A successful trial required that the participant completed the COD correctly, following the desired trajectories, with the entire stance foot landing within the force plate. The order by which the subjects performed each COD was randomised in an effort to minimise fatigue and habituation.

Only the stance phase of each COD, which is to say, the time the foot was in contact with the force plate, was analysed. The stance phase starts with the Initial Contact (IC) phase, when the foot first contacts the force plate, which is followed by the Weight Acceptance (WA) and Acceleration phases, and terminates with Toe-off.[57] Figure 3.4 shows the different phases of a COD performed with the described laboratory settings.

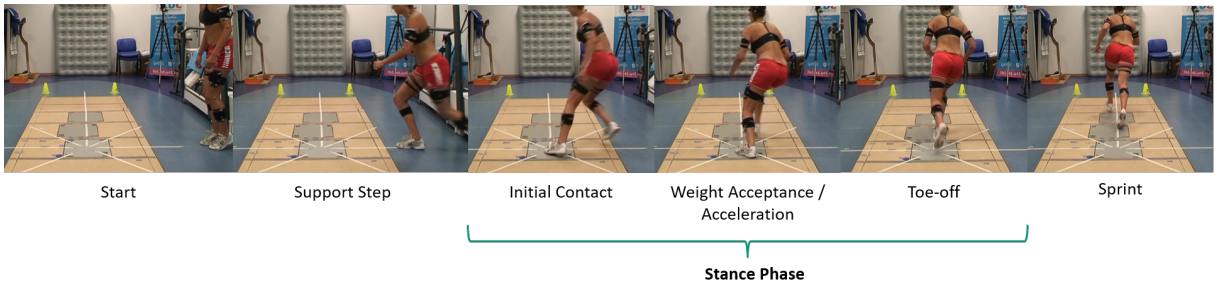

Figure 3.4: Example of the COD phases for the 90° COD executed with the left foot.

3.2 Data Processing

3.2.1 Pre-Processing

All data files were obtained using the Qualisys© software. Markers' trajectories were exported to .c3d files and then converted to .trc files using the C3D Tools software[64] for all static and dynamic COD trials. External forces' files were exported as .tsv files. A series of pre-processing steps was executed in MATLAB to produce the data files required by OpenSim to perform the kinematic and dynamic analysis. Firstly, markers' trajectories that were incomplete or incorrect (due to acquisition errors) were reconstructed from the trajectories of clusters' markers, using the relationships between markers calculated from the static acquisition files. These files were also used to calculate the coordinates of the joint centres of the hips and shoulders. This was done based on the regression models proposed by Hara et al. (2016)[65] and Campbell et al. (2009),[66] respectively. Both .trc and .tsv files were then filtered using low-pass Butterworth filters with cut-off frequencies calculated through residual analysis, as proposed by Winter (2009).[67] After that, all files were transformed to be in the OpenSim global reference frame. Finally, external forces' files were treated to eliminate residual forces from the time frames where there was no foot contact with the force plate and were exported as .mot files. These .mot files are the input files containing GRFs OpenSim uses to execute its Static Optimization (SO) analysis.

3.2.2 Musculoskeletal model

The general musculoskeletal model used in this work was developed by Rajagopal et al. (2016)[7] and consists of 22 articulating rigid bodies actuated by 80 massless MTU actuators (40 in each leg) and 17 ideal torque actuators (upper body), resulting in 35 Degrees of Freedom (DOF)s. Joint geometries and their corresponding DOFs are summarised in Table 3.1. The reference frames for joint origins and DOFs of the most relevant joints for this work are presented in Figure 3.5.

The generic MTU actuators and the parameters used to define them are described in Table 3.2. Their geometry and placement are also shown in Figure 3.5.

Table 3.1: Joint Geometry and DOFs. Wrist flexion and deviation, ankle inversion and toe flexion DOFs are locked to ensure a proper representation of the desired motion.[7]

Joint Name	Rigid Bodies	Geometry	DOF Name	Range of Motion (degrees)
Lumbar	Head and Torso with Pelvis	Ball-and-socket joint	Lumbar Extension	-90° to 90°
			Lumbar Bending	-90° to 90°
			Lumbar Rotation	-90° to 90°
Shoulder	Humerus with Torso	Ball-and-socket joint	Arm Flexion	-90° to 90°
			Arm Adduction	-120° to 90°
			Arm Rotation	-90° to 90°
Elbow	Ulna with Humerus	Pin joint	Elbow Flexion	0° to 150°
Wrist	Ulna with Radius	Pin joint	Forearm Pronation	0° to 90°
	Hand with Radius	Universal joint	Wrist Flexion	locked
			Wrist Deviation	locked
Pelvis	Pelvis with Ground	Custom 3DOF joint	Pelvis Tilt	-90° to 90°
			Pelvis List	-90° to 90°
			Pelvis Rotation	-90° to 90°
Hip	Femur with Pelvis	Ball-and-socket joint	Hip Flexion	-30° to 120°
			Hip Adduction	-50° to 30°
			Hip Rotation	-40° to 40°
Knee	Tibia with Femur	Custom 1DOF joint	Knee Flexion	0° to 120°
Ankle	Talus with Tibia	Pin joint	Ankle Dorsiflexion	-40° to 30°
Subtalar	Calcaneus with Talus	Pin joint	Ankle Inversion	locked
Metatarsophalangeal	Toes with Calcaneus	Pin joint	Toe Flexion	locked

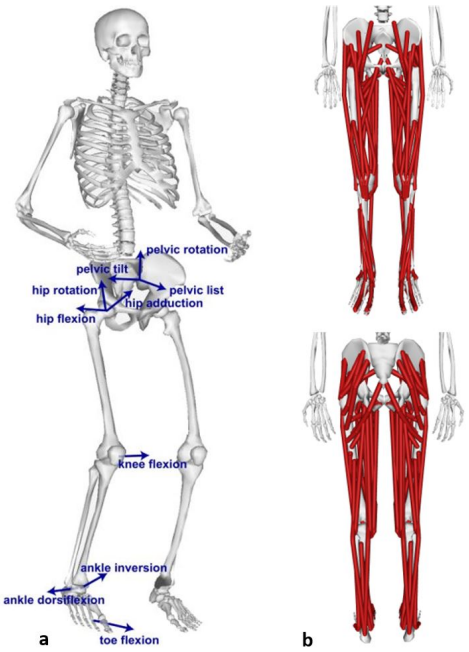

Figure 3.5: Representation of the rigid bodies and DOFs in the model, labeled for the right limb (a) and the MTU actuators of the model's lower limbs (b).[7] Image obtained with OpenSim.

Table 3.2: MTUs' parameters.[7]

Muscle	Optimal force (N)	Optimal fiber length (cm)	Pennation angle (°)
Adductor brevis	626	10.3	6.6
Adductor longus	917	10.8	7.9
Adductor magnus (distal)	597	17.7	11.2
Adductor magnus (ischial)	597	15.6	9.6
Adductor magnus (middle)	597	13.8	11.9
Adductor magnus (proximal)	597	10.6	17.8
Biceps femoris long head	1313	9.8	10.1
Biceps femoris short head	557	11.0	15.1
Extensor digitorum longus	603	6.9	12.5
Extensor hallucis longus	286	7.5	11.3
Flexor digitorum longus	423	4.5	12.9
Flexor hallucis longus	908	5.3	14.8
Gastrocnemius lateral head	1575	5.9	12.0
Gastrocnemius medial head	3116	5.1	9.5
Gluteus maximus (superior)	984	14.7	20.3
Gluteus maximus (middle)	1406	15.7	21.0
Gluteus maximus (inferior)	948	16.7	21.9
Gluteus medius (anterior)	1093	7.3	18.1
Gluteus medius (middle)	765	7.3	18.1
Gluteus medius (posterior)	871	7.3	18.1
Gluteus minimus (anterior)	374	6.8	10.0
Gluteus minimus (middle)	395	5.6	0.0
Gluteus minimus (posterior)	447	3.8	1.0
Gracilis	281	22.8	9.9
Iliacus	1021	10.7	16.0
Peroneus brevis	521	4.5	11.8
Peroneus longus	1115	5.1	14.2
Piriformis	1030	2.6	10.0
Psoas	1427	11.7	12.3
Rectus femoris	2192	7.6	12.4
Sartorius	249	40.3	1.5
Semimembranosus	2201	6.9	14.6
Semitendinosus	591	19.3	13.8
Soleus	6195	4.4	21.9
Tensor fascia latae	411	9.5	3.0
Tibialis anterior	1227	6.8	11.2
Tibialis posterior	1730	3.8	13.0
Vastus intermedius	1697	9.9	3.6
Vastus lateralis	5149	9.9	14.5
Vastus medialis	2748	9.7	24.2

To improve the accuracy of the multi-body simulations, the generic model used was scaled to match the anthropometric data of each subject using the Scale Tool of OpenSim. The scale factors are calculated as the ratio of the distance between pairs of markers on the static trial file and the distance between the same pairs of markers on the model, in the default body position. Then, the scale factors obtained from these measurements are used to scale joint frame locations, centre of mass location, force appli-

cation points, and muscle attachment points in each body segment. The mass of all body segments is also scaled by the scale factor calculated for each segment. The subject's input mass is divided by the sum of the masses of all scaled body segments. This provides a second scale factor for the mass of all body segments, used to ensure preservation of the mass distribution and making sure the mass of the model corresponds to the mass of the subject. Scaling the length-dependent components of MTUs is done by computing the ratio between the length before scaling and the length after scaling, maintaining the configuration and proportions of the MTUs. Lastly, the markers position on the model is moved to match the markers locations of the inputted static trial.[46]

3.2.3 Inverse Kinematics

A kinematic study comprises the characterisation of the position and trajectory of a system and the motions it is performing without considering the forces that generate them. Kinematic variables can be either linear or angular displacements, velocities, and accelerations.[67] Inverse Kinematics (IK) is a method that allows the determination of these variables during the movement of a body's segments.

IK requires displacement data, acquired for several anatomical landmarks, such as anatomical prominences, ends of limb segments, in order to obtain the position of a number of fixed elements of the system, throughout the movement.[67]

In this case, the IK tool in OpenSim was used to calculate joint angles and translations during the execution of the CODs. It works by forcing the model, respecting its joint's DOFs, to assume the position that better corresponds to the experimental marker coordinates obtained from the motion capture system, at each time frame. This is achieved by solving of a weighted least squares problem (see Equation 3.1) The objective is to find the vector of generalised coordinates,$\mathbf{q}$, that minimises the distance between the experimental marker's position and the position of the marker on the model (marker error), as well as the difference between the experimental coordinate values (i.e. joint angles calculated outside OpenSim) and the coordinate values estimated by the IK (coordinate errors).[46] Since no experimental coordinate values were inputted to OpenSim, the cost function used in IK was as follows:

$$f = \sum_{i=0}^{markers} \omega_i \left\| \left(x_i^{subjet} - x(q)_i^{model} \right) \right\|^2 \tag{3.1}$$

where q is the vector of generalised coordinates, ω_i is the weight factor and $x_i^{subject}$ and x_i^{model} are the three-dimensional positions of the i^{th} marker for the subject and model, respectively.[46] The weight factors indicate how strongly the error term of a specific marker must be minimised. For this work, weight factors were the same as those used by Rajagopal et al. (2016) in their running simulations.[7]

IK produces a motion file containing the generalised coordinate trajectories, which include joint angles, for each time frame of the analysed motion.

3.2.4 Inverse Dynamics

A dynamic analysis studies the motions as a result of the external forces applied to the system and the inertial characteristics of its elements. Inverse Dynamics (ID) is the process by which it is possible to calculate the internal forces that produce a certain movement, by systematically solving the Equations of Motion (EoM) of a system. In order to do that, anthropometric measurements, mass, inertia and location of the centre of mass must be known for every segment of the system. The kinematic variables are also necessary for this process. The EoM that describe a motion can be written as follows:

$$\mathbf{M}(\mathbf{q})\ddot{\mathbf{q}} + \mathbf{C}(\mathbf{q}, \dot{\mathbf{q}}) + \mathbf{G}(\mathbf{q}) = \tau \tag{3.2}$$

where $\mathbf{q}, \dot{\mathbf{q}}, \ddot{\mathbf{q}} \in \mathbb{R}^N$ are the vectors of generalised positions, velocities and accelerations, respectively, $\mathbf{M}(\mathbf{q}) \in \mathbb{R}^{N \times N}$ is the system mass matrix, $\mathbf{C}(\mathbf{q}, \dot{\mathbf{q}}) \in \mathbb{R}^N$ is the vector of Coriolis and centrifugal forces, $\mathbf{G}(\mathbf{q}) \in \mathbb{R}^N$ is the vector of gravitational forces and $\tau \in \mathbb{R}^N$ is the vector of generalised forces, with N representing the total number of DOFs in the system.[46]

After conducting IK, generalised positions, velocities and accelerations are fully determined. Calculating the remainder of parameters on the left side of equation 3.2 requires knowledge of the external forces resulting from the movement of the system, which can be obtained through experimental acquisition using force plates. Once all these variables are fully known, it is possible to solve the EoM for the unknown generalised forces vector τ. This allows the calculation of the joint net forces and moments that generate the motion that is being analysed.[46]

Utilising the ID tool in OpenSim results in a file that, for every time frame, contains the net joint forces and torques, acting along each coordinate axis, that generate the accelerations calculated from experimentally measured motion and external forces.

Before performing ID, given that the velocities and accelerations are calculated through differentiation, the generalised coordinate file resulting from IK was low-pass filtered in OpenSim with a cut-off frequency of 6Hz.[7,12,49]

3.2.5 Muscle Force Estimation

The SO tool is an extension of the ID tool used to estimate individual muscle forces acting on the system to produce its motion. It does so by decomposing the net joint forces and torques into individual muscle forces, while taking into account force-length-velocity properties of the MTU actuators (Equation 3.3).

$$\sum_{m=1}^{n} \left[a_m f(F_m^0, l_m, v_m) \right] r_{m,j} = \tau_j \tag{3.3}$$

where n is the number of MTUs in the model, a_m is the activation of the m^{th} muscle at a given time

step, F^0_m, l_m and v_m are its maximum isometric force, length and shortening velocity, respectively, $f(F^0_m, l_m, v_m)$ is its force-length-velocity surface, $r_{m,j}$ is its moment arm about the j^{th} joint axis and τ_j is the generalised force acting about that joint axis.

This generates an under-determined system of equations, as there are more unknowns than the number of DOFs in the model, which results in an infinite number of solutions. This optimisation strategy surpasses this problem by finding the solution that minimises a specific objective function. In this work, the SO was instructed to solve the EoM for the generalised forces while minimising the squared sum of their activations (Equation 3.4).

$$J = \sum_{m=1}^{n} (a_m)^2 \tag{3.4}$$

SO does not take activation dynamics into account. Furthermore, it also assumes tendon to be rigid, meaning their passive force production does not depend on the stress-strain relationship of actual tendons.

This process, which is summarised by the schematics presented in Figure 3.6, is repeated independently for each time-step of the analysed motion.

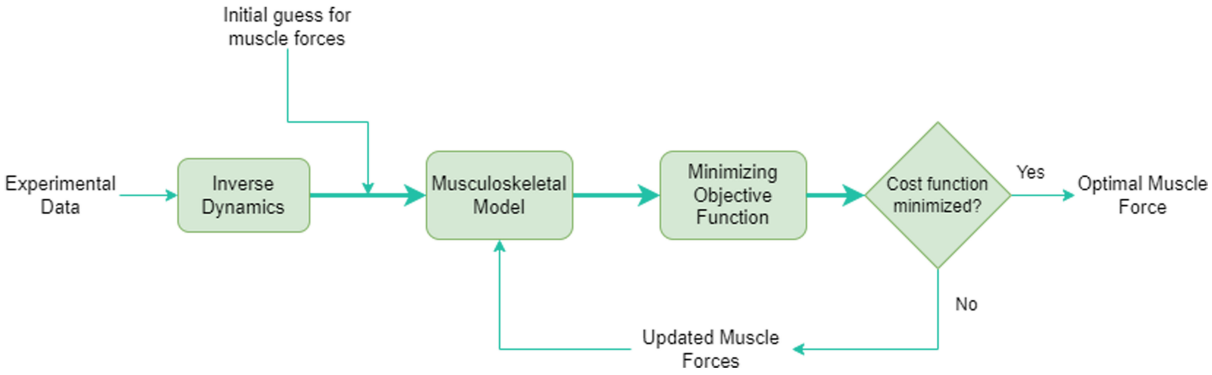

Figure 3.6: Schematic representation of the Static Optimisation process [7]

SO produces files containing the muscles' activation and force for every time frame.

In order to ensure convergence of the algorithm and reliable results, 2 additional tasks must be performed before SO. Just like in ID, the generalised coordinates were low-pass filtered with a cut-off frequency of 6Hz.[7,12,49] Furthermore, reserve actuators were added to the model at this point, in an effort to make up for residual forces that result from inconsistencies between the motion that was modelled and the experimental external forces, as well as from the musculoskeletal properties of the model not completely matching those of the subjects. For this work, the reserve actuators added and their optimal force were defined according to the running simulations of Rajagopal et al.(2016), and are specified in Table 3.3.

Table 3.3: Reserve actuators' names, types, bodies or translations they drive and their maximum generalised force.[7]

Name	Body/Coordinate	Maximum Force/Moment (N/Nm)
FX	Pelvis	10
FY	Pelvis	10
FZ	Pelvis	10
MX	Pelvis - Ground	15
MY	Pelvis - Ground	15
MZ	Pelvis - Ground	15
Hip Flexion	Hip flexion	2.5
Hip Adduction	Hip adduction	5
Hip Rotation	Hip rotation	10
Knee Angle	Knee angle	1
Ankle Angle	Ankle angle	1

3.3 Statistical Analysis

After obtaining the outcomes from IK, ID and SO, for every trial of the 11 subjects, the output files of interest were post-treated in Matlab. All results were low-pass filtered, using a Butterworth filter with a cut-off frequency defined through Residual Analysis. They were normalised in the time-domain and ploted in terms of percentage of COD completion, so that 0% corresponds to the first instant of contact with the force plate and 100% to the last. Joint moments and muscle forces were also normalised by the mass of the subjects.

For each subject, results were computed as an average of all successful trials. For some subjects, available trials were less than 5 due to acquisition issues. The most common issues that led to trial dismissal were the subject not placing the entirety of the stance foot on the force plate and loss of marker information (due to falling or interference) that could not be reconstructed. The mean of the 11 subjects' individual averages was computed and plotted, together with the corresponding standard deviation, for every variable of interest: joint angles, joint moments, muscle activations and muscle forces.

SPM was used to assess inter-limb differences between the total average results on the 3 COD angles.[55,57] It was also implemented to statistically compare the total average results across the different COD angles, in order to investigate angle dependence of the variables of interest.[53] SPM allows to conduct t-test statistics analysis on continuous data, producing statistical results that are also continuous.[31,68,69] By performing topological inference over the full data field utilising Random Field Theory (RFT),[70] it investigates the statistical significance of events based on the size and height of supra-threshold clusters, which are clusters of statistics (e.g. t) that cross a critical threshold (t^*).[68] In this case, 2-tailed paired t-tests were used to compare pairs of results, and the null-hypothesis corresponds to no difference between these results. The defined statistical significance of $\alpha = 0.05$ signifies that for every instant the SPM produces a t value that surpasses the critical threshold, t^*, the null-hypothesis is

rejected with a confidence level of 95%. SPM produces p-values across the full time-series, indicating the probability of the supra-threshold cluster being as large (in the time domain) as the observed cluster in the statistical test.[68,71] Specific portions of COD execution can be identified as being significantly different depending on limb or COD angle. SPM analysis was performed using the open-source Matlab package *spm1d* (spm1d.org, ©T. Pataky).

In an effort to quantify the differences between these specific portions, the mean Effect Size (ES) was calculated for those time sections. ES, based on Cohens' D, is a measure of difference in terms of standard deviations.[57,72]

4

Results

Contents

The focal point of this chapter is the presentation of the results obtained from the processes described in Chapter 3. The joint angles and moments studied are those regarding hip flexion-extension, hip abduction-adduction, hip medial-lateral rotation, knee flexion-extension, and ankle flexion-extension. The muscles analysed here are the primary muscles that are responsible for those joint motions. The IK and ID outcomes are shown as the total average and standard deviations. SPM outcomes comparing joint angles, moments and muscle forces between the 3 COD tasks are also presented here. All results are presented in terms of percentage of completion of the stance phase of the COD. The first 10% of the movement correspond to IC. From that mark to around the 50% mark, it is considered to correspond to the WA phase. From there until the 90% mark, it corresponds to the Acceleration phase, and from the 90% mark to 100% completion it is considered to be the Toe-off phase.

4.1 Differences between COD angles

A direct biomechanical analysis of the average joint kinematics and dynamics allows to better understand the outcomes of the SPM studies. The significant differences in joint kinematics and dynamics between COD are presented together with the corresponding IK, ID and SO results. This section only contains result plots corresponding to the analysis of the dominant limb. The plots corresponding to IK, ID and SO results for the non-dominant limb are shown in Appendix A.

4.1.1 Kinematic Analysis

The IK strategy allowed for the calculation of the joint angles during the execution of the CODs. The variables of interest are hip flexion, hip adduction, hip rotation, knee flexion and ankle flexion angles of the stance leg. This technique also provided the assessment of the execution velocity of each COD, represented by the velocity of the Centre of Mass (CM) of each subject. The individual average velocities for the subjects executing the 3 CODs are presented in Figure 4.1.

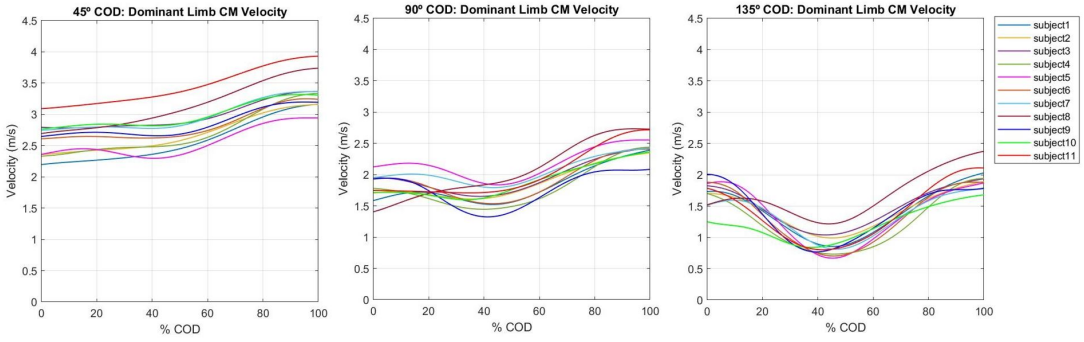

Figure 4.1: Individual average CM Velocities, in $\mathrm{m/s}$, in terms of percentage of completion of the stance phase of the COD.

The velocity profiles are similar for all subjects, and the sharper the COD angle, the lower and less linear the velocity. For the 45° COD, almost no deceleration is visible, whereas for the 135° COD, a clear deceleration is observed until the velocity reaches values close to $0.9\mathrm{m}/s$ around the 45% mark of COD completion. Moreover, the velocity at Toe-off averages around $3.4\mathrm{m}/s$ for the 45° COD, $2.5\mathrm{m}/s$ for the 90° and only $2.0\mathrm{m}/s$ for the 135°.

Regarding hip joint movement, the results from IK are shown in Figure 4.2 and SPM results for the comparison of joint kinematics between the different COD angles are presented in Figure 4.3.

The flexion patterns of the hip joint show some differences according to the COD angle. The largest flexion angles are verified for IC of the 45° COD, after which there is a continuous extension of the joint until Toe-off. For the 90° COD, some subjects continue this movement pattern, whereas most subjects show more hip flexion between during the WA phase, and only then begin extending the joint. This behaviour is associated with braking during the WA phase (as shown by the velocity profiles) and is more noticeable for the 135° COD. A slight flexion movement is present at Toe-off of the 135° COD, indicating these subjects are using hip flexion to accelerate the manoeuvre.

Regarding hip motion in the frontal plane, although the general shape of the curve is maintained, the adduction / abduction angles change considerably with COD angle. Overall, sharper angles involve larger hip abduction angles throughout the entire movement. Even so, the end of the WA phase is associated with a local minima of hip abduction, whereas Acceleration shows maximum hip abduction for all CODs. The sharper the COD, the sooner these peaks present.

The results for the hip rotation angle show a general increase in internal rotation after IC and then an increase of external rotation until Toe-off. Sharper CODs present steeper increases in hip external rotation. This culminates with the greatest external rotation angles, verified for the 135° COD Toe-off. The standard deviation in these results shows that even though the tendencies are the same, some trials were executed with a mostly externally rotated hip while others with a mostly internally rotated hip.

For the hip joint, differences in joint motion are more significant between the 45° and both other COD angles. Even so, DOFs of the hip joint are affected differently by the variation of COD angle. Differences for hip flexion are focused towards IC and the beginning of WA, where flexion angles become smaller with the increase in COD angle. For hip rotation, an increase in COD angles implies larger external rotation towards the end of Acceleration and Toe-off. Hip adduction is considerably different for the 45° throughout the entire movement. Hip abduction is significantly larger for the 90° and 135° CODs. It is even larger during the IC phase of the 135° COD. These results also show that for most of the movement, the hip joint behaves similarly for 90° and 135° CODs, as ESs are smaller than for the other comparisons. The ESs calculated for the hip joint are negative, which signifies that in the regions of significant difference, hip angles defined as positive become smaller and hip angles defined as negative become larger as COD angle increases, for all DOFs.

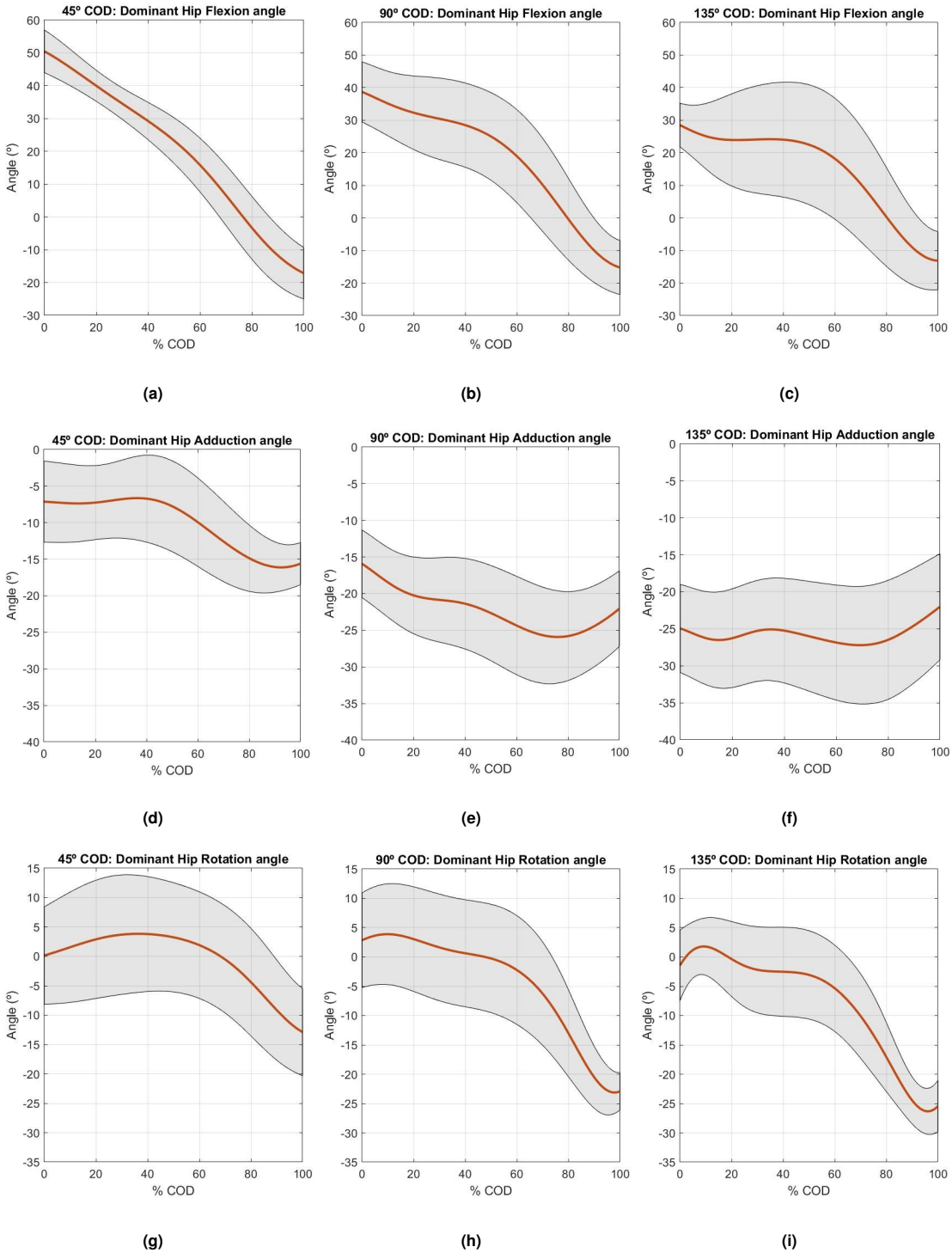

Figure 4.2: Total average (orange) and standard deviation (shaded area) for the hip joint flexion angle. Dominant hip flexion/extension angle (+flexion) for the 45° COD (a), 90° COD (b) and 135° COD (c). Dominant hip adduction/abduction angle (+adduction) for the 45° COD (d), 90° COD (e) and 135° COD (f). Dominant hip internal/external rotation angle (+internal) for the 45° COD (g), 90° COD (h) and 135° COD (i). In degrees, in terms of percentage of completion of the stance phase of the COD.

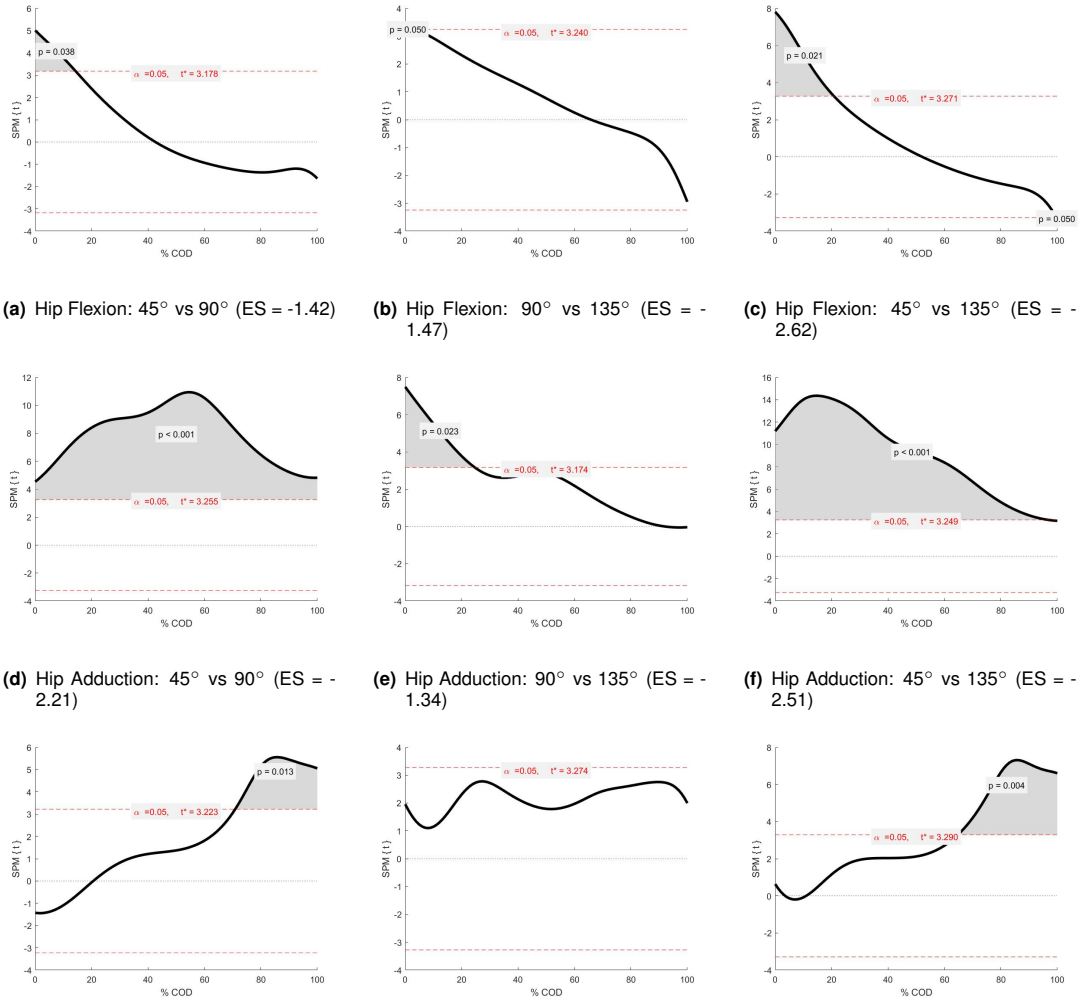

(a) Hip Flexion: 45° vs 90° (ES = -1.42)

(b) Hip Flexion: 90° vs 135° (ES = -1.47)

(c) Hip Flexion: 45° vs 135° (ES = -2.62)

(d) Hip Adduction: 45° vs 90° (ES = -2.21)

(e) Hip Adduction: 90° vs 135° (ES = -1.34)

(f) Hip Adduction: 45° vs 135° (ES = -2.51)

(g) Hip Rotation: 45° vs 90° (ES = -1.33)

(h) Hip Rotation: 90° vs 135°

(i) Hip Rotation: 45° vs 135° (ES = -1.71)

Figure 4.3: SPMt (black line) of a 2-tailed t-test between: hip joint flexion angles of the 45° and 90° CODs (a), hip joint flexion angles of the 90° and 135° CODs (b), hip joint flexion angles of the 45° and 135° CODs (c); hip joint adduction angles of the 45° and 90° CODs (d), hip joint adduction angles of the 90° and 135° CODs (e), hip joint adduction angles of the 45° and 135° CODs (f); hip joint rotation angles of the 45° and 90° CODs (g), hip joint rotation angles of the 90° and 135° CODs (h), hip joint rotation angles of the 45° and 135° CODs (i). In terms of percentage of completion of the stance phase of the COD. Critical threshold (red lines), t^*, at significance ($\alpha = 0.05$), supra-threshold cluster region (shaded area) and corresponding p-value.

IK results for the knee and ankle joints are presented in Figure 4.4 and the corresponding SPM results are shown in Figure 4.5.

The average result for the 45° COD presents an increase in knee flexion until around the 50% mark and then a decrease until around 90% completion, which indicates the end of the Acceleration phase, where the knee is more extended than at the start. A slight knee flexion can be observed after that point. The 90° and 135° CODs mostly show the same pattern.

As the COD angles get sharper, knee flexion at IC become smaller, whereas knee flexion at Toe-off remains the same. Sharper CODs possess larger peak flexion angles. The greatest knee flexion angles occur around the 50% mark of the 135° COD, which coincides with the end of the WA portion of stance phase.

The ankle joint's movement has a similar behaviour to the knee. For the 45° CODs, most subjects start with a slight dorsiflexion of the ankle, which increases until the 60% mark and then decreases until maximum plantarflexion is reached at Toe-off. As COD angles become sharper, IC dorsiflexion angle becomes smaller, even changing to plantarflexion instead. Moreover, larger ankle dorsiflexion angles are achieved sooner for the sharper CODs, and are maintained across a larger portion of the task completion.

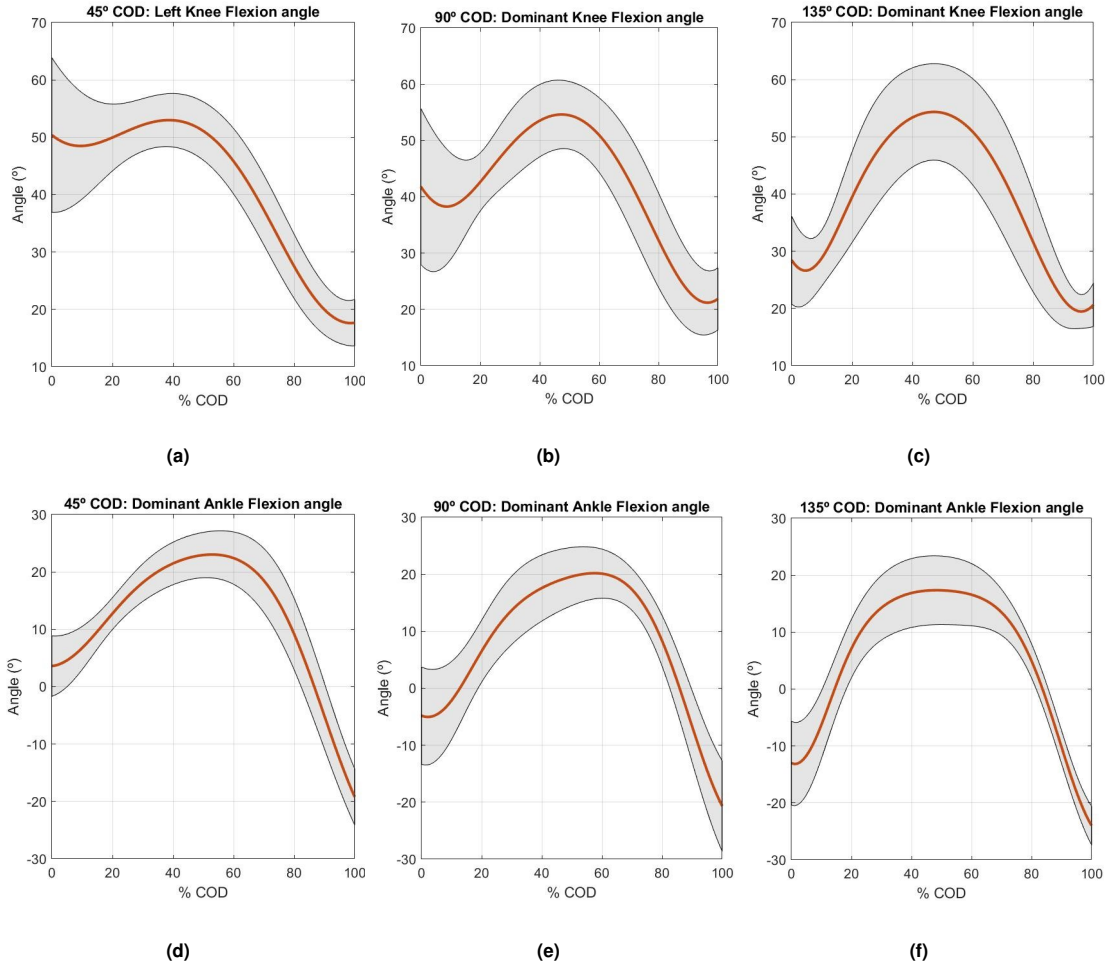

Figure 4.4: Total average (orange) and standard deviation (shaded area) for the knee joint flexion angle. Dominant knee flexion/extension angle (+flexion) for the 45° COD (a), 90° COD (b) and 135° COD (c). Dominant ankle dorsiflexion/-plantarflexion angle (+dorsiflexion) for the 45° COD (d), 90° COD (e) and 135° COD (f). In degrees, in terms of percentage of completion of the stance phase of the COD.

Kinematics of the knee and ankle joints only present significant differences between COD angles towards the beginning of the movement (until the 25% mark). These results also show that, for the same COD angles, significant differences in flexion angles occur simultaneously for these two joints. Similarly to the hip joint, the period where there are significant differences between the 90° and 135° CODs is shorter than when compared with the 45° COD. Furthermore, the largest differences are observed between the 135° and 45° CODs, as indicated by the biggest ESs. These negative ESs correspond to a decrease in knee flexion and ankle dorsiflexion during the initial portion of the CODs that happen with the increase in COD angle.

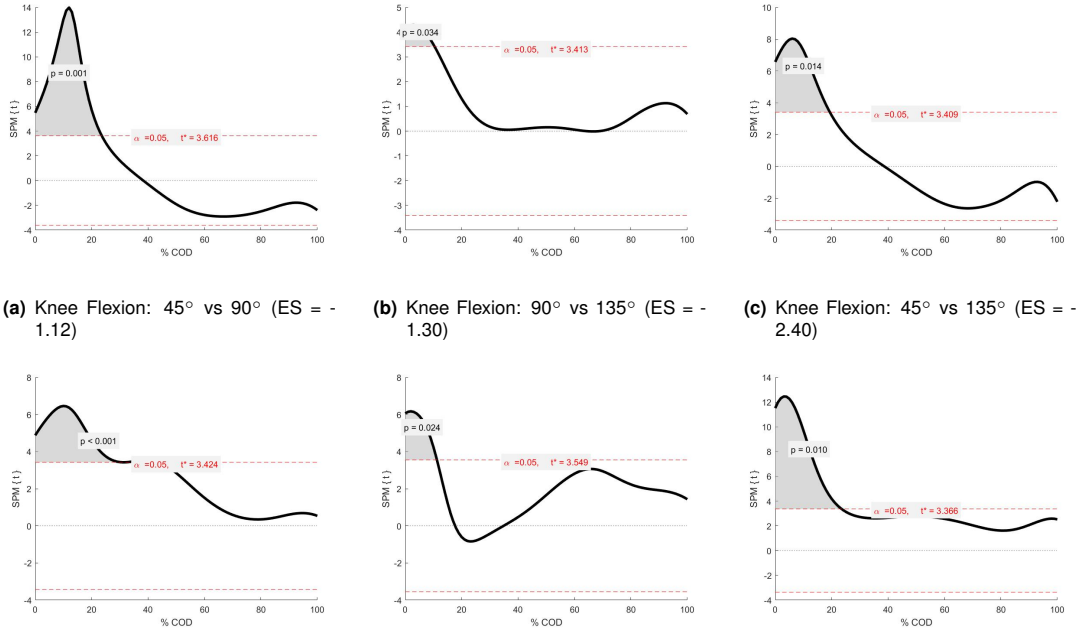

(a) Knee Flexion: 45° vs 90° (ES = -1.12)

(b) Knee Flexion: 90° vs 135° (ES = -1.30)

(c) Knee Flexion: 45° vs 135° (ES = -2.40)

(d) Ankle Flexion: 45° vs 90° (ES = -1.51)

(e) Ankle Flexion: 90° vs 135° (ES = -0.79)

(f) Ankle Flexion: 45° vs 135° (ES = -2.47)

Figure 4.5: SPMt (black line) of a 2-tailed t-test between: knee joint flexion angles of the 45° and 90° CODs (a), knee joint flexion angles of the 90° and 135° CODs (b), knee joint flexion angles of the 45° and 135° CODs (c); ankle joint flexion angles of the 45° and 90° CODs (d), ankle joint flexion angles of the 90° and 135° CODs (e), ankle joint flexion angles of the 45° and 135° CODs (f). In terms of percentage of completion of the stance phase of the COD. Critical threshold (red lines), t^*, at significance ($\alpha = 0.05$), supra-threshold cluster region (shaded area) and corresponding p-value.

Table 4.1 provides a summary of the most relevant results obtained from IK. The average maximum and minimum velocities, maximum and minimum joint angles and their respective timings are presented for the 3 COD angles, executed with the dominant and non-dominant limb.

Table 4.1: Inverse Kinematics Results: maximum and minimum average velocities; peak hip flexion(+) and extension(-); peak hip adduction(+) and abduction(-); peak hip internal(+) and external(-) rotation; peak knee flexion(+) and extension(-); peak ankle dorsiflexion(+) and plantarflexion(-) average joint angles(°). Respective timings presented in % of COD execution. Results presented as average ± standard deviation, for all COD angles, for the dominant (top) and non-dominant (bottom) limbs.

Inverse Kinematics						
Dominant Limb						
	45°		90°		135°	
	Vel. (m/s)	% COD	Vel. (m/s)	% COD	Vel. (m/s)	% COD
Velocitiy (Max/Min)	3.4 ± 0.5 / 2.6 ± 0.4	100% / 0%	2.5 ± 0.4 / 1.6 ± 0.3	100% / 45%	2.0 ± 0.4 / 0.9 ± 0.4	100% / 45%
	Angle (°)	% COD	Angle (°)	% COD	Angle (°)	% COD
Hip Flexion-Extension (Max/Min)	50.0 ± 6.7 / -16.7 ± 7.8	0% / 100%	38.9 ± 8.3 / -14.4 ± 8.3	0% / 100%	28.9 ± 6.7 / -13.3 ± 8.9	0% / 100%
Hip Addcution-Abduction (Max/Min)	-6.0 ± 6.0 / -15.5 ± 3.5	36% / 88%	-15.8 ± 5.0 / -26.0 ± 6.5	0% / 73%	-22.0 ± 7.0 / -27.0 ± 8.0	100% / 67%
Hip Internal-External Rotation (Max/Min)	4.4 ± 10.0 / -12.5 ± 7.5	33% / 100%	-4.4 ± 8.8 / -23.1 ± 3.8	9% / 93%	2.5 ± 5.0 / -26.3 ± 3.8	9% / 93%
Knee Flexion-Extension (Max/Min)	52.1 ± 4.3 / 17.1 ± 3.6	37% / 100%	-53.6 ± 5.7 / -20.7 ± 5.7	45% / 92%	53.6 ± 7.9 / -19.3 ± 2.9	47% / 92%
Ankle Dorsiflexion-Plantarflexion (Max/Min)	22.1 ± 3.6 / -9.3 ± 4.3	51% / 100%	-19.6 ± 4.3 / -20.7 ± 7.9	57% / 100%	16.4 ± 5.7 / -24.3 ± 3.6	47% / 100%
Non-dominant Limb						
	45°		90°		135°	
	Vel. (m/s)	% COD	Vel. (m/s)	% COD	Vel. (m/s)	% COD
Velocitiy (Max/Min)	3.4 ± 0.7 / 2.6 ± 0.6	100% / 0%	2.5 ± 0.3 / 1.7 ± 0.2	100% / 45%	2.0 ± 0.3 / 0.8 ± 0.3	100% / 45%
	Angle (°)	% COD	Angle (°)	% COD	Angle (°)	% COD
Hip Flexion-Extension (Max/Min)	50.0 ± 10.0 / -15.6 ± 7.2	0% / 100%	36.7 ± 5.6 / -15.6 ± 5.6	0% / 100%	30.0 ± 7.8 / -10.0 ± 8.3	0% / 100%
Hip Addcution-Abduction (Max/Min)	-4.5 ± 5.0 / -12.5 ± 5.0	0% / 85%	-15.5 ± 6.0 / -21.0 ± 7.0	100% / 63%	-20.0 ± 7.0 / -25.5 ± 4.0	100% / 12%
Hip Internal-External Rotation (Max/Min)	3.1 ± 8.1 / -14.4 ± 10.6	24% / 100%	6.3 ± 8.1 / -22.5 ± 10.0	9% / 100%	5.6 ± 8.8 / -24.4 ± 8.1	15% / 95%
Knee Flexion-Extension (Max/Min)	54.3 ± 4.3 / -17.1 ± 3.6	41% / 100%	55.0 ± 5.0 / -18.6 ± 2.9	45% / 93%	58.6 ± 7.9 / -21.4 ± 5.7	44% / 91%
Ankle Dorsiflexion-Plantarflexion (Max/Min)	22.1 ± 3.6 / -19.3 ± 3.6	52% / 100%	22.1 ± 3.6 / -21.4 ± 4.3	49% / 100%	20.0 ± 5.0 / -23.6 ± 4.3	47% / 100%

4.1.2 Dynamic Analysis

ID resulted in the calculation of the net joint moments responsible for the movement described by the kinematic data. These moments are the outcome of the internal muscle forces acting across a joint axis as a response to the external moment generated by the external forces (GRFs) about the same joint axis.

The joint moments calculated for hip joint the DOFs considered in the kinematic analysis are presented in Figure 4.6. SPM results regarding the comparison of those outcomes between COD angles are presented in Figure 4.7.

Regarding the hip's DOFs, the hip joint goes from peak flexion, at IC, to peak extension at Toe-off, in the 3 CODs. That motion is translated by the hip extension moment peaking at IC, becoming a flexor moment and reaching peak flexion moment at Toe-off, since they counteracting the action of external forces. A similar correspondence is also verified for hip adduction moments. Furthermore, these results also show hip flexion and adduction moments at IC becoming larger as COD angle increases. Hip rotation moments are close to zero for all CODs, which results from averaging trial data from CODs performed with internally and externally rotated hips, as observed in the kinematic results. Internall and external rotator moments are symmetrical and therefore nullify each other when calculating their mean.

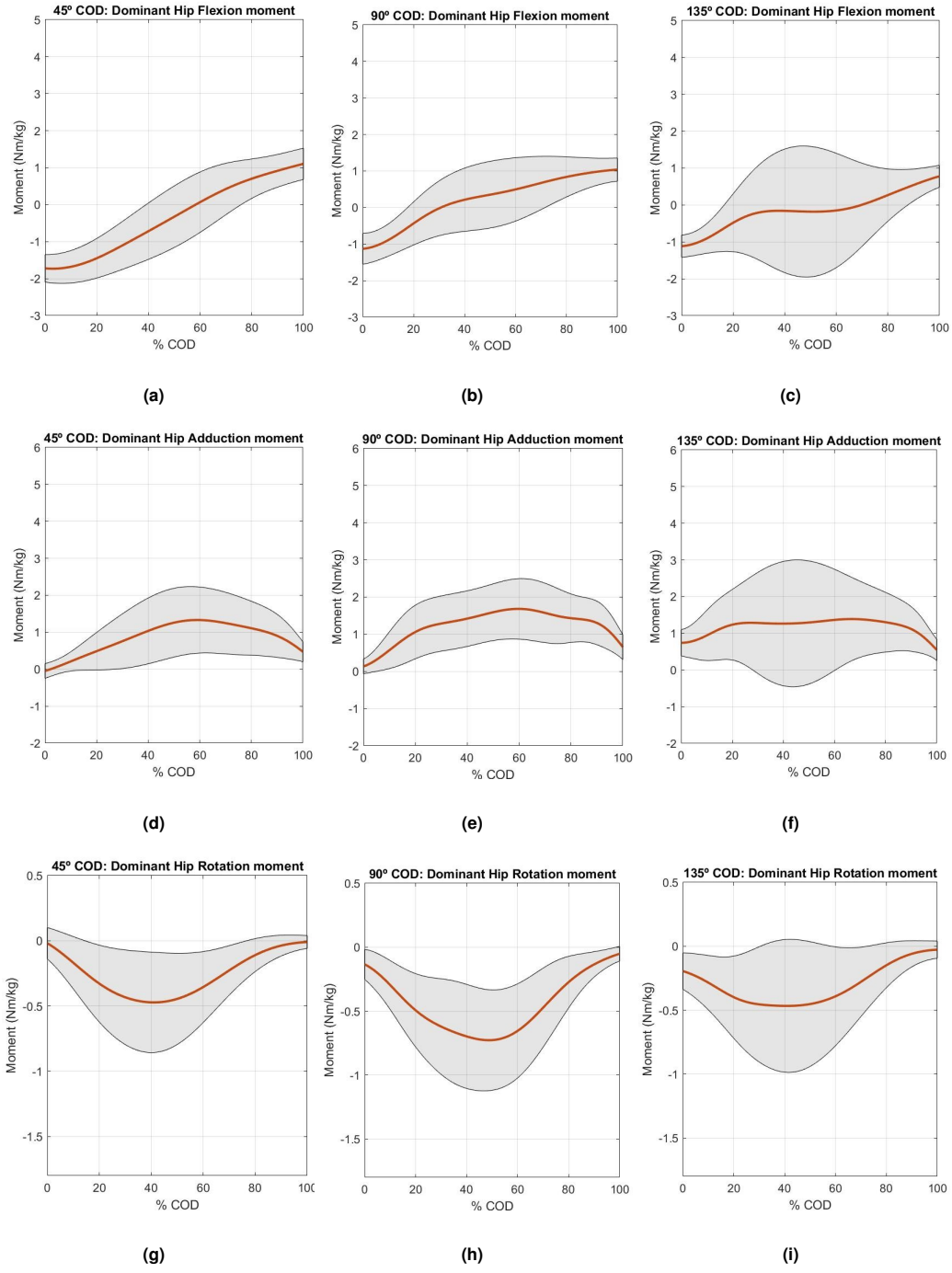

Figure 4.6: Total average (orange) and standard deviation (shaded area) for the hip joint flexion moment. Dominant hip flexion/extension moment (+flexion) for the 45° COD (a), 90° COD (b) and 135° COD (c). Dominant hip adduction/abduction moment (+adduction) for the 45° COD (d), 90° COD (e) and 135° COD (f). Dominant hip internal/external rotation moment (+internal) for the 45° COD (g), 90° COD (h) and 135° COD (i). In Nm/kg, in terms of percentage of completion of the stance phase of the COD.

Portions of significant difference resulting from the SPM regarding hip joint moments do not correspond directly to those of hip joint angles. For example, hip flexion moments are significantly different

between the 45° and 90° CODs during all the IC phase and almost the entire WA phase, which is much longer than the difference verified for hip flexion angles of the same CODs. Even so, ESs calculated for these comparisons still present the 90° and 135° CODs as being the most similar CODs when it comes to the dynamic behaviour of the hip joint, regardless of DOFs. The positive values of ES verified for the hip joint flexion and adduction DOFs reflect the decrease in hip extensor and increase in hip adductor moments that happen for the IC phase with the increase in COD angle.

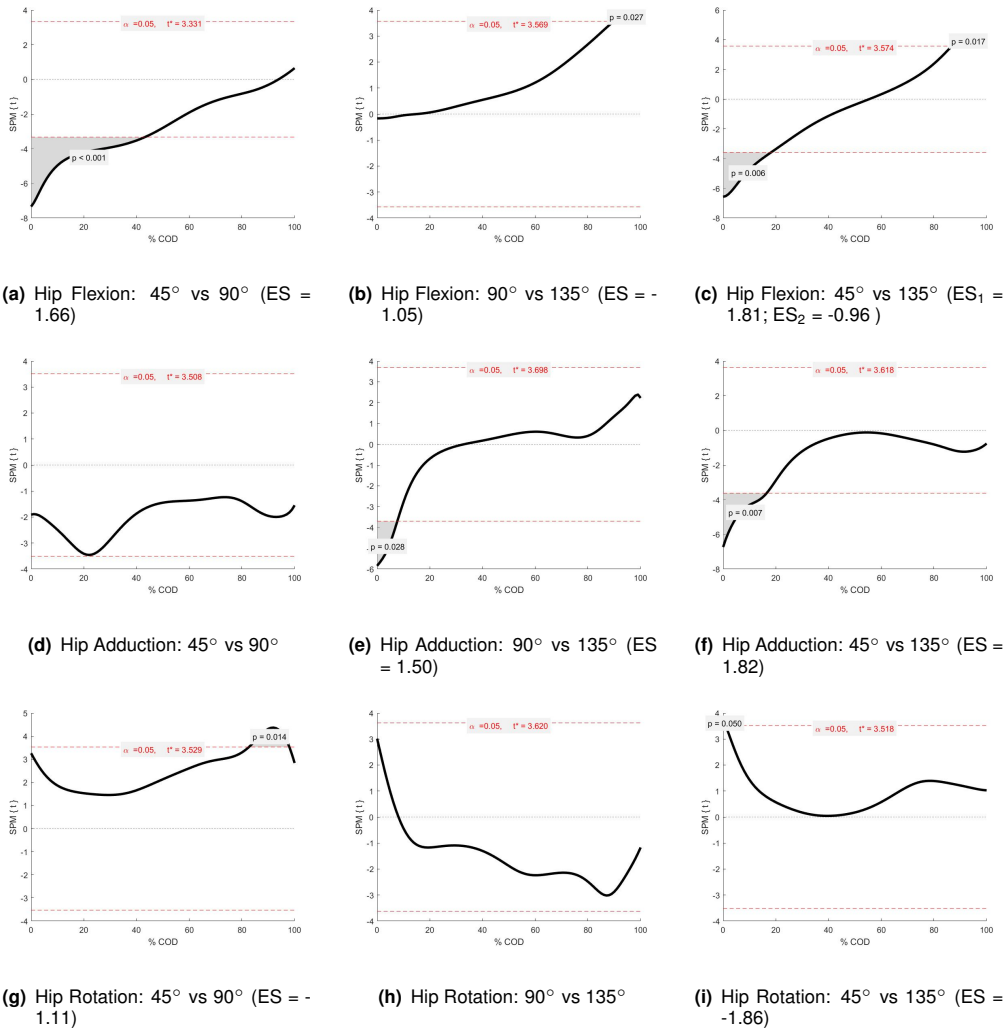

(a) Hip Flexion: 45° vs 90° (ES = 1.66)

(b) Hip Flexion: 90° vs 135° (ES = -1.05)

(c) Hip Flexion: 45° vs 135° (ES_1 = 1.81; ES_2 = -0.96)

(d) Hip Adduction: 45° vs 90°

(e) Hip Adduction: 90° vs 135° (ES = 1.50)

(f) Hip Adduction: 45° vs 135° (ES = 1.82)

(g) Hip Rotation: 45° vs 90° (ES = -1.11)

(h) Hip Rotation: 90° vs 135°

(i) Hip Rotation: 45° vs 135° (ES = -1.86)

Figure 4.7: SPMt (black line) of a 2-tailed t-test between: hip joint flexion moments of the 45° and 90° CODs (a), hip joint flexion moments of the 90° and 135° CODs (b), hip joint flexion moments of the 45° and 135° CODs (c); hip joint adduction moments of the 45° and 90° CODs (d), hip joint adduction moments of the 90° and 135° CODs (e), hip joint adduction moments of the 45° and 135° CODs (f); hip joint rotation moments of the 45° and 90° CODs (g), hip joint rotation moments of the 90° and 135° CODs (h), hip joint rotation moments of the 45° and 135° CODs (i). In terms of percentage of completion of the stance phase of the COD. Critical threshold (red lines), t^*, at significance ($\alpha = 0.05$), supra-threshold cluster region (shaded area) and corresponding p-value.

ID results for the knee and ankle joints are presented in Figure 4.8 and the corresponding SPM results are shown in Figure 4.9.

Regarding the knee joint, as knee flexion angles increase during WA, so do knee extensor moments, and as knee flexion angles decrease, knee extensor moments that oppose them also decrease. The 90° COD have larger peak extensor moments than the other CODs, and the 135° COD shows overall smaller knee extensor moments throughout Acceleration. Ankle joint moments also correspond to the observed kinematic behavior of the ankle. Peak plantarflexion moment is visible for the 45° COD, where peak dorsiflexion angle is also present. The 90° COD shows the smallest ankle dorsiflexion moments, in particular during IC and WA.

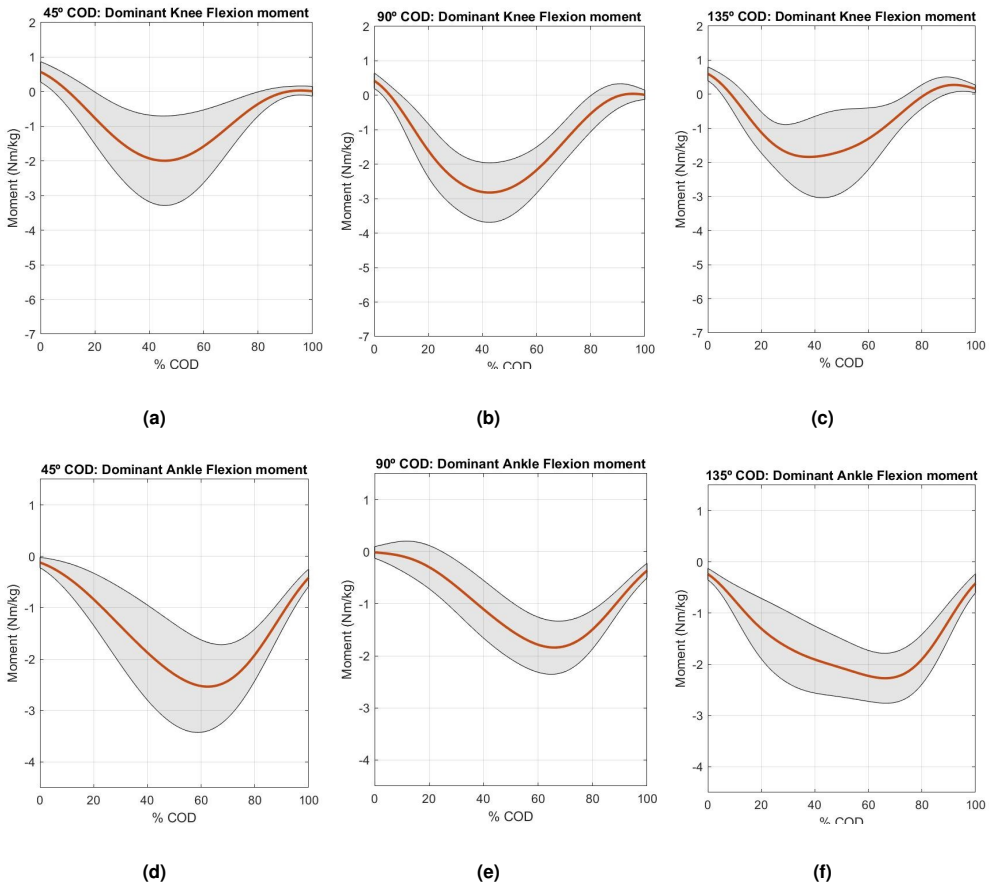

Figure 4.8: Total average (orange) and standard deviation (shaded area) for the knee joint flexion moment. Dominant knee flexion/extension moment (+flexion) for the 45° COD (a), 90° COD (b) and 135° COD (c). Dominant ankle dorsiflexion/plantarflexion moment (+dorsiflexion) for the 45° COD (d), 90° COD (e) and 135° COD (f). In Nm/kg, in terms of percentage of completion of the stance phase of the COD.

SPM results for the dynamics of the knee and ankle joints show the 90° and 135° as the only pair of CODs with significant difference between each other. This difference is more significant for ankle flexion moments than for knee flexion moments. The ES calculated to asses the difference between knee joint moments at the end of the Acceleration phase of the 90° and 135° CODs confirms the larger flexor moment verified in the ID results. The ES regarding the ankle joint refers to the the increase in plantarflexor moment during the IC and WA phases of the 135° COD when compared to the 90° COD.

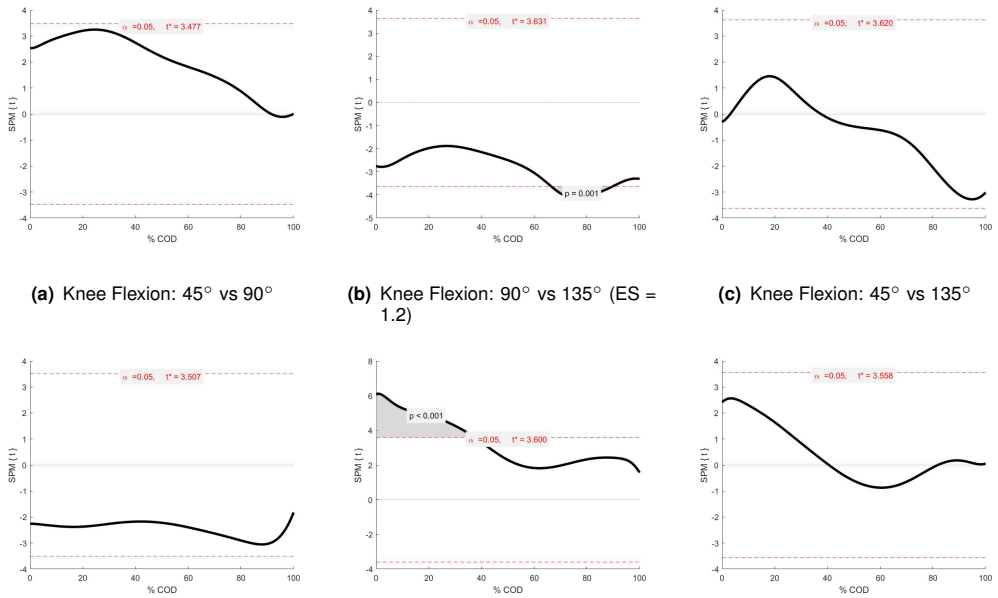

(a) Knee Flexion: 45° vs 90°

(b) Knee Flexion: 90° vs 135° (ES = 1.2)

(c) Knee Flexion: 45° vs 135°

(d) Ankle Flexion: 45° vs 90°

(e) Ankle Flexion: 90° vs 135° (ES = -1.96)

(f) Ankle Flexion: 45° vs 135°

Figure 4.9: SPMt (black line) of a 2-tailed t-test between: knee joint flexion moments of the 45° and 90° CODs (a), knee joint flexion moments of the 90° and 135° CODs (b), knee joint flexion moments of the 45° and 135° CODs (c); ankle joint flexion moments of the 45° and 90° CODs (d), ankle joint flexion moments of the 90° and 135° CODs (e), ankle joint flexion moments of the 45° and 135° CODs (f). In terms of percentage of completion of the stance phase of the COD. Critical threshold (red lines), t^*, at significance ($\alpha = 0.05$), supra-threshold cluster region (shaded area) and corresponding p-value.

The most relevant results from ID are summarised in Table 4.2. The average maximum and minimum joint moments and their respective timings are presented for the 3 COD angles, executed with the dominant and non-dominant limb.

Table 4.2: Inverse Dynamics Results: peak hip flexion(+) and extension(-); peak hip adduction(+) and abduction(-); peak hip internal(+) and external(-) rotation; peak knee flexion(+) and extension(-); peak ankle dorsiflexion(+) and plantarflexion(-) average joint moments (Nm/kg). Respective timings presented in % of COD execution. Results presented as average ± standard deviation, for all COD angles, for the dominant (top) and non-dominant (bottom) limbs.

Inverse Dynamics						
Dominant Limb						
	45°		**90°**		**135°**	
	Moment (Nm/kg)	% COD	Moment (Nm/kg)	% COD	Moment (Nm/kg)	% COD
Hip Flexion-Extension (Max/Min)	1.2 ± 0.4 / -1.7 ± 0.4	100% / 0%	1.1 ± 0.3 / -1.1 ± 0.4	100% / 0%	0.9 ± 0.3 / -1.9 ± 0.3	100% / 0%
Hip Addcution-Abduction (Max/Min)	1.4 ± 0.9 / -0.0 ± 0.2	56% / 0%	1.8 ± 0.8 / 0.2 ± 0.2	61% / 0%	1.5 ± 1.1 / 0.6 ± 0.3	63% / 100%
Hip Internal-External Rotation (Max/Min)	0.0 ± 0.1 / -0.5 ± 0.4	0% / 39%	-0.1 ± 0.1 / -0.7 ± 0.4	100% / 50%	-0.1 ± 0.1 / -0.5 ± 0.5	100% / 43%
Knee Flexion-Extension (Max/Min)	0.7 ± 0.3 / -2.0 ± 1.3	0% / 44%	0.4 ± 0.1 / -2.9 ± 0.8	0% / 43%	0.7 ± 0.2 / -1.8 ± 1.0	0% / 36%
Ankle Dorsiflexion-Plantarflexion (Max/Min)	-0.1 ± 0.1 / -2.6 ± 0.8	0% / 64%	0.0 ± 0.1 / -1.9 ± 0.4	0% / 67%	-0.3 ± 0.1 / -2.4 ± 0.4	0% / 67%
Non-dominant Limb						
	45°		**90°**		**135°**	
	Moment (Nm/kg)	% COD	Moment (Nm/kg)	% COD	Moment (Nm/kg)	% COD
Hip Flexion-Extension (Max/Min)	1.3 ± 0.4 / -1.8 ± 0.4	100% / 0%	1.2 ± 0.3 / -1.3 ± 0.4	100% / 0%	1.0 ± 0.2 / -1.0 ± 0.2	100% / 0%
Hip Addcution-Abduction (Max/Min)	0.8 ± 1.0 / -0.1 ± 0.3	56% / 0%	1.3 ± 1.0 / 0.2 ± 0.3	34% / 0%	1.0 ± 0.3 / 0.6 ± 0.2	100% / 0%
Hip Internal-External Rotation (Max/Min)	0.0 ± 0.2 / -0.3 ± 0.3	0% / 41%	-0.1 ± 0.1 / -0.6 ± 0.4	100% / 43%	0.1 ± 0.1 / -0.4 ± 0.3	100% / 40%
Knee Flexion-Extension (Max/Min)	0.7 ± 0.2 / -2.4 ± 1.2	0% / 46%	0.7 ± 0.2 / -3.6 ± 1.2	0% / 43%	0.6 ± 0.1 / -2.4 ± 0.9	0% / 34%
Ankle Dorsiflexion-Plantarflexion (Max/Min)	0.0 ± 0.2 / -2.4 ± 0.8	0% / 64%	0.0 ± 0.1 / -1.8 ± 0.6	0% / 66%	-0.3 ± 0.1 / -2.0 ± 0.6	0% / 66%

4.1.3 Muscle Analysis

Figures 4.10, 4.12, 4.14 and 4.16 present the results of the SO for the most relevant muscle forces, grouped according to their location on the body: gluteal, hip, thigh and leg muscles, respectively. Figures 4.11, 4.13, 4.15 and 4.17 show the corresponding SPM results.

Compared to the other gluteal muscles, the *Gluteus maximus* produced the largest forces. The magnitude of the *Gluteus minimus* looks negligible in the context of the other gluteal forces. For the *Gluteus maximus* and *Gluteus medius* it is possible to observe they produce higher forces during the IC and WA phases, and that the forces become smaller as COD angle increase.

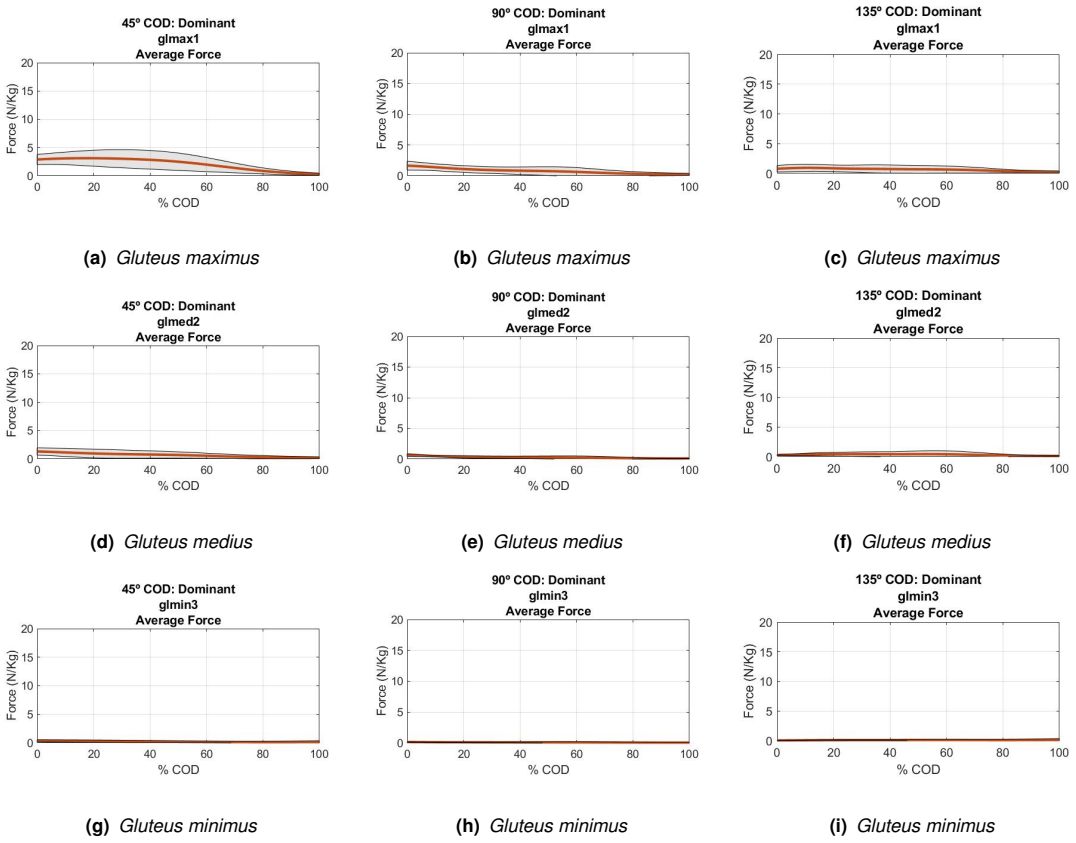

(a) *Gluteus maximus* **(b)** *Gluteus maximus* **(c)** *Gluteus maximus*

(d) *Gluteus medius* **(e)** *Gluteus medius* **(f)** *Gluteus medius*

(g) *Gluteus minimus* **(h)** *Gluteus minimus* **(i)** *Gluteus minimus*

Figure 4.10: Total average (orange) and standard deviation (shaded area) for the estimated muscle forces: *Gluteus maximus*:45° COD (a), 90° COD (b) and 135° COD (c); *Gluteus medius*: 45° COD (d), 90° COD (e) and 135° COD (f); *Gluteus minimus*: 45° COD (g), 90° COD (h) and 135° COD (i). In N/kg and in terms of percentage of completion of the stance phase of the COD.

The results from the SPM analysis confirm that gluteal force during IC and beginning of WA become smaller as COD angle increases, as indicated by the negative ES values. This signifies these muscles contribute less to hip extension and abduction moments of the hip during this portion of the CODs as they become sharper. The *Gluteus maximus* shows significant differences between the 45° COD and the other CODs for much longer periods of the task than the other gluteal muscles.

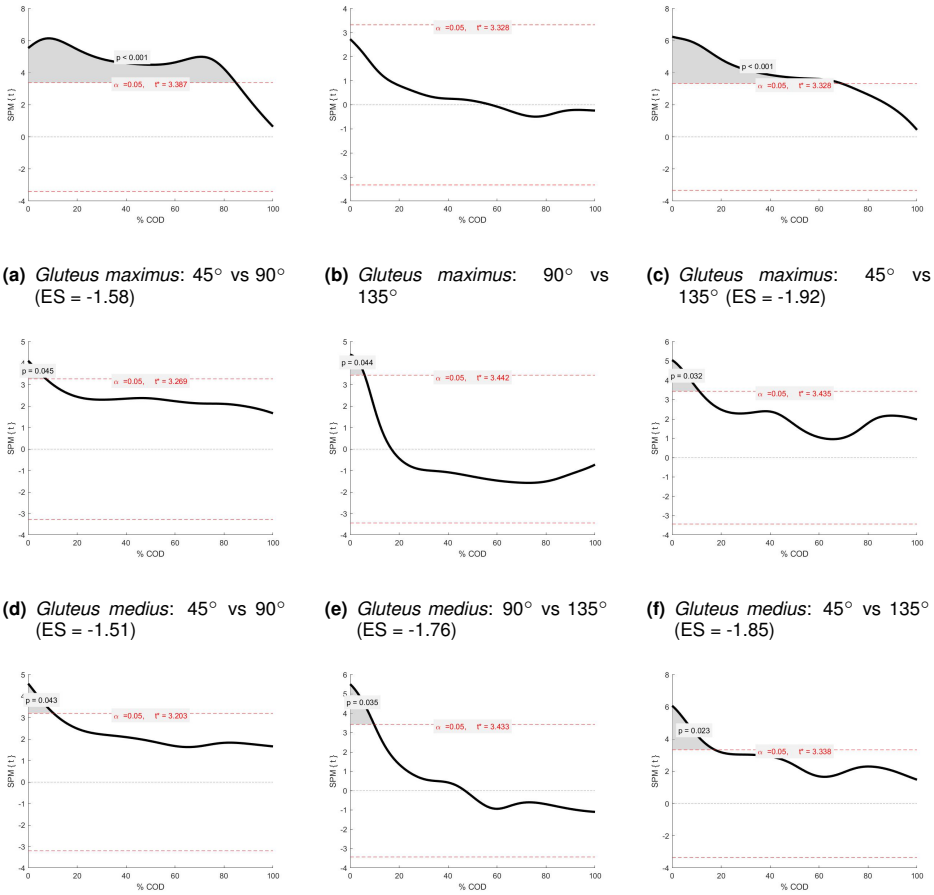

(a) *Gluteus maximus*: 45° vs 90° (ES = -1.58)

(b) *Gluteus maximus*: 90° vs 135°

(c) *Gluteus maximus*: 45° vs 135° (ES = -1.92)

(d) *Gluteus medius*: 45° vs 90° (ES = -1.51)

(e) *Gluteus medius*: 90° vs 135° (ES = -1.76)

(f) *Gluteus medius*: 45° vs 135° (ES = -1.85)

(g) *Gluteus minimus*: 45° vs 90° (ES = -1.49)

(h) *Gluteus minimus*: 90° vs 135° (ES = -1.43)

(i) *Gluteus minimus*: 45° vs 135° (ES = -1.84)

Figure 4.11: SPMt (black line) of a 2-tailed t-test between: *Gluteus maximus* muscle force of the 45° and 90° CODs (a), *Gluteus maximus* muscle force of the 90° and 135° CODs (b), *Gluteus maximus* muscle force of the 45° and 135° CODs (c); *Gluteus medius* muscle force of the 45° and 90° CODs (d), *Gluteus medius* muscle force of the 90° and 135° CODs (e), *Gluteus medius* muscle force of the 45° and 135° CODs (f); *Gluteus minimus* muscle force of the 45° and 90° CODs (g), *Gluteus minimus* muscle force of the 90° and 135° CODs (h), *Gluteus minimus* muscle force of the 45° and 135° CODs (i). In terms of percentage of completion of the stance phase of the COD. Critical threshold (red lines), t^*, at significance ($\alpha = 0.05$), supra-threshold cluster region (shaded area) and corresponding p-value.

The *Piriformis* muscle follows the same pattern as the gluteal muscles, producing its highest level of force during the IC and WA phases of the 45° COD. This is the muscle that produces the least amount of force out of the presented hip muscles. Both *Adductor* muscles show similar patterns of force production across the COD angles, with the *Adductor longus* showing larger magnitude forces. For the 45° and 90° CODs, these muscles forces continuously increase throughout COD execution until the Acceleration phase, where they peak. For the 135° COD, however, there is a dip in the magnitude of force around the 50% mark, where WA ends. The *Psoas* muscle presents the largest forces in this muscle group. The *Psoas* muscle force increases throughout COD execution, reaching its highest values at the end of Toe-off. This muscle shows an overall larger average force for the 90° COD than for the other angles.

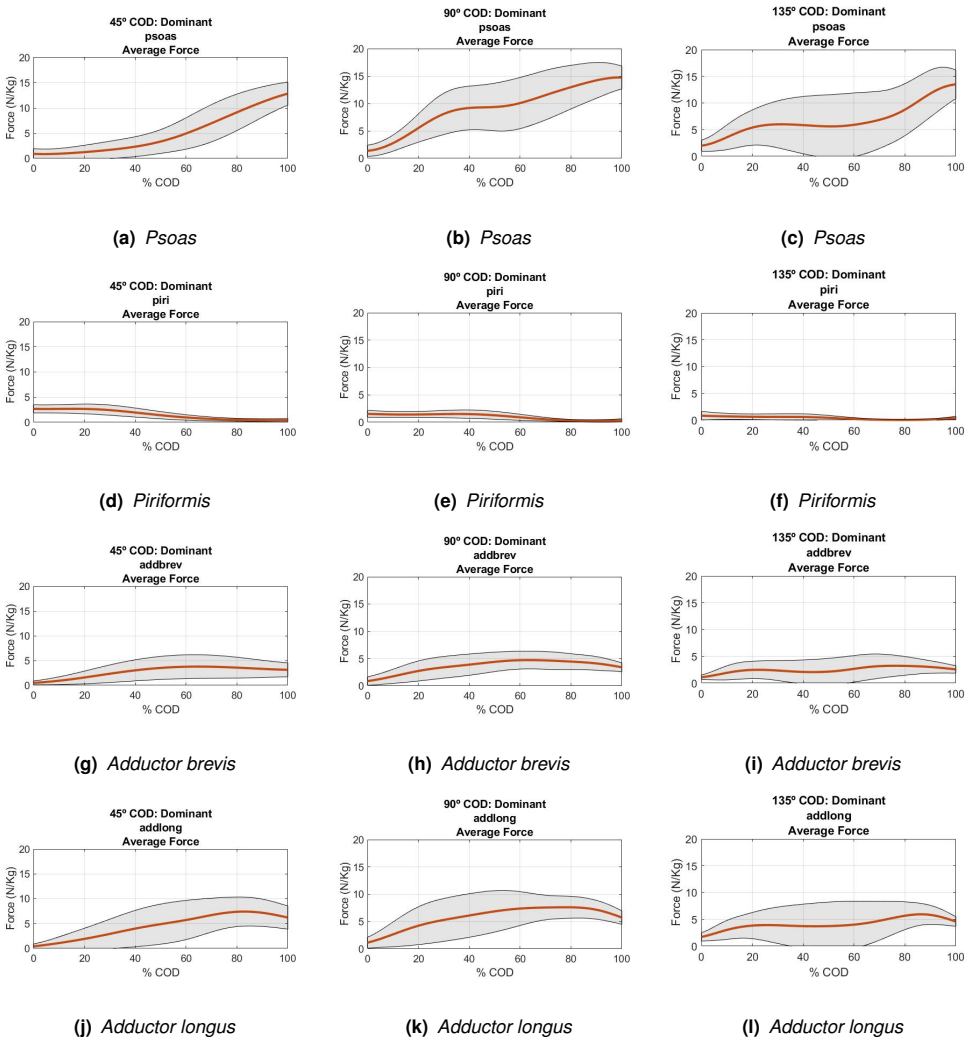

(a) *Psoas* **(b)** *Psoas* **(c)** *Psoas*

(d) *Piriformis* **(e)** *Piriformis* **(f)** *Piriformis*

(g) *Adductor brevis* **(h)** *Adductor brevis* **(i)** *Adductor brevis*

(j) *Adductor longus* **(k)** *Adductor longus* **(l)** *Adductor longus*

Figure 4.12: Total average (orange) and standard deviation (shaded area) for the estimated muscle forces: *Psoas*:45° COD (a), 90° COD (b) and 135° COD (c); *Piriformis*: 45° COD (d), 90° COD (e) and 135° COD (f); *Adductor brevis*: 45° COD (g), 90° COD (h) and 135° COD (i); *Adductor longus*: 45° COD (j), 90° COD (k) and 135° COD (l). In N/kg and in terms of percentage of completion of the stance phase of the COD.

Figure 4.13 shows that the *Psoas* generates significantly larger forces for the sharper CODs than for 45°. As primarily a hip flexor muscle, this tendency shows its contribution to a hip flexor moment is less needed for the less sharp COD. The *Adductors* show a significant decrease in their generated force towards the end of Acceleration and Toe-off of the 90° COD when compared to the 135°, and an increase during IC when comparing 135° to 45°. The *Piriformis* and the *Adductors* have opposing roles with respect to hip adduction and rotation. *Piriformis*'s force production diminishes as COD angle increases. Therefore, decreasing *Piriformis* while increasing *Adductors* forces, as is visible during IC when comparing the 45° and 135° CODs, contributes to the adduction and external rotation of the hip. The *Adductor brevis* and *Adductor longus* show the same behavior with the change in COD angle, indicating these muscles always act together.

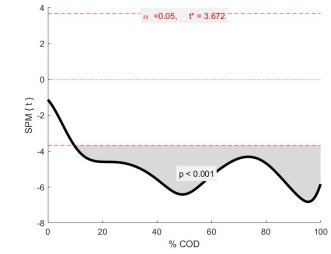

(a) *Psoas*: 45° vs 90° (ES = 1.55)

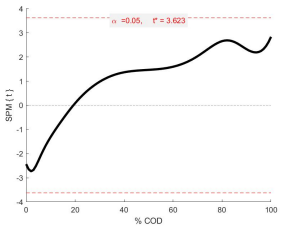

(b) *Psoas*: 90° vs 135°

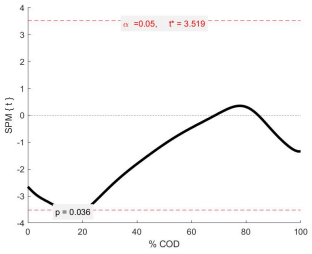

(c) *Psoas*: 45° vs 135° (ES = 2.19)

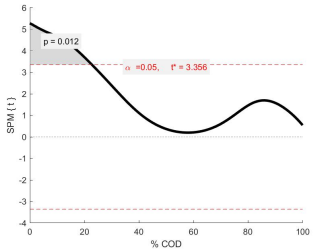

(d) *Piriformis*: 45° vs 90° (ES = -1.77)

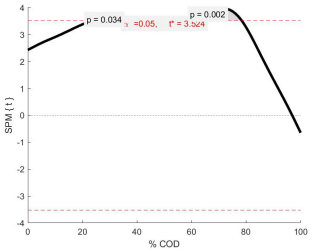

(e) *Piriformis*: 90° vs 135° (ES_1 = -1.47; ES_2 = -1.81)

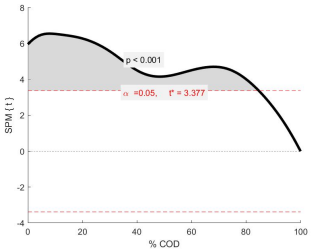

(f) *Piriformis*: 45° vs 135° (ES = -2.12)

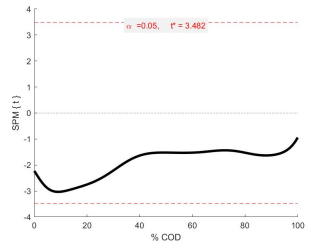

(g) *Adductor brevis*: 45° vs 90°

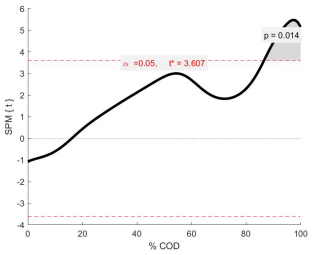

(h) *Adductor brevis*: 90° vs 135° (ES = -1.01)

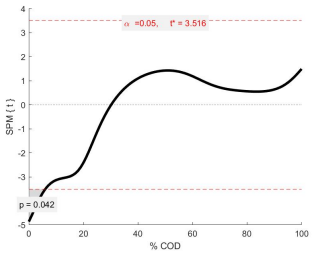

(i) *Adductor brevis*: 45° vs 135° (ES = 1.38)

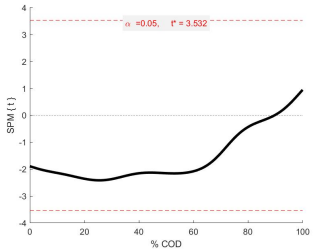

(j) *Adductor longus*: 45° vs 90°

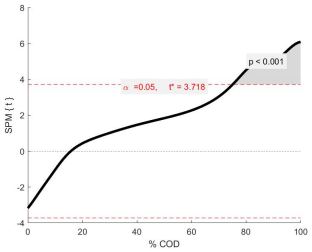

(k) *Adductor longus*: 90° vs 135° (ES = -0.87)

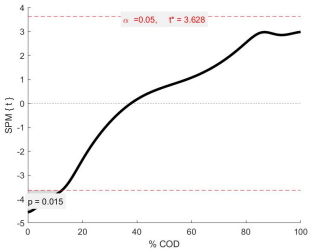

(l) *Adductor longus*: 45° vs 135° (ES = 1.55)

Figure 4.13: SPMt (black line) of a 2-tailed t-test between: *Psoas* muscle force of the 45° and 90° CODs (a), *Psoas* muscle force of the 90° and 135° CODs (b), *Psoas* muscle force of the 45° and 135° CODs (c); *Piriformis* muscle force of the 45° and 90° CODs (d), *Piriformis* muscle force of the 90° and 135° CODs (e), *Piriformis* muscle force of the 45° and 135° CODs (f); *Adductor brevis* muscle force of the 45° and 90° CODs (g), *Adductor brevis* muscle force of the 90° and 135° CODs (h), *Adductor brevis* muscle force of the 45° and 135° CODs (i); *Adductor longus* muscle force of the 45° and 90° CODs (j), *Adductor longus* muscle force of the 90° and 135° CODs (k), *Adductor longus* muscle force of the 45° and 135° CODs (l). In terms of percentage of completion of the stance phase of the COD. Critical threshold (red lines), t^*, at significance ($\alpha = 0.05$), supra-threshold cluster region (shaded area) and corresponding p-value.

Regarding the thigh muscles (Figure 4.14), the *Semitendinosus* msucles produced an almost negligible force when compared to the others considered here. The *Semimebranosus* shows peak force production at IC, which decreases as the COD progresses. That decrease becomes less steep as COD angles increase. The *Rectus femoris* presents the largest forces out of these thigh muscles. As COD angle increases, this muscle's force reaches its peak sooner in the COD. The 90° COD shows the highest magnitudes of *Rectus femoris* force.

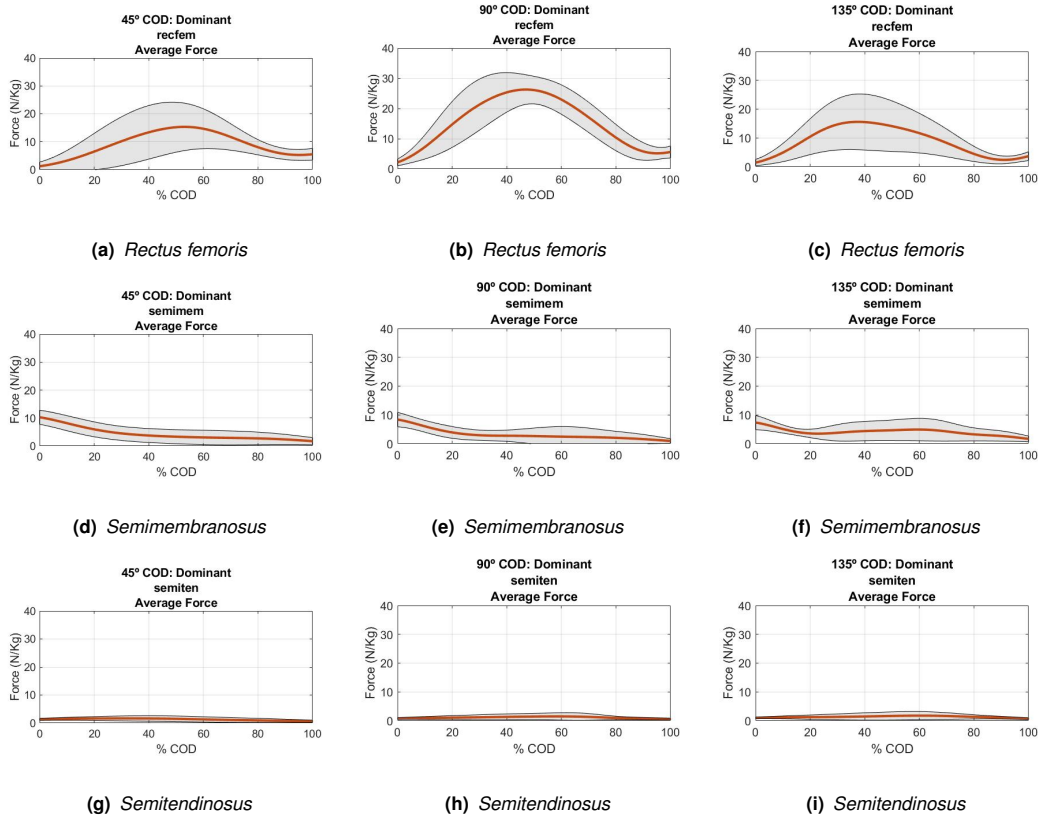

(a) *Rectus femoris* **(b)** *Rectus femoris* **(c)** *Rectus femoris*

(d) *Semimembranosus* **(e)** *Semimembranosus* **(f)** *Semimembranosus*

(g) *Semitendinosus* **(h)** *Semitendinosus* **(i)** *Semitendinosus*

Figure 4.14: Total average (orange) and standard deviation (shaded area) for the estimated muscle forces: *Rectus femoris*:45° COD (a), 90° COD (b) and 135° COD (c); *Semimembranosus*: 45° COD (d), 90° COD (e) and 135° COD (f); *Semitendinosus*: 45° COD (g), 90° COD (h) and 135° COD (i). In N/kg and in terms of percentage of completion of the stance phase of the COD.

The SPM results regarding thigh muscles show that the *Rectus femoris* force towards the end of the Acceleartion phase and Toe-off is smaller for the sharper CODs. The results regarding the *Semimembranosus* and *Semitendinosus* muscles show them to be less affected by the COD angle, as significant differences between CODs are only seen around IC. The reported ESs relate a decrease in force at the beginning of the movement with the sharper CODs. These results are associated with smaller hip extensor and internal rotator moments, as well as smaller knee flexor moments.

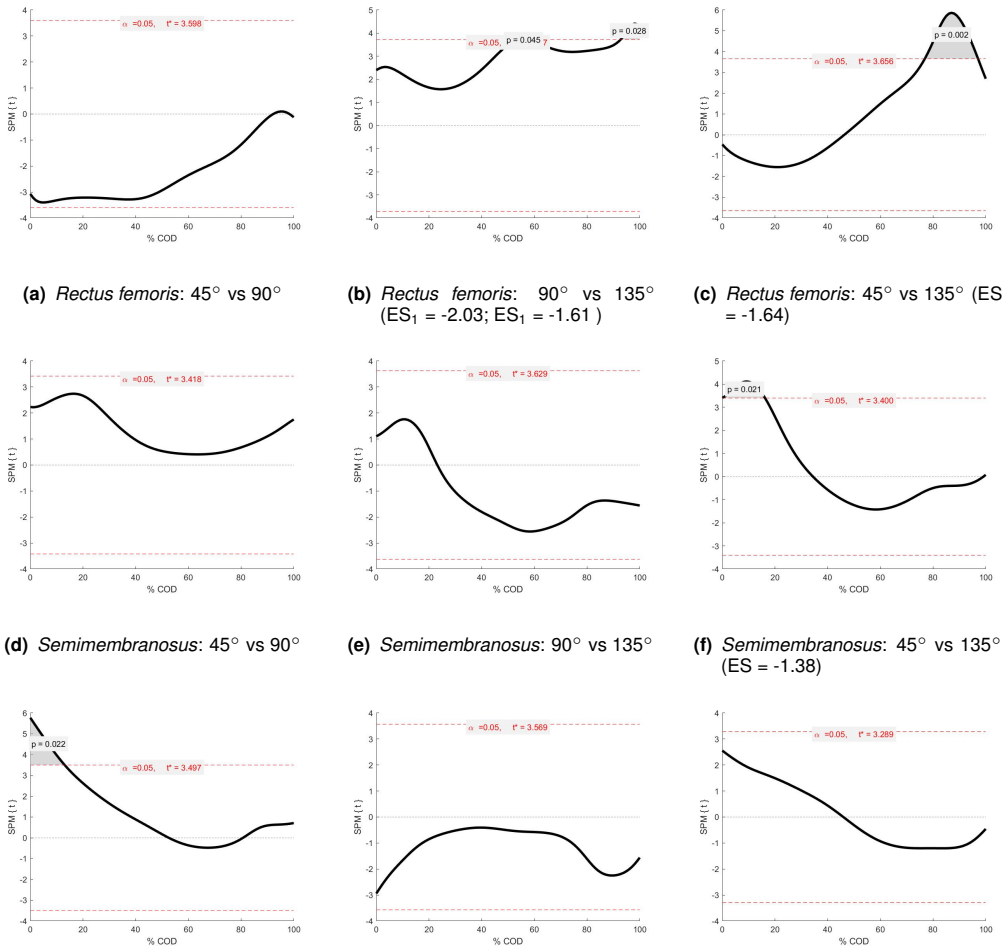

(a) *Rectus femoris*: 45° vs 90°

(b) *Rectus femoris*: 90° vs 135° (ES_1 = -2.03; ES_1 = -1.61)

(c) *Rectus femoris*: 45° vs 135° (ES = -1.64)

(d) *Semimembranosus*: 45° vs 90°

(e) *Semimembranosus*: 90° vs 135°

(f) *Semimembranosus*: 45° vs 135° (ES = -1.38)

(g) *Semitendinosus*: 45° vs 90° (ES = -1.25)

(h) *Semitendinosus*: 90° vs 135°

(i) *Semitendinosus*: 45° vs 135°

Figure 4.15: SPMt (black line) of a 2-tailed t-test between: *Rectus femoris* muscle force of the 45° and 90° CODs (a), *Rectus femoris* muscle force of the 90° and 135° CODs (b), *Rectus femoris* muscle force of the 45° and 135° CODs (c); *Semimembranosus* muscle force of the 45° and 90° CODs (d), *Semimembranosus* muscle force of the 90° and 135° CODs (e), *Semimembranosus* muscle force of the 45° and 135° CODs (f); *Semitendinosus* muscle force of the 45° and 90° CODs (g), *Semitendinosus* muscle force of the 90° and 135° CODs (h), *Semitendinosus* muscle force of the 45° and 135° CODs (i). In terms of percentage of completion of the stance phase of the COD. Critical threshold (red lines), t^*, at significance ($\alpha = 0.05$), supra-threshold cluster region (shaded area) and corresponding p-value.

Out of the leg muscles presented here, the *Tibilais anterior* is the one with the lowest magnitude forces. Even so, a slight peak in its force is visible during the Toe-off phase. Both the *Tibilais posterior* and the *Gastrocnemius* muscles present the same pattern of force production during the CODs. Magnitude of the average force for these muscles is shown to increase until the middle of the Acceleration phase, and does not appear to be affected by the variation in COD angle. The *Soleus* muscle shows its overall lowest average forces for the 90° COD. The 135° COD presents a larger span of COD execution with greater forces than the other COD angles.

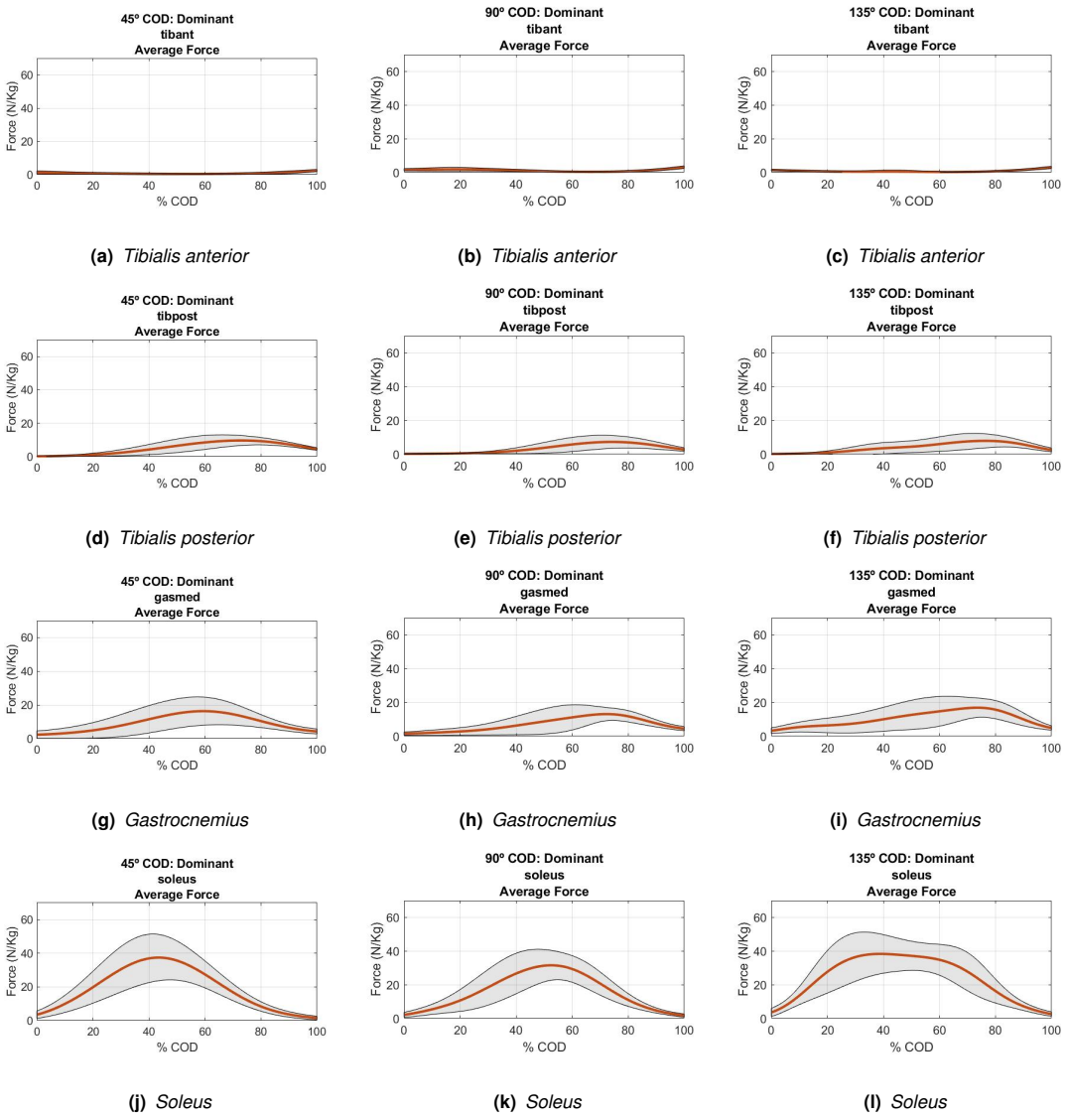

(a) *Tibialis anterior* **(b)** *Tibialis anterior* **(c)** *Tibialis anterior*

(d) *Tibialis posterior* **(e)** *Tibialis posterior* **(f)** *Tibialis posterior*

(g) *Gastrocnemius* **(h)** *Gastrocnemius* **(i)** *Gastrocnemius*

(j) *Soleus* **(k)** *Soleus* **(l)** *Soleus*

Figure 4.16: Total average (orange) and standard deviation (shaded area) for the estimated muscle forces: *Tibialis anterior*:45° COD (a), 90° COD (b) and 135° COD (c); *Tibialis posterior*: 45° COD (d), 90° COD (e) and 135° COD (f); *Gastrocnemius*: 45° COD (g), 90° COD (h) and 135° COD (i); *Soleus*: 45° COD (j), 90° COD (k) and 135° COD (l). In N/kg and in terms of percentage of completion of the stance phase of the COD.

Figure 4.17 contains the SPM results for the muscles that control ankle flexion. The *Tibialis anterior* is the primary muscle responsible for ankle dorsiflexion. This muscle presents shorter periods of significant differences between CODs, when compared to the others. The *Tibialis poterior*, *Gastrocnemius* and *Soleus* muscles participate in ankle plantarflexion. The last two muscles' behaviour responds similarly to the increase in COD angle, with that change being more significant when going from cutting at 90° to 135°. The 135° COD results show both muscles working together, producing larger forces during IC, the beginning of WA and also towards the end of Acceleration.

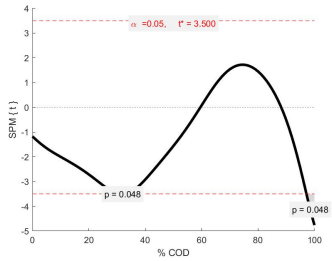

(a) *Tibialis anterior*: 45° vs 90° (ES_1 = 1.63; ES_1 = 0.96)

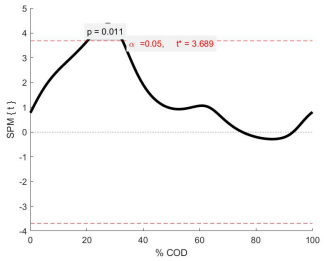

(b) *Tibialis anterior*: 90° vs 135° (ES = -1.70)

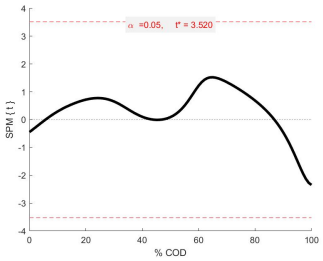

(c) *Tibialis anterior*: 45° vs 135°

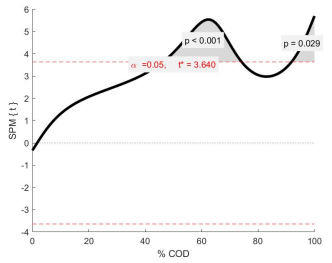

(d) *Tibialis posterior*: 45° vs 90° (ES_1 = 0.74; ES_1 =-1.72)

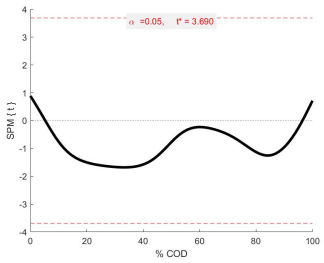

(e) *Tibialis posterior*: 90° vs 135°

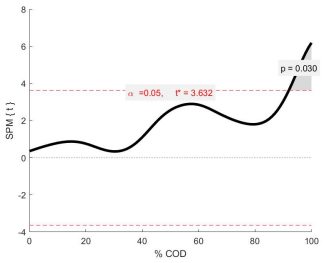

(f) *Tibialis posterior*: 45° vs 135° (ES = -2.11)

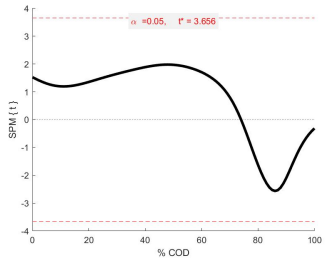

(g) *Gastrocnemius*: 45° vs 90°

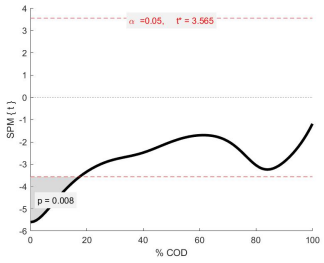

(h) *Gastrocnemius*: 90° vs 135° (ES = 1.38)

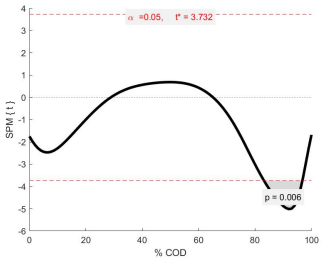

(i) *Gastrocnemius*: 45° vs 135° (ES = 1.12)

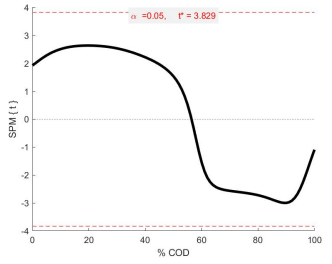

(j) *Soleus*: 45° vs 90°

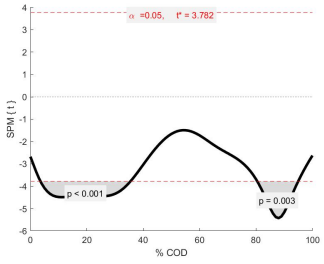

(k) *Soleus*: 90° vs 135° (ES_1 = 1.68; ES_1 = 1.19)

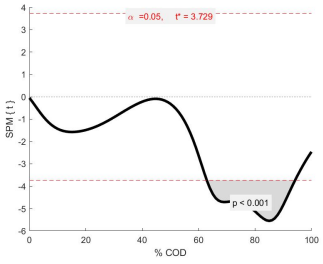

(l) *Soleus*: 45° vs 135° (ES = 1.44)

Figure 4.17: SPMt (black line) of a 2-tailed t-test between: *Tibialis anterior* muscle force of the 45° and 90° CODs (a), *Tibialis anterior* muscle force of the 90° and 135° CODs (b), *Tibialis anterior* muscle force of the 45° and 135° CODs (c); *Tibialis posterior* muscle force of the 45° and 90° CODs (d), *Tibialis posterior* muscle force of the 90° and 135° CODs (e), *Tibialis posterior* muscle force of the 45° and 135° CODs (f); *Gastrocnemius* muscle force of the 45° and 90° CODs (g), *Gastrocnemius* muscle force of the 90° and 135° CODs (h), *Gastrocnemius* muscle force of the 45° and 135° CODs (i); *Soleus* muscle force of the 45° and 90° CODs (j), *Soleus* muscle force of the 90° and 135° CODs (k), *Soleus* muscle force of the 45° and 135° CODs (l). In terms of percentage of completion of the stance phase of the COD. Critical threshold (red lines), t^*, at significance ($\alpha = 0.05$), supra-threshold cluster region (shaded area) and corresponding p-value.

Table 4.3 provides a summary of the most relevant results obtained from SO. The average maximum and minimum estimated muscle forces and their respective timings are presented for the 3 COD angles, executed with the dominant and non-dominant limb.

Table 4.3: Static Optimization Results: maximum and minimum *Gluteus maximus*, *Gluteus medius*, *Gluteus minimus*, *Psoas*, *Piriformis*, *Adductor brevis*, *Adductor longus*, *Semimembranosus*, *Semitendinosus*, *Tibialis anterior*, *Tibialis posterior*, *Gastrocnemius* and *Soleus* average force (N/kg). Respective timings presented in % of COD execution. Results presented as average ± standard deviation, for all COD angles, for the dominant (top) and non-dominant (bottom) limbs.

Static Optimization						
Dominant Limb						
	45°		**90°**		**135°**	
	Force (N/kg)	% COD	Force (N/kg)	% COD	Force (N/kg)	% COD
Gluteus maximus (Max/Min)	3.0 ± 1.4 / 0.0 ± 0.0	20% / 100%	2.1 ± 0.4 / 0.0 ± 0.0	0% / 100%	1.3 ± 0.4 / 0.0 ± 0.0	13% / 100%
Gluteus medius (Max/Min)	1.5 ± 0.6 / 0.0 ± 0.0	0% / 100%	0.8 ± 0.0 / 0.0 ± 0.0	0% / 100%	0.8 ± 0.0 / 0.0 ± 0.0	30% / 100%
Gluteus minimus (Max/Min)	0.3 ± 0.0 / 0.0 ± 0.0	0% / 100%	0.0 ± 0.0 / 0.0 ± 0.0	0% / 100%	0.0 ± 0.0 / 0.0 ± 0.0	0% / 100%
Psoas (Max/Min)	12.9 ± 2.1 / 0.9 ± 2.7	100% / 0%	15.0 ± 1.8 / 1.8 ± 0.9	100% / 0%	13.8 ± 2.5 / 2.1 ± 1.3	100% / 0%
Piriformis (Max/Min)	2.7 ± 1.0 / 0.0 ± 0.0	20% / 100%	1.7 ± 0.4 / 0.0 ± 0.0	0% / 87%	0.8 ± 0.8 / 0.0 ± 0.0	0% / 79%
Adductor brevis (Max/Min)	4.1 ± 2.3 / 0.5 ± 0.0	65% / 0%	5.0 ± 1.7 / 0.8 ± 0.4	64% / 0%	3.3 ± 2.1 / 1.3 ± 0.4	74% / 0%
Adductor longus (Max/Min)	7.7 ± 2.7 / 0.5 ± 0.0	84% / 0%	7.9 ± 2.1 / 1.3 ± 0.8	78% / 0%	6.3 ± 1.7 / 1.7 ± 0.4	87% / 0%
Rectus femoris (Max/Min)	15.9 ± 8.3 / 1.7 ± 0.8	54% / 0%	26.2 ± 4.6 / 2.3 ± 0.8	48% / 0%	16.7 ± 10.0 / 0.8 ± 0.8	37% / 0%
Semimembranosus (Max/Min)	10.0 ± 2.5 / 1.7 ± 0.8	0% / 100%	8.3 ± 2.5 / 0.8 ± 0.0	0% / 100%	7.5 ± 2.5 / 1.7 ± 0.8	0% / 100%
Semitendinosus (Max/Min)	2.3 ± 0.0 / 0.0 ± 0.0	19% / 100%	1.7 ± 0.8 / 0.0 ± 0.0	64% / 100%	1.7 ± 0.8 / 0.8 ± 0.0	60% / 100%
Tibialis anterior (Max/Min)	2.9 ± 0.0 / 0.0 ± 0.0	100% / 57%	4.3 ± 0.0 / 0.0 ± 0.0	100% / 71%	2.9 ± 0.0 / 0.0 ± 0.0	100% / 64%
Tibialis posterior (Max/Min)	10.0 ± 2.9 / 0.0 ± 0.0	73% / 0%	7.1 ± 4.3 / 0.0 ± 0.0	74% / 0%	8.6 ± 2.9 / 0.0 ± 0.0	78% / 0%
Gastrocnemius (Max/Min)	15.7 ± 8.6 / 2.9 ± 1.4	61% / 0%	14.3 ± 4.3 / 1.4 ± 0.0	74% / 0%	17.1 ± 4.3 / 2.9 ± 1.4	75% / 0%
Soleus (Max/Min)	37.1 ± 14.3 / 0.0 ± 0.0	44% / 100%	32.9 ± 8.6 / 1.4 ± 0.0	53% / 100%	38.6 ± 12.9 / 2.9 ± 0.0	37% / 100%
Non-dominant Limb						
	45°		**90°**		**135°**	
	Force (N/kg)	% COD	Force (N/kg)	% COD	Force (N/kg)	% COD
Gluteus maximus (Max/Min)	3.1 ± 1.2 / 0.3 ± 0.1	20% / 100%	2.1 ± 1.0 / 0.0 ± 0.0	0% / 100%	1.6 ± 1.5 / 0.0 ± 0.0	50% / 100%
Gluteus medius (Max/Min)	1.6 ± 0.9 / 0.3 ± 0.1	0% / 100%	0.7 ± 0.3 / 0.0 ± 0.0	0% / 100%	0.7 ± 0.8 / 0.0 ± 0.0	39% / 100%
Gluteus minimus (Max/Min)	0.4 ± 0.2 / 0.1 ± 0.0	0% / 100%	0.2 ± 0.0 / 0.0 ± 0.0	0% / 100%	0.1 ± 0.1 / 0.0 ± 0.0	41% / 100%
Psoas (Max/Min)	14.2 ± 3.0 / 0.7 ± 0.4	100% / 0%	14.7 ± 2.0 / 1.4 ± 1.0	100% / 0%	13.4 ± 1.9 / 3.9 ± 1.4	100% / 0%
Piriformis (Max/Min)	2.6 ± 0.8 / 0.4 ± 0.2	0% / 100%	1.7 ± 1.1 / 0.0 ± 0.0	35% / 96%	1.6 ± 1.5 / 0.2 ± 0.0	37% / 90%
Adductor brevis (Max/Min)	3.3 ± 1.8 / 0.3 ± 0.1	65% / 0%	4.9 ± 2.2 / 0.8 ± 0.1	61% / 0%	3.0 ± 1.7 / 1.5 ± 0.2	68% / 0%
Adductor longus (Max/Min)	6.6 ± 2.7 / 0.4 ± 0.1	65% / 0%	7.6 ± 2.7 / 1.0 ± 0.0	77% / 0%	5.4 ± 2.1 / 2.6 ± 0.1	87% / 0%
Rectus femoris (Max/Min)	14.2 ± 7.1 / 1.3 ± 0.9	48% / 0%	26.1 ± 8.4 / 2.4 ± 0.9	43% / 0%	19.9 ± 8.6 / 1.8 ± 0.4	33% / 0%
Semimembranosus (Max/Min)	10.1 ± 2.9 / 1.5 ± 1.0	0% / 100%	9.2 ± 2.2 / 1.1 ± 0.7	0% / 100%	6.1 ± 2.2 / 1.4 ± 0.6	0% / 100%
Semitendinosus (Max/Min)	1.5 ± 0.6 / 0.4 ± 0.1	20% / 100%	1.1 ± 1.2 / 0.0 ± 0.0	42% / 0%	1.1 ± 0.5 / 0.5 ± 0.2	17% / 100%
Tibialis anterior (Max/Min)	2.9 ± 0.0 / 0.6 ± 0.1	100% / 62%	3.5 ± 0.1 / 0.6 ± 0.0	100% / 73%	3.3 ± 0.8 / 0.4 ± 0.5	100% / 67%
Tibialis posterior (Max/Min)	9.4 ± 2.7 / 0.0 ± 0.0	73% / 0%	8.8 ± 3.4 / 0.0 ± 0.0	69% / 0%	7.2 ± 3.1 / 0.0 ± 0.0	81% / 0%
Gastrocnemius (Max/Min)	16.0 ± 5.6 / 2.2 ± 0.9	56% / 0%	12.0 ± 6.1 / 1.9 ± 0.8	67% / 0%	16.8 ± 7.4 / 3.3 ± 0.6	72% / 0%
Soleus (Max/Min)	35.1 ± 11.2 / 0.0 ± 0.0	44% / 100%	30.7 ± 9.3 / 0.0 ± 0.0	59% / 100%	40.0 ± 0.9 / 0.0 ± 0.0	40% / 100%

4.2 Inter-limb differences

The results of the SPM analysis regarding inter-limb differences show no significant differences between kinematic, dynamic or muscular behaviour during CODs performed with the subjects' dominant and non-dominant limb. Thus, COD execution with either leg is shown to be equivalent.

5

Discussion

Direct validation of the results by comparison with the literature is difficult due to differences in methodology. Many factors can interfere with the results, including the angle of COD tasks studied, the populations evaluated or the techniques used to simulate the COD tasks in the laboratory. Since no other studies were found analysing the same cutting angles for female handball players, comparisons with the literature regarding the kinematic and kinetic results obtained must consider this limitation.

Maniar[49] utilised OpenSim to study a healthy male population performing cutting tasks, using a single-leg hop technique. The curves shown regarding hip flexion, adduction, rotation, knee flexion and ankle flexion angles for a 45° COD are similar in profile and magnitude to those presented in this work. Knee flexion and ankle dorsiflexion moments reported by Maniar[49] for the 45° CODs are also similar in shape to those obtained in this work.

Regarding joint motion in the sagittal plane, hip and knee flexion angles obtained in this work are in agreement with those reported by Dos'Santos et al.[30] and Schreurs et al.[24] In both cases, flexion at IC decreased with the increase in cutting angle. Ankle dorsiflexion followed the same pattern, showing greater angles at IC for the 45° COD. The statistical analysis in this work did not identify significant differences in peak knee flexion and ankle dorsiflexion for the different COD angles. Rather, this analysis highlights IC as the COD phase where cutting angle influences the sagittal plane kinematics the most.

As another measure of the impact the cutting angle has on COD execution, this work found that sharper CODs are performed at lower velocities. Not only that, initial and terminal velocities also decrease with the increase in cutting angle. These findings are in accordance with those by Dos'Santos et al.,[25,30] which reported a trade-off between velocity and COD angle. Moreover, as COD angle increases, the WA and Acceleration phases correspond to steeper deceleration and acceleration, respectively. Mateus et al.[29] found the *Soleus* muscle to be one of the main contributors to the deceleration during tasks like CODs. Maniar et al.[50] also reported the *Gastrocnemius* to play a significant role in deceleration when changing direction. This information indicates that these muscles are expected to increase their produced force with the increasing COD angles.

Since the *Soleus* and *Gastrocnemius* muscles are both plantarflexor muscles, their behaviour reflects on the ankle joint moment. This work's statistical analysis of the ankle motion revealed plantarflexor moments to be smaller for the first 40% of the 90°COD than for the 135° COD, which is to say, during the phase where deceleration occurs. These results also found a significant increase in force production by these two muscles towards Toe-off of the 135° COD. As no deceleration is present at this time, this may indicate these muscles have another function other than braking, which is also accentuated by the increase in COD angle.

Regarding the knee joint, statistical comparison of the joint moments across the COD angles suggested the 135° COD presented smaller knee extensor moments at the end of Acceleration phase when compared to the 90° COD. This coincides with the observation that the *Gatrocnemius* has an increase in

force around the Toe-off of the 135° COD, as it is also a knee flexor muscle, which force opposes the extensor moment. Regarding the other knee flexor muscles, *Semimembranosus* and *Semitendinosus*, the increase in COD angle mostly affects their participation during IC and Toe-off, which show a decrease in their generated force. The *Rectus femoris*, as a knee extensor muscle, appears to be responsible for the peak in knee extensor moment verified for the 90° COD, as it showed significantly higher force for the 90° COD when compared to the 135° COD during the beginning of the Acceleration phase.

These 3 thigh muscles also participate in hip flexion and extension, where the *Rectus femoris* has an opposing role to the *Semimembranosus* and *Semitendinosus* muscles. The *Psoas* and *Gluteus maximus* muscles are also involved in the control of this hip joint motion. This work found that hip flexion angles at IC decrease as COD angle increases. Similar reports were also made by Dos'Santos et al.[25] To the larger IC flexion angles verified for the 45° COD correspond larger extensor moments observed during IC of that COD, when compared with the other CODs. This alludes to an increased contribution of the hip extensor muscles during the initial phase of the 45° COD, verified by the statistical analysis.

The gluteal muscles showed a decrease their participation, particularly during the IC phase, with the increase in COD angle. These muscles were found by Maniar et al.[50] to be the largest contributors to acceleration towards the desired direction. However, the difference in the Acceleration phase of the movements showed by the velocity profiles of the various COD angles is not reflected in a significant change in the gluteal muscle's force production. Moreover, the magnitude of the gluteal forces showed during the Acceleration phases of the movements are smaller than those of other muscles, in particular, the *Psoas* and the *Adductor* muscles. This suggests these hip muscles may play a more important role in accelerating the movement towards the desired new direction. As a hip flexor, the *Psoas* contributes to approximate the trunk and thigh segments, potentiating acceleration. The 90° COD showed higher levels of force for this muscle than the other CODs, with a particularly significant increase when compared to the 45° COD. The *Adductor brevis* and *Adductor longus* muscles' function is to move the thigh (and leg) away from the mid-line of the body, in the frontal plane. As COD angle increases, so does the hip adduction moment at IC, as a result of the increased force generated by these two muscles, combined with the decrease in force produced by the hip abductor muscles (i.e. gluteal muscles). The *Adductor* muscles also show more contribution towards the Acceleration and Toe-off phases for the 90° COD than for the others. However, this is not translated in the hip adduction moment, which found no significant differences between COD angles during those phases. That is probably due the action of the abductor muscles of the hip, opposing that motion.

Since hip joint rotation is controlled by muscles which primary function is the generation of force involved in other motions, hip behaviour in this DOF becomes whatever results from the control of those other motions. The possibility of executing the CODs with an externally or internally rotated hip, as shown by the results in this work, implies that hip rotation is not critical to COD execution.

This work, similarly to Dos'Santos et al.,[57] who evaluated inter-limb variance during 180° COD tasks, found no significant differences between COD execution with the subjects' dominant or non-dominant limb. This may be an indicator that elite athletes sports involving COD manoeuvres may be less susceptible to between-limb asymmetries due to their training.

The findings of the present work may be of significant importance when understanding injury risk in an athlete. Knee adduction and rotation moments have been described as good indicators of ACL injury risk.[30] Even though these moments were not calculated in this study, some correlations have been found between them and other joint parameters. Little hip and knee flexion as well as hip internal rotation have been found to be associated with larger knee valgus, and to contribute greatly to an increase in acACL loading.[16,17,25,30] The present study found the 135° CODs to have the most dangerous combination of these factors.

6

Conclusion

Contents

6.1 Conclusions

The objective of this work was to evaluate and compare hip, knee and ankle joint angles and moments and lower limb muscle forces estimated from experimental data of female handball athletes executing COD manoeuvres with different angles.

The methodology applied allowed the computation of joint kinematics and kinetics, which were shown to be consistent with the literature. Additionally, muscle activity was also computed.

The main findings pertain to the dependence of the biomechanics of the COD task on the cutting angle. Sharper CODs are associated with lower velocity profiles, steeper deceleration and acceleration and more extended hips.

The COD angles differ from each other by 45 degrees. However, the differences in kinematic and dynamic behaviour of the lower limbs between the 90° and 135° CODs are generally smaller than the difference between the 45° and 90° CODs. This implies lower limb biomechanics do not have a linear response to the increase in COD angle.

When it comes to knee and ankle, the change in these joint's moments is not proportional to the variation in COD angle, nor to change in kinematics. Even though the kinematics of the CODs are not as impacted when the cutting angle goes from 90° to 135°, the internal forces acting on the knee and ankle change the most with that angle increment.

The *Rectus femoris*, the *Adductors*, the *Psoas* and the *Tibialis anterior* showed largest peak forces for the 90 ° CODs, while the *Soleus*, the *Gastrocnemius* and the *Tibialis posterior* showed the smallest peak forces for those CODs. All the remaining muscles showed decreasing peak force with the increase in COD angle.

The 90° COD was found to be the task where the *Soleus* and *Gastrocnemius* muscles contributed less to the IC and WA phases of the manoeuvres. This is of particular importance, since these muscles have been proposed by literature to be responsible for the abrupt deceleration during the first half of the stance phase of COD tasks.

The comparison between biomechanical profiles of the COD tasks executed with the subjects' dominant and non-dominant limbs revealed no significant asymmetries in the evaluated population.

6.2 Limitations

This study carries a set of limitations, starting by having been performed in a laboratory setting. Even though this type of experimental acquisition allows for more accurate data to be extracted, the simplification of the task to fit within the laboratory's requirements may distance it from what would be an actual in-game situation. Furthermore, intensity and fatigue levels in the laboratory environment can be smaller than those experienced in-game, thus not accurately reflecting the events trying to be reproduced.

The musculoskeletal model used also has its limitations mostly regarding degrees of freedom that could not be considered in order to successfully reproduce the desired motion. The knee and ankle joints were only considered to have movement on the sagittal plane, which is not true for natural human motion. Furthermore, the subtalar and metatarsal-phalangeal joints were considered to have no movement at all. These foot motions could play an important role in the execution of the CODs. Moreover, the muscle parameters utilized were obtained from works with different subjects, body types and strategies, and may not truly represent the subjects analysed here. Another limitation comes from the static optimization process, which considers tendons to be inextensible and therefore does not take into account muscle's parallel elastic element's contribution.

Acquiring electromyography data was not considered due to the necessary time required for preparation of subjects, which would have made even longer the already long laboratory sessions, and the difficulties imposed by the measuring device on the their mobility. Lack of electromyography data limited the validation of the estimated muscles' activations and forces.

Finally, another important limitation of this study was the small population it evaluated. Larger populations allow for more robust statistical analysis results.

6.3 Future Work

The outcomes of this study are valuable for the development of training programs to further improve these athletes' performance while decreasing their injury risk.[30,49] Factors like increasing braking and propulsion capacity, through muscle training, as well as joint positions through technique training can be evaluated with similar studies.[16] Other than the possibility of analysing a particular athlete in detail, which is extremely valuable for elite athletes, this methodology can be applied for larger populations to identify the most common motion patterns, and introduce that knowledge in training at the younger formative levels.

An example of this work's application is the identification of limb asymmetries, at both kinematic and muscular levels, which presents an opportunity to assess the effectiveness of training of the COD manoeuvres of these athletes, as it is desirable that athletes are able to perform them equally well with both their legs. These data can be used to design specific training plans for each athlete, and to understand which muscles and which motions they must work on.

In order to produce better results, the first step on improving this work would be to increase the population size. In order to make generalized claims about the biomechanics involved in COD tasks for female handball players, studies similar to this should include more athletes.

Analysing each subject individually could provide more focused and detailed information on their execution of the CODs. This would be extremely helpful for elite athletes trying to assess their injury risk

and enhance their performance.

It would also be of particular interest to study smaller increments in COD angle, to better understand the knee and ankle joints response. This would also account for a wider range of game-like situations.

Performing similar studies focusing on subjects that have prior history of injury, in particular, ACL injury, and have then recovered, could provide valuable insight on the strategies athletes use to overcome said injuries and how the bodies adapt to them. Moreover, it could highlight the differences between healthy subjects and recovered subjects, which can impact performance and injury (or re-injury) risk.

Finally, another important improvement on this work would be to investigate the possibility to measure biomechanical data in-game. This would allow for a more accurate representation of the COD tasks to be studied, and would even enable the study of other in-game situations that are not reproducible in laboratory settings.

References

[1] L. Peterson and P. Renström, *Sports Injuries: Prevention, Treatment and Rehabilitation, Fourth Edition*. CRC Press, 2017, vol. 13.

[2] B. Elling and K. M. Elling, *Anatomy I& Physiology for the Prehospital Provider, 2nd edition*. American Academy of Orthopaedic Surgeons, 2014.

[3] D. Knudson, *Fundamentals of Biomechanics, 2nd edition*. Springer Nature Switzerland AG, 2021.

[4] B. F. Fremgen and S. S. Frucht, *Medical Terminology: A Living Language, 6th edition*. Pearson, 2015.

[5] A. Sensini and L. Cristofolini, "Biofabrication of electrospun scaffolds for the regeneration of tendons and ligaments. materials," *Basel, Switzerland*, vol. 11,10, 2018.

[6] M. Schuenke, E. Schulte, and U. Schumacher, *General Anatomy and Musculoskeletal System*. Thieme, 2006, vol. 88.

[7] A. Rajagopal, C. L. Dembia, M. S. DeMers, D. D. Delp, J. L. Hicks, and S. L. Delp, "Full-Body Musculoskeletal Model for Muscle-Driven Simulation of Human Gait," *IEEE Transactions on Biomedical Engineering*, vol. 63, no. 10, pp. 2068–2079, 2016.

[8] R. L. Drake, W. Vogl, A. W. M. Mitchell, R. Tibbitts, and P. Richardson. Elsevier, 2015.

[9] H. Nygaard Falch, H. Guldteig Rædergård, and R. van den Tillaar, "Effect of Different Physical Training Forms on Change of Direction Ability: a Systematic Review and Meta-analysis," *Sports Medicine - Open*, vol. 5, no. 1, 2019.

[10] J. Bencke, P. Aagaard, and M. K. Zebis, "Muscle activation during ACL injury risk movements in young female athletes: A narrative review," *Frontiers in Physiology*, vol. 9, no. MAY, pp. 1–10, 2018.

[11] J. Raya-González, F. M. Clemente, M. Beato, and D. Castillo, "Injury profile of male and female senior and youth handball players: A systematic review," *International Journal of Environmental Research and Public Health*, vol. 17, no. 11, 2020.

[12] R. Mateus, “Model-based estimation of muscle and joint reaction forces exerted during an abrupt horizontal deceleration task performed by elite athletes,” 2018.

[13] A. G. Schache, H.-j. Kim, D. L. Morgan, and M. G. Pandy, “Gait I& Posture Hamstring muscle forces prior to and immediately following an acute sprinting-related muscle strain injury,” *Gait I& Posture*, vol. 32, no. 1, pp. 136–140, 2010.

[14] C. M. Powers, “The influence of abnormal hip mechanics on knee injury: A biomechanical perspective,” *Journal of Orthopaedic and Sports Physical Therapy*, vol. 40, no. 2, pp. 42–51, 2010.

[15] S. Sasaki, Y. Nagano, S. Kaneko, T. Sakurai, and T. Fukubayashi, “The relationship between performance and trunk movement during change of direction,” *Journal of Sports Science and Medicine*, vol. 10, no. 1, pp. 112–118, 2011.

[16] E. Kristianslund and T. Krosshaug, “Comparison of drop jumps and sport-specific sidestep cutting: Implications for anterior cruciate ligament injury risk screening,” *American Journal of Sports Medicine*, vol. 41, no. 3, pp. 684–688, 2013.

[17] J. Bencke, D. Curtis, C. Krogshede, L. K. Jensen, T. Bandholm, and M. K. Zebis, “Biomechanical evaluation of the side-cutting manoeuvre associated with ACL injury in young female handball players,” *Knee Surgery, Sports Traumatology, Arthroscopy*, vol. 21, no. 8, pp. 1876–1881, 2013.

[18] E. Kristianslund, O. Faul, R. Bahr, G. Myklebust, and T. Krosshaug, “Sidestep cutting technique and knee abduction loading: Implications for ACL prevention exercises,” *British Journal of Sports Medicine*, vol. 48, no. 9, pp. 779–783, 2014.

[19] K. Weiss and C. Whatman, “Biomechanics Associated with Patellofemoral Pain and ACL Injuries in Sports,” *Sports Medicine*, vol. 45, no. 9, pp. 1325–1337, 2015.

[20] S. M. Sigward, G. M. Cesar, and K. L. Havens, “Predictors of frontal plane knee moments during side-step cutting to 45 and 110 degrees in men and women: Implications for anterior cruciate ligament injury,” *Clinical Journal of Sport Medicine*, vol. 25, no. 6, pp. 529–534, 2015.

[21] H. T. Van Der Does, M. S. Brink, A. Benjaminse, C. Visscher, and K. A. Lemmink, “Jump Landing Characteristics Predict Lower Extremity Injuries in Indoor Team Sports,” *International Journal of Sports Medicine*, vol. 37, no. 3, pp. 251–256, 2016.

[22] E. F. Hyte, C. Richter, S. O’Connor, and K. Moran, “Nvestigation of the,” *Journal of Strength and Conditioning Research*, vol. 32, no. 6, pp. 1583–1593, 2018.

[23] A. Franklyn-Miller, C. Richter, E. King, S. Gore, K. Moran, S. Strike, and E. C. Falvey, “Athletic groin pain (part 2): A prospective cohort study on the biomechanical evaluation of change of direction

identifies three clusters of movement patterns," *British Journal of Sports Medicine*, vol. 51, no. 5, pp. 460–468, 2017.

[24] M. J. Schreurs, A. Benjaminse, and K. A. Lemmink, "Sharper angle, higher risk? The effect of cutting angle on knee mechanics in invasion sport athletes," *Journal of Biomechanics*, vol. 63, pp. 144–150, 2017.

[25] T. Dos'Santos, C. Thomas, P. Comfort, and P. A. Jones, "The Effect of Angle and Velocity on Change of Direction Biomechanics: An Angle-Velocity Trade-Off," *Sports Medicine*, vol. 48, no. 10, pp. 2235–2253, 2018.

[26] A. S. Fox, "Change-of-Direction Biomechanics: Is What's Best for Anterior Cruciate Ligament Injury Prevention Also Best for Performance?" *Sports Medicine*, vol. 48, no. 8, pp. 1799–1807, 2018.

[27] E. Hosseini, A. Daneshjoo, and M. Sahebozamani, "Comparing the Knee Joint Kinematic Parameters of Female Athletes During Sidestep Cutting Task Before and After Fatigue in Predictable and Unpredictable Settings," *Journal of Sport Biomechanics*, vol. 5, no. 3, pp. 178–187, 2020.

[28] N. J. Nedergaard, S. Dalbø, S. V. Petersen, M. K. Zebis, and J. Bencke, "Biomechanical and neuromuscular comparison of single- and multi-planar jump tests and a side-cutting maneuver: Implications for ACL injury risk assessment," *Knee*, vol. 27, no. 2, pp. 324–333, 2020.

[29] R. B. Mateus, V. Ferrer-Roca, F. João, and A. P. Veloso, "Muscle contributions to maximal single-leg forward braking and backward acceleration in elite athletes," *Journal of Biomechanics*, vol. 112, p. 110047, 2020.

[30] T. Dos'Santos, C. Thomas, and P. A. Jones, "The effect of angle on change of direction biomechanics: Comparison and inter-task relationships," *Journal of Sports Sciences*, vol. 00, no. 00, pp. 1–14, 2021.

[31] B. L. S. Bedo, G. M. Cesar, R. Moraes, F. P. Mariano, L. H. P. Vieira, V. L. Andrade, and P. R. P. Santiago, "Influence of side uncertainty on knee kinematics of female handball athletes during sidestep cutting maneuvers," *Journal of Applied Biomechanics*, vol. 37, no. 3, pp. 188–195, 2021.

[32] T. Hahn, A. Foldspang, and T. Ingemann-Hansen, "Prevalence of knee instability in relation to sports activity," *Scandinavian Journal of Medicine and Science in Sports*, vol. 11, no. 4, pp. 233–238, 2001.

[33] E. Pappas, F. Zampeli, S. A. Xergia, and A. D. Georgoulis, "Lessons learned from the last 20 years of ACL-related in vivo-biomechanics research of the knee joint," *Knee Surgery, Sports Traumatology, Arthroscopy*, pp. 755–766, 2013.

[34] T. Dos'Santos, C. Thomas, P. Comfort, and P. A. Jones, "The Effect of Training Interventions on Change of Direction Biomechanics Associated with Increased Anterior Cruciate Ligament Loading: A Scoping Review," *Sports Medicine*, vol. 49, no. 12, pp. 1837–1859, 2019.

[35] F. João, A. Veloso, S. Cabral, and V. Moniz-pereira, "Human Movement Science Synergistic interaction between ankle and knee during hopping revealed through induced acceleration analysis," *Human Movement Science*, vol. 33, pp. 312–320, 2014.

[36] T. D. C. Thomas, P. Comfort, and P. A. Jones, "Comparison of Change of Direction Speed Performance and Asymmetries between Team-Sport Athletes: Application of Change of Direction Deficit," *Sports*, vol. 6, no. 4, p. 174, 2018.

[37] S. A. Roelker, E. J. Caruthers, R. K. Hall, N. C. Pelz, A. M. Chaudhari, and R. A. Siston, "Effects of optimization technique on simulated muscle activations and forces," *Journal of Applied Biomechanics*, vol. 36, no. 4, pp. 259–278, 2020.

[38] A. S. Arnold, F. C. Anderson, M. G. Pandy, and S. L. Delp, "Muscular contributions to hip and knee extension during the single limb stance phase of normal gait: A framework for investigating the causes of crouch gait," *Journal of Biomechanics*, vol. 38, no. 11, pp. 2181–2189, 2005.

[39] K. L. Siegel, T. M. Kepple, and S. J. Stanhope, "Using induced accelerations to understand knee stability during gait of individuals with muscle weakness," vol. 23, pp. 435–440, 2006.

[40] H. J. Kim, J. W. Fernandez, M. Akbarshahi, J. P. Walter, B. J. Fregly, and M. G. Pandy, "Evaluation of Predicted Knee-Joint Muscle Forces during Gait Using an Instrumented Knee Implant," no. October, pp. 1326–1331, 2009.

[41] Y. C. Lin, J. P. Walter, S. A. Banks, M. G. Pandy, and B. J. Fregly, "Simultaneous prediction of muscle and contact forces in the knee during gait," *Journal of Biomechanics*, vol. 43, no. 5, pp. 945–952, 2010.

[42] K. B. Shelburne, M. R. Torry, and M. G. Pandy, "Muscle, ligament, and joint-contact forces at the knee during walking," *Medicine and Science in Sports and Exercise*, vol. 37, no. 11, pp. 1948–1956, 2005.

[43] P. Sritharan, Y. C. Lin, and M. G. Pandy, "Muscles that do not cross the knee contribute to the knee adduction moment and tibiofemoral compartment loading during gait," *Journal of Orthopaedic Research*, vol. 30, no. 10, pp. 1586–1595, 2012.

[44] T. T. Dao, F. Marin, and M. C. Hobatho, "Sensitivity of the anthropometrical and geometrical parameters of the bones and muscles on a musculoskeletal model of the lower limbs," *Proceedings of the*

31st Annual International Conference of the IEEE Engineering in Medicine and Biology Society: Engineering the Future of Biomedicine, EMBC 2009, pp. 5251–5254, 2009.

[45] I. Roupa, M. Rodrigues, F. Marques, S. B. Gonçalves, P. Flores, and M. Tavares, *On the Modeling of Biomechanical Systems for Human Movement Analysis : A Narrative Review*. Springer Netherlands, 2022, no. 0123456789.

[46] S. L. Delp, F. C. Anderson, A. S. Arnold, P. Loan, A. Habib, C. T. John, E. Guendelman, and D. G. Thelen, "Delp2007.pdf," *IEEE Transactions on Biomechanical Engineering*, vol. 54, no. 11, pp. 1940–1950, 2007.

[47] A. Seth, J. L. Hicks, T. K. Uchida, A. Habib, L. Dembia, J. J. Dunne, C. F. Ong, M. S. Demers, A. Rajagopal, M. Millard, S. R. Hamner, E. M. Arnold, R. Yong, S. K. Lakshmikanth, M. A. Sherman, J. P. Ku, and S. L. Delp, "OpenSim : Simulating musculoskeletal dynamics and neuromuscular control to study human and animal movement," *PLOS Computational Biology*, pp. 1–20, 2018.

[48] S. R. Hamner, A. Seth, and S. L. Delp, "Muscle contributions to propulsion and support during running," *Journal of Biomechanics*, vol. 43, no. 14, p. 2709–2716, 2011.

[49] N. Maniar, "Muscle force contributions to knee joint loading," *Thesis, Australian Catholic Universitys*, 2017.

[50] N. Maniar, A. G. Schache, M. H. Cole, and D. A. Opar, "Lower-limb muscle function during sidestep cutting," *Journal of Biomechanics*, vol. 82, no. October, pp. 186–192, 2019.

[51] K. Steffen, A. Nilstad, E. K. Kristianslund, G. Myklebust, R. Bahr, S. Medicine, O. Sports, and S. Sciences, "Association between Lower Extremity Muscle," *Official Journal of the American College of Sports Medicine*, no. 23, pp. 2082–2089, 2016.

[52] K. Sinsurin, R. Vachalathiti, W. Jalayondeja, and W. Limroongreungrat, "Knee muscular control during jump landing in multidirections," *Asian Journal of Sports Medicine*, vol. 7, no. 2, 2016.

[53] E. C. Honert and T. C. Pataky, "Timing of gait events affects whole trajectory analyses: A statistical parametric mapping sensitivity analysis of lower limb biomechanics," *Journal of Biomechanics*, vol. 119, p. 110329, 2021.

[54] W. D. Penny, K. J. Friston, J. T. Ashburner, S. J. Kiebel, and T. E. Nichols, *Statistical parametric mapping: the analysis of functional brain images*. Elsevier, 2011.

[55] C. N. Hughes-Oliver, K. A. Harrison, D. B. Williams, and R. M. Queen, "Statistical parametric mapping as a measure of differences between limbs: Applications to clinical populations," *Journal of Applied Biomechanics*, vol. 35, no. 6, pp. 377 – 387, 2019.

[56] E. King, C. Richter, A. Franklyn-Miller, K. Daniels, R. Wadey, R. Moran, and S. Strike, “Whole-body biomechanical differences between limbs exist 9 months after acl reconstruction across jump/landing tasks,” *Scandinavian Journal of Medicine & Science in Sports*, vol. 28, no. 12, pp. 2567–2578, 2018.

[57] T. Dos’Santos and C. Thomas, “Between-limb differences during 180 turns in female soccer players: Application of statistical parametric mapping,” *Journal of Strength and Conditioning Research*, 2021.

[58] S. J. Hall, *Basic Biomechanics, 6th edition*. CMcGraw-Hill, 2012.

[59] A. Seth, M. Sherman, P. Eastman, and S. Delp, “Minimal formulation of joint motion for biomechanisms,” *Nonlinear Dynamics*, vol. 62, no. 1-2, pp. 291–303, 2010.

[60] A. V. Hill, *The heat of shortening and the dynamic constants of muscle*. Department of Physiology, University College, London, 1938.

[61] ——, *The abrupt transition from rest to activity in muscle*. Biophysics Research Unit, University College, London, 1949.

[62] F. E. Zajac, “Muscle and tendon: properties, models, scaling, and application to biomechanics and motor control,” *Critical reviews in biomedical engineering*, vol. 17, p. 359–411, 1989.

[63] M. Millard, T. Uchida, A. Seth, and S. L. Delp, “Flexing computational muscle: Modeling and simulation of musculotendon dynamics,” *Journal of Biomechanical Engineering*, vol. 135, no. 2, pp. 1–11, 2013.

[64] B. S. N. Milas, “Bsnlab,” 2021, accessed: 2021-04-21. [Online]. Available: http://www.bsnlab.com

[65] R. Hara, J. Mcginley, C. Briggs, R. Baker, and M. Sangeux, “Predicting the location of the hip joint centres , impact of age group and sex,” *Nature Publishing Group*, pp. 1–9, 2016.

[66] A. C. Campbell, D. G. Lloyd, J. A. Alderson, and B. C. Elliott, “MRI development and validation of two new predictive methods of glenohumeral joint centre location identification and comparison with established techniques MRI development and validation of two new predictive methods of glenohumeral joint centre location identification and comparison with established techniques,” *Journal of Biomechanics*, no. December 2018, pp. 1–6, 2009.

[67] D. A. Winter, *Biomechanics and Motor Control of Human Movement, Fourth Edition*. John Wiley and Sons, Inc., 2009.

[68] B. Serrien, M. Goossens, and J.-P. Baeyens, “Statistical parametric mapping of biomechanical one-dimensional data with bayesian inference,” *International Biomechanics*, vol. 6, no. 1, pp. 9–18, 2019.

[69] E. F. Whyte, C. Richter, S. O’Connor, and K. A. Moran, “Investigation of the effects of high-intensity, intermittent exercise and unanticipation on trunk and lower limb biomechanics during a side-cutting maneuver using statistical parametric mapping,” *Journal of Strength and Conditioning Research*, vol. 32, no. 6, pp. 1583–1593, 2018.

[70] R. J. Adler, *The Geometry of Random Fields*. Society for Industrial and Applied Mathematics, 2010.

[71] T. C. Pataky, “Generalized n-dimensional biomechanical field analysis using statistical parametric mapping,” *Journal of Biomechanics*, vol. 43, no. 10, pp. 1976–1982, 2010.

[72] J. Cohen, *Statistical Power Analysis for the Behavioral Sciences, 2nd Edition*. Lawrence Erlbaum Associates, 1988.

A

Biomechanical Analysis: Non-dominant Limb

A.1 Inverse Kinematics

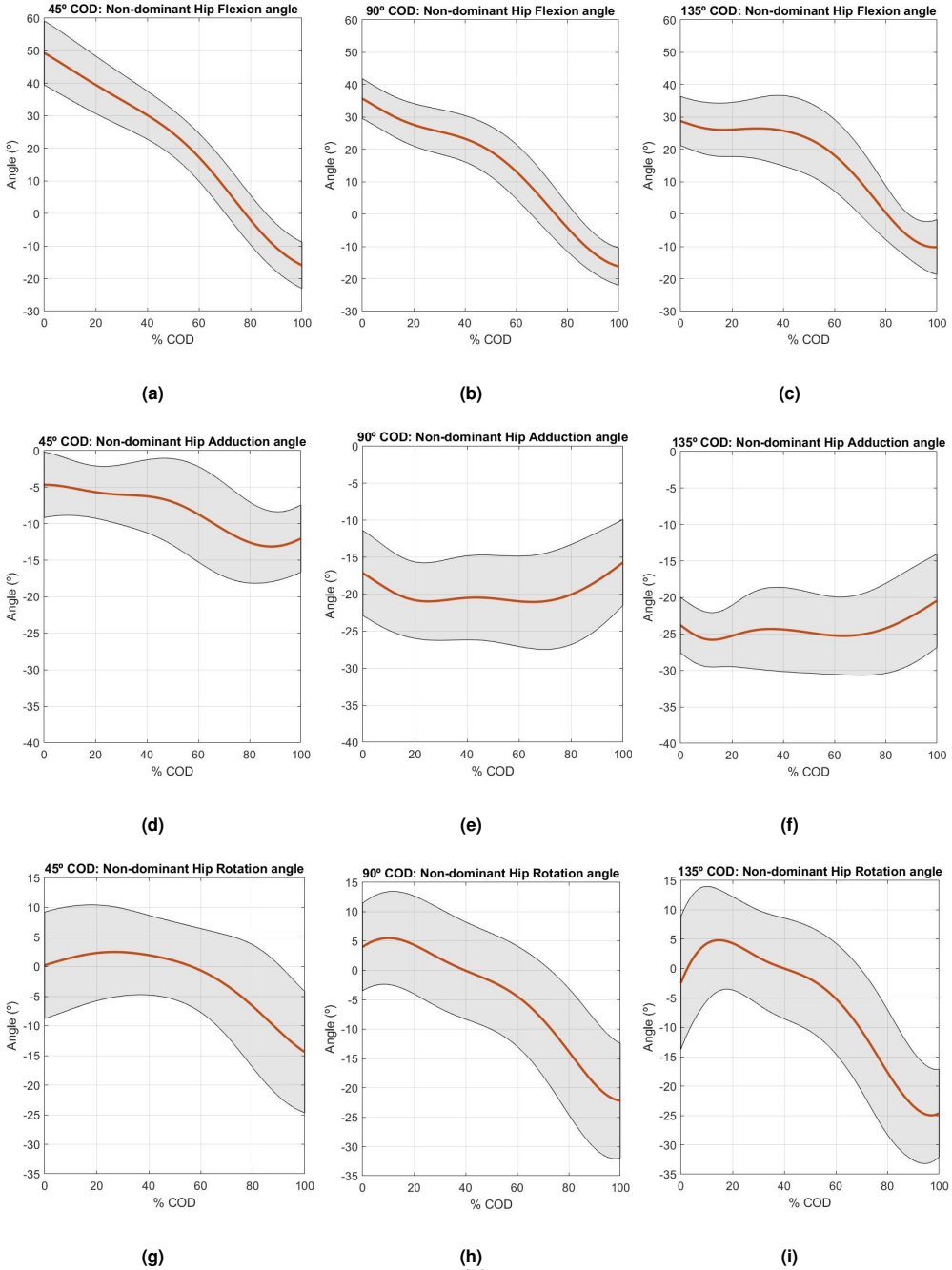

Figure A.1: Total average (orange) and standard deviation (shaded area) for the hip joint flexion angle. Non-dominant hip flexion/extension angle (+flexion) for the 45° COD (a), 90° COD (b) and 135° COD (c). Non-dominant hip adduction/abduction angle (+adduction) for the 45° COD (d), 90° COD (e) and 135° COD (f). Non-dominant hip internal/external rotation angle (+internal) for the 45° COD (g), 90° COD (h) and 135° COD (i). In degrees, in terms of percentage of completion of the stance phase of the COD.

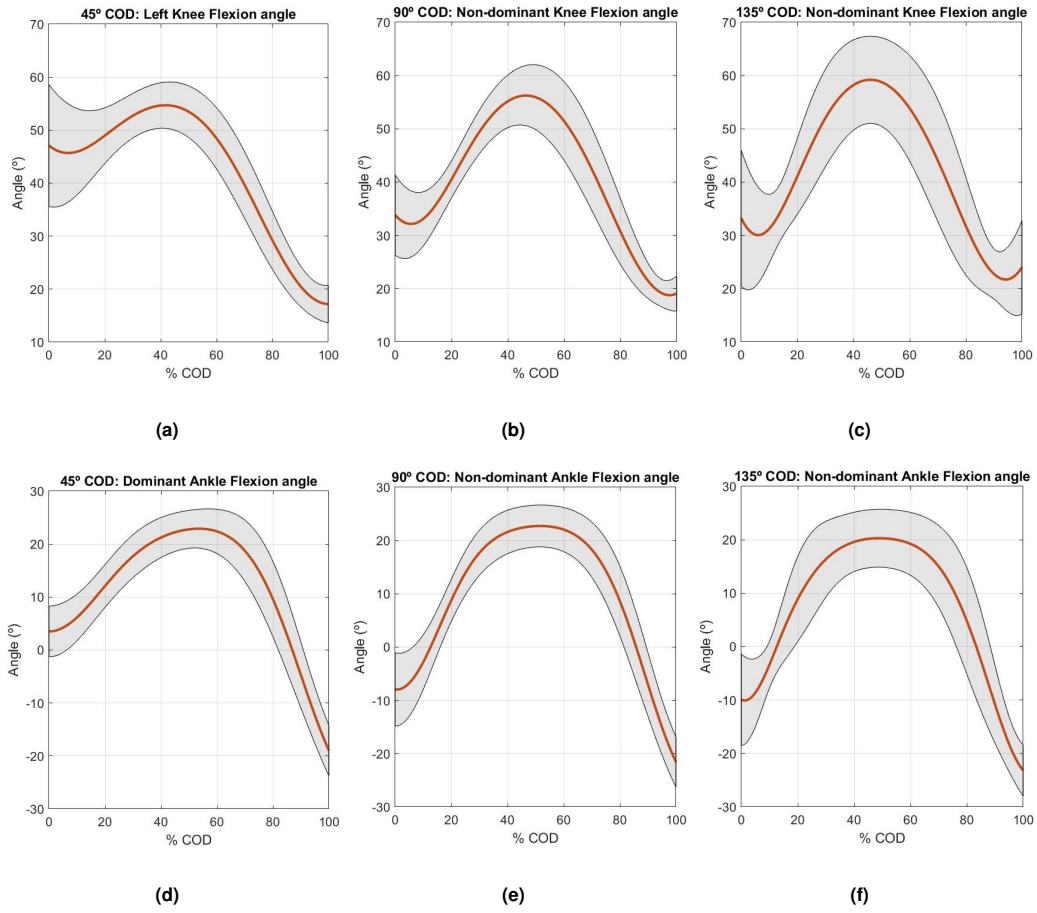

Figure A.2: Total average (orange) and standard deviation (shaded area) for the knee joint flexion angle. Non-dominant knee flexion/extension angle (+flexion) for the 45° COD (a), 90° COD (b) and 135° COD (c). Non-dominant ankle dorsiflexion/plantarflexion angle (+dorsiflexion) for the 45° COD (d), 90° COD (e) and 135° COD (f). In degrees, in terms of percentage of completion of the stance phase of the COD.

A.2 Inverse Dynamics

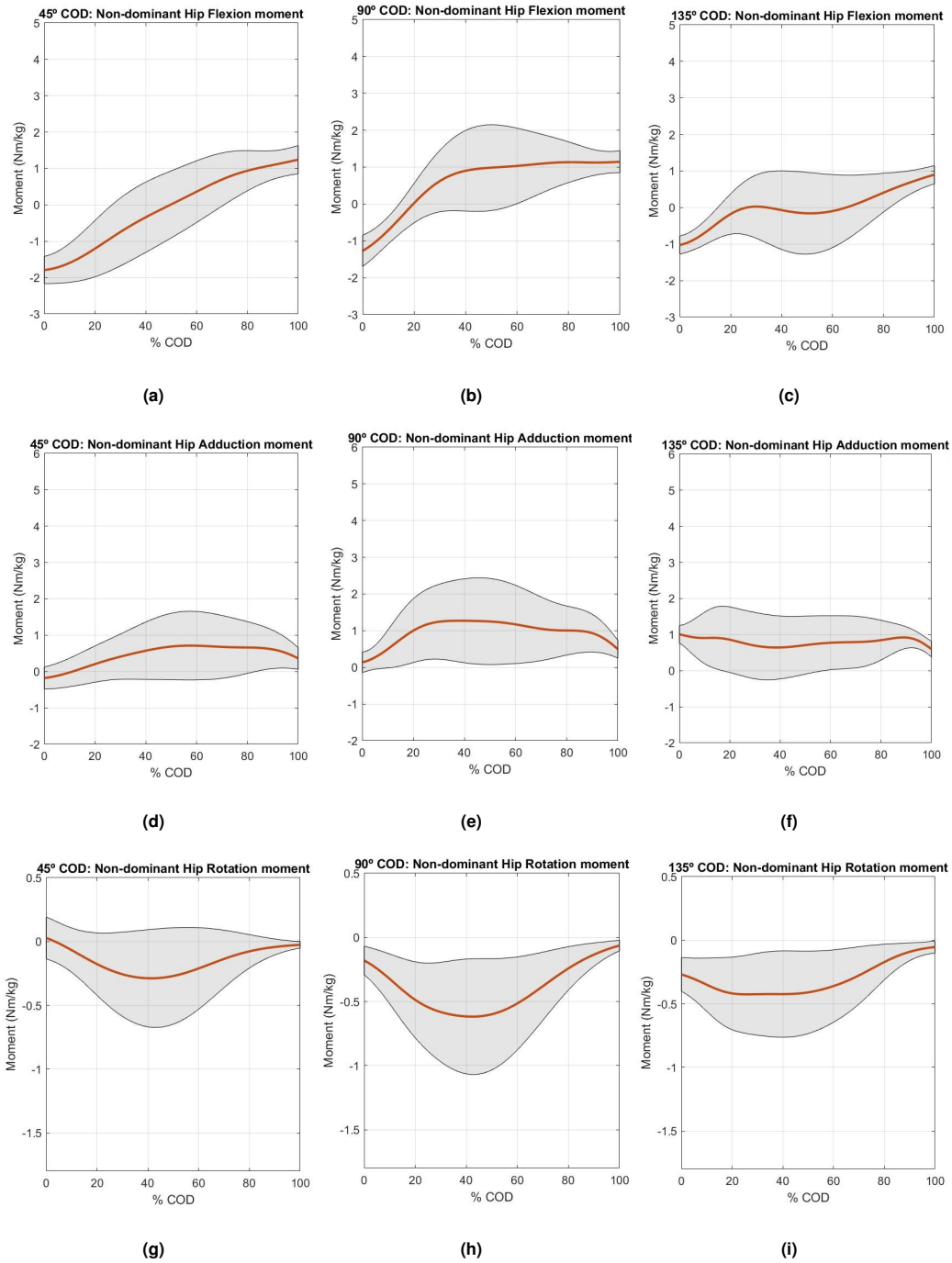

Figure A.3: Total average (orange) and standard deviation (shaded area) for the hip joint flexion moment. Non-dominant hip flexion/extension moment (+flexion) for the 45° COD (a), 90° COD (b) and 135° COD (c). Non-dominant hip adduction/abduction moment (+adduction) for the 45° COD (d), 90° COD (e) and 135° COD (f). Non-dominant hip internal/external rotation moment (+internal) for the 45° COD (g), 90° COD (h) and 135° COD (i). In Nm/kg, in terms of percentage of completion of the stance phase of the COD.

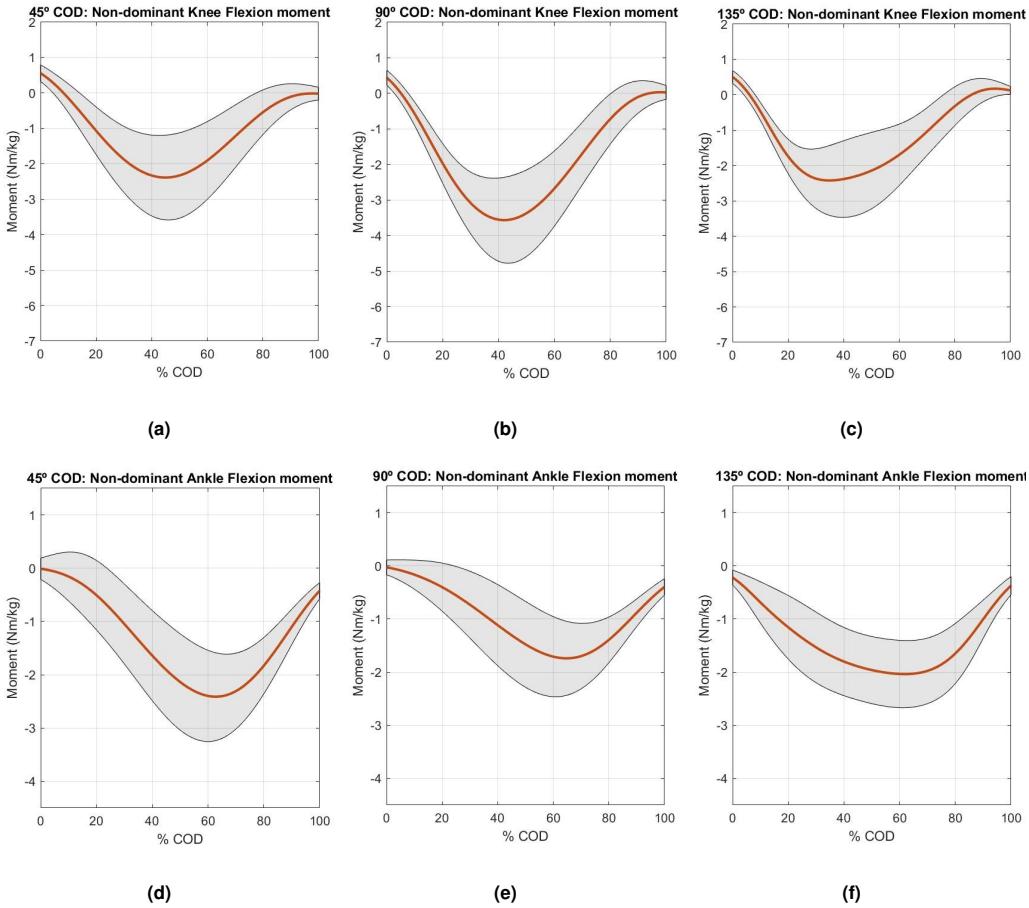

Figure A.4: Total average (orange) and standard deviation (shaded area) for the knee joint flexion moment. Non-dominant knee flexion/extension moment (+flexion) for the 45° COD (a), 90° COD (b) and 135° COD (c). Non-dominant ankle dorsiflexion/plantarflexion moment (+dorsiflexion) for the 45° COD (d), 90° COD (e) and 135° COD (f). In Nm/kg, in terms of percentage of completion of the stance phase of the COD.

A.3 Static Optimization

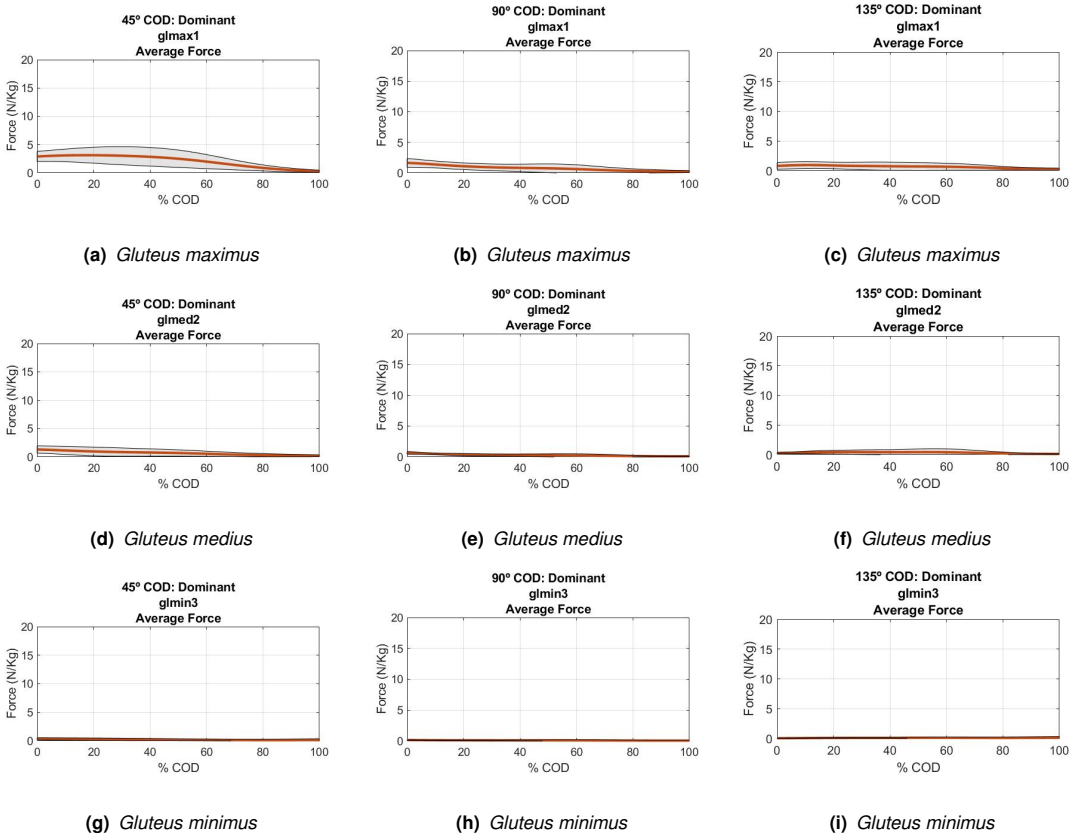

(a) *Gluteus maximus* **(b)** *Gluteus maximus* **(c)** *Gluteus maximus*

(d) *Gluteus medius* **(e)** *Gluteus medius* **(f)** *Gluteus medius*

(g) *Gluteus minimus* **(h)** *Gluteus minimus* **(i)** *Gluteus minimus*

Figure A.5: Total average (orange) and standard deviation (shaded area) for the estimated muscle forces: *Gluteus maximus*:45° COD (a), 90° COD (b) and 135° COD (c); *Gluteus medius*: 45° COD (d), 90° COD (e) and 135° COD (f); *Gluteus minimus*: 45° COD (g), 90° COD (h) and 135° COD (i). In N/kg and in terms of percentage of completion of the stance phase of the COD.

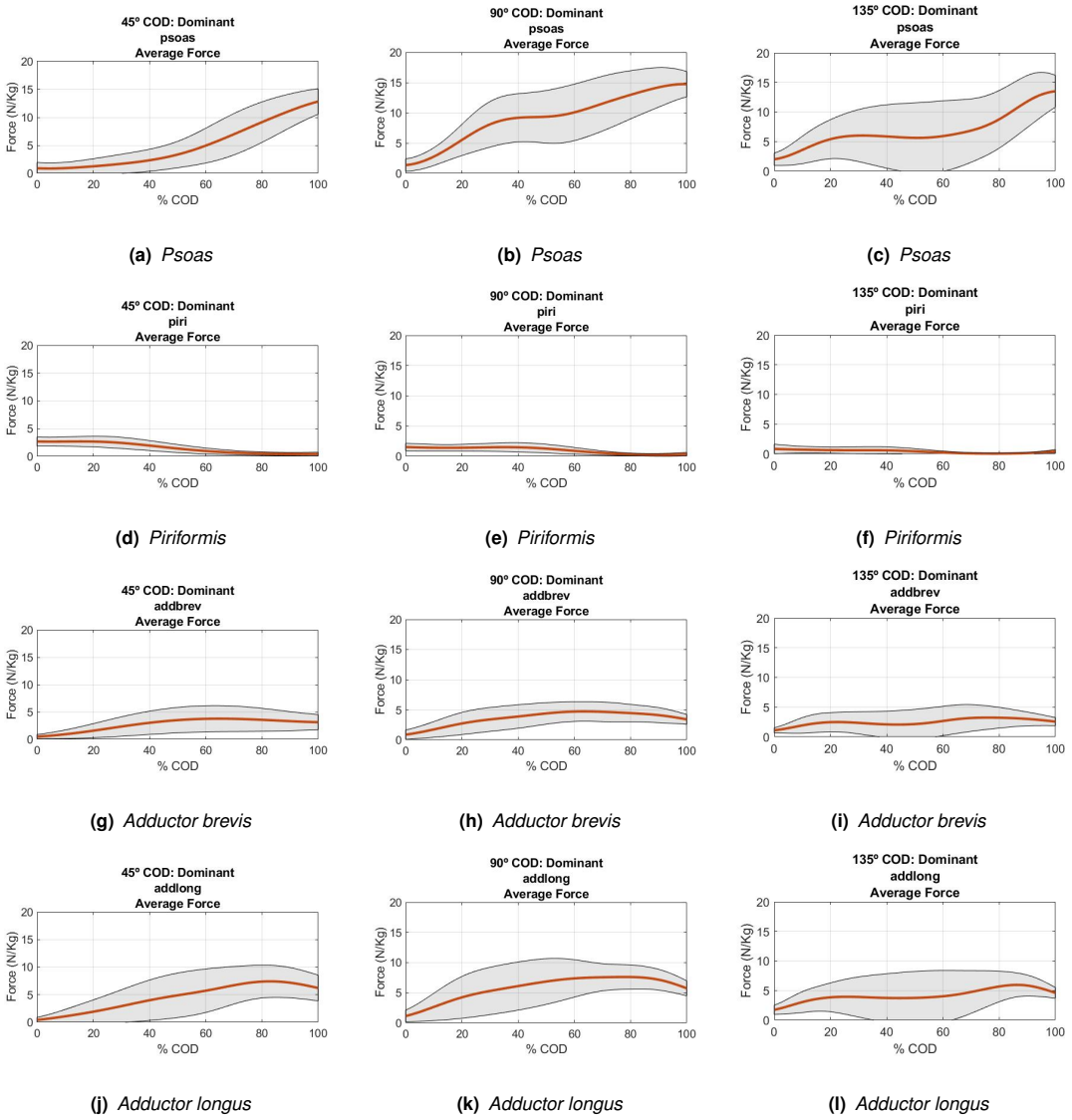

(a) *Psoas* **(b)** *Psoas* **(c)** *Psoas*

(d) *Piriformis* **(e)** *Piriformis* **(f)** *Piriformis*

(g) *Adductor brevis* **(h)** *Adductor brevis* **(i)** *Adductor brevis*

(j) *Adductor longus* **(k)** *Adductor longus* **(l)** *Adductor longus*

Figure A.6: Total average (orange) and standard deviation (shaded area) for the estimated muscle forces: *Psoas*:45° COD (a), 90° COD (b) and 135° COD (c); *Piriformis*: 45° COD (d), 90° COD (e) and 135° COD (f); *Adductor brevis*: 45° COD (g), 90° COD (h) and 135° COD (i); *Adductor longus*: 45° COD (j), 90° COD (k) and 135° COD (l). In N/kg and in terms of percentage of completion of the stance phase of the COD.

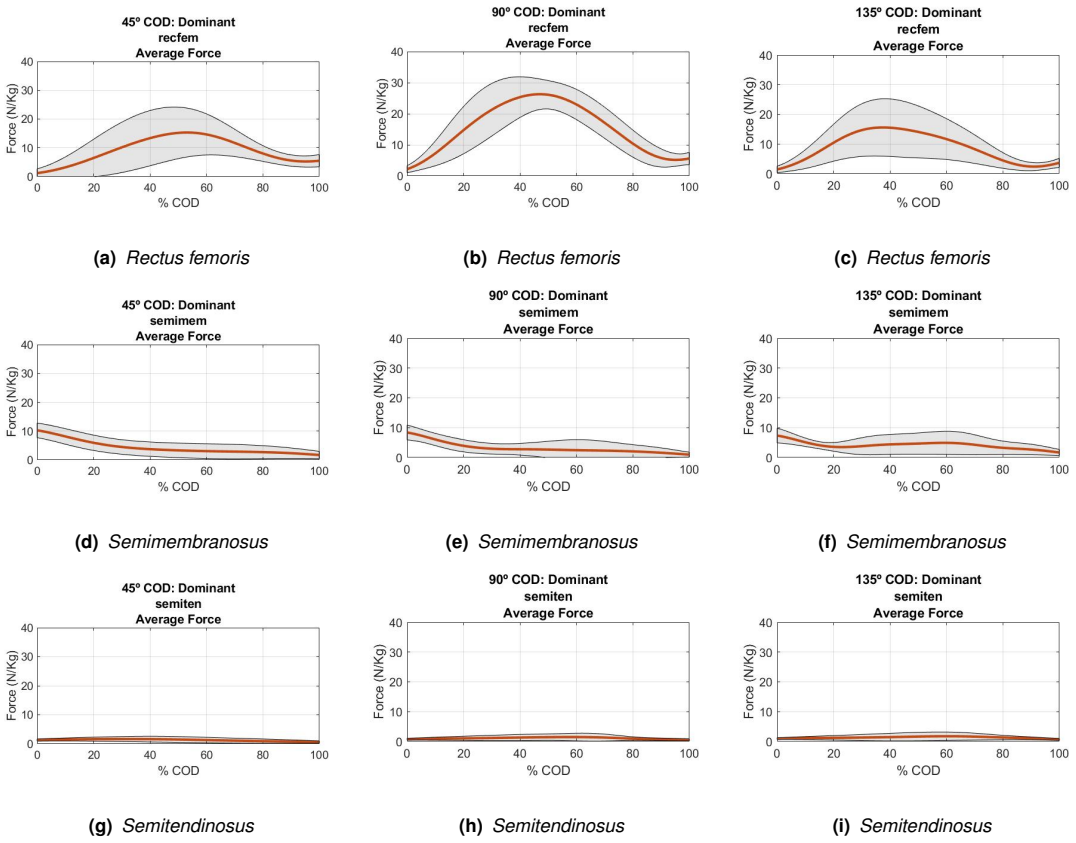

(a) *Rectus femoris* **(b)** *Rectus femoris* **(c)** *Rectus femoris*

(d) *Semimembranosus* **(e)** *Semimembranosus* **(f)** *Semimembranosus*

(g) *Semitendinosus* **(h)** *Semitendinosus* **(i)** *Semitendinosus*

Figure A.7: Total average (orange) and standard deviation (shaded area) for the estimated muscle forces: *Rectus femoris*:45° COD (a), 90° COD (b) and 135° COD (c); *Semimembranosus*: 45° COD (d), 90° COD (e) and 135° COD (f); *Semitendinosus*: 45° COD (g), 90° COD (h) and 135° COD (i). In N/kg and in terms of percentage of completion of the stance phase of the COD.

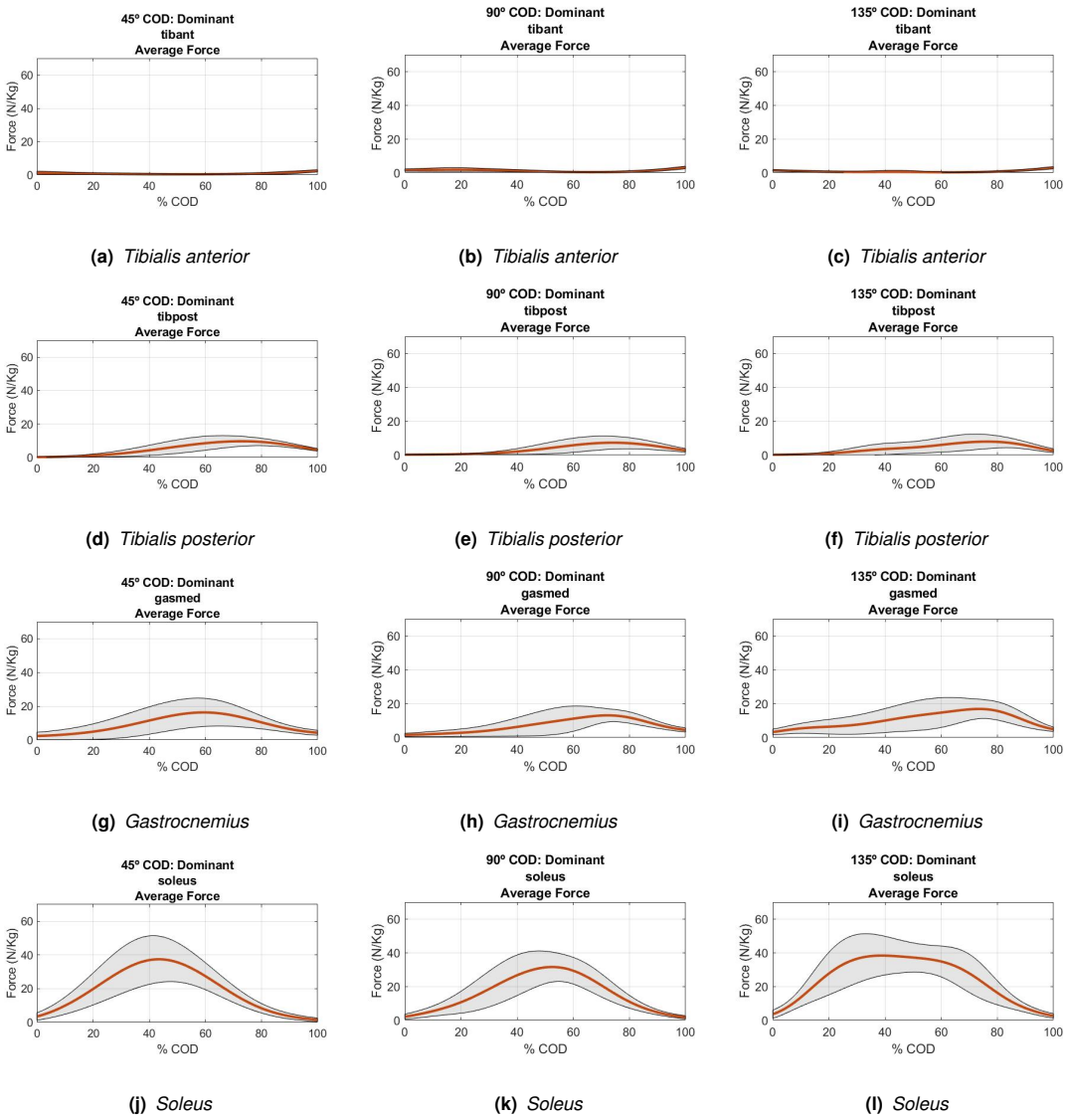

(a) *Tibialis anterior* **(b)** *Tibialis anterior* **(c)** *Tibialis anterior*

(d) *Tibialis posterior* **(e)** *Tibialis posterior* **(f)** *Tibialis posterior*

(g) *Gastrocnemius* **(h)** *Gastrocnemius* **(i)** *Gastrocnemius*

(j) *Soleus* **(k)** *Soleus* **(l)** *Soleus*

Figure A.8: Total average (orange) and standard deviation (shaded area) for the estimated muscle forces: *Tibialis anterior*:45° COD (a), 90° COD (b) and 135° COD (c); *Tibialis posterior*: 45° COD (d), 90° COD (e) and 135° COD (f); *Gastrocnemius*: 45° COD (g), 90° COD (h) and 135° COD (i); *Soleus*: 45° COD (j), 90° COD (k) and 135° COD (l). In N/kg and in terms of percentage of completion of the stance phase of the COD.